Lecture 3

Lattice and thermal transport, Electronic transport, Wannier-isation, Transport from MD autocorrelation functions, Thermoelectric materials

Thermoelectric materials

TE are particularly suitable for the generation of electrical power from temperature gradients, for example for harvesting low-grade waste heat into usable electrical energy in industrial plants, automotive exhaust systems, solar energy converters, and any other sources of waste heat.

Difficult area for innovation, specific properties!

Crystal structure as well as electronic structure are important.

Electrical conduction as well as thermal conduction critical.

In a thermodynamic perspective, thermoelectrics are *heat engines*.

Pressure/Volume

Temperature/Entropy

Heat Flux

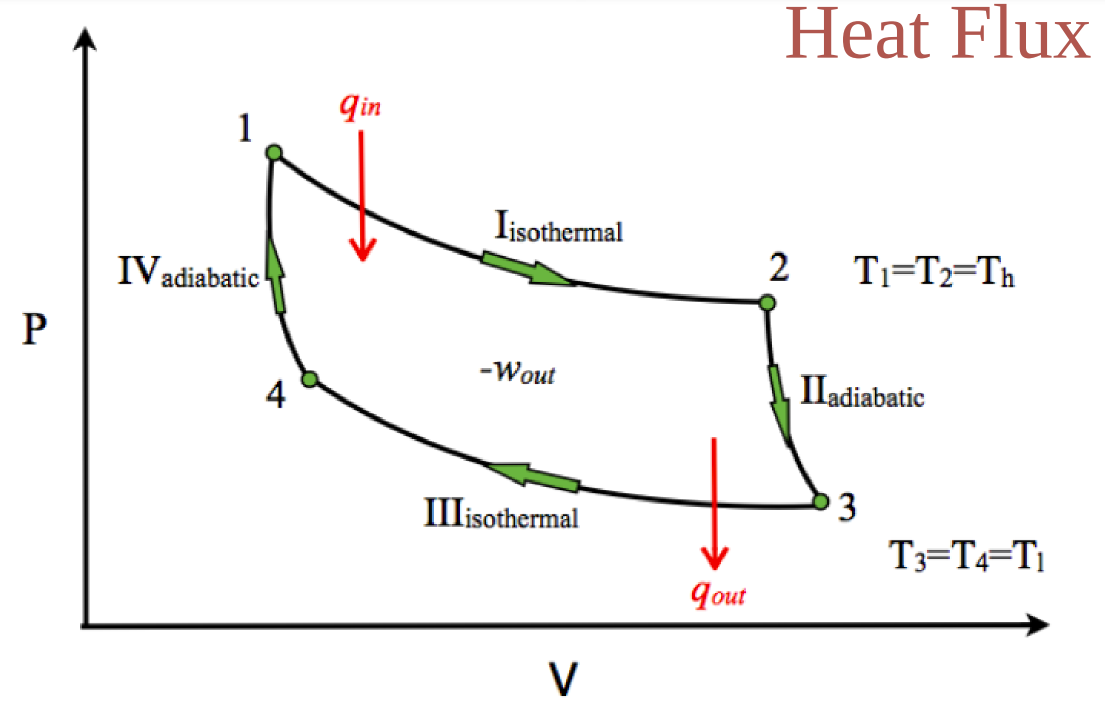

Figure 2. A P-V diagram of the Carnot Cycle.

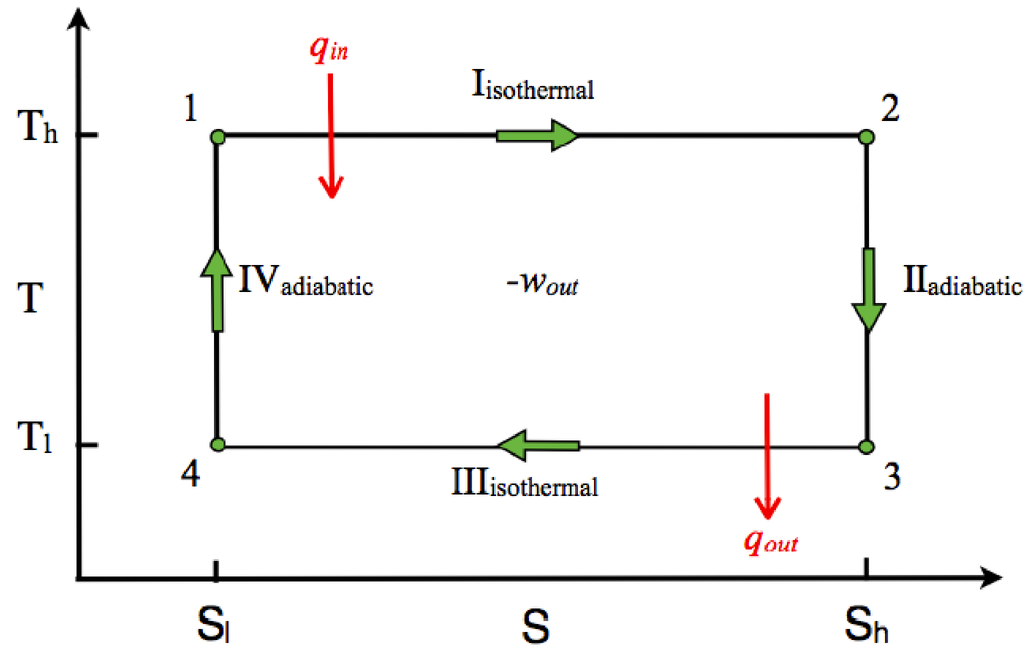

Figure 3. A T-S diagram of the Carnot Cycle.

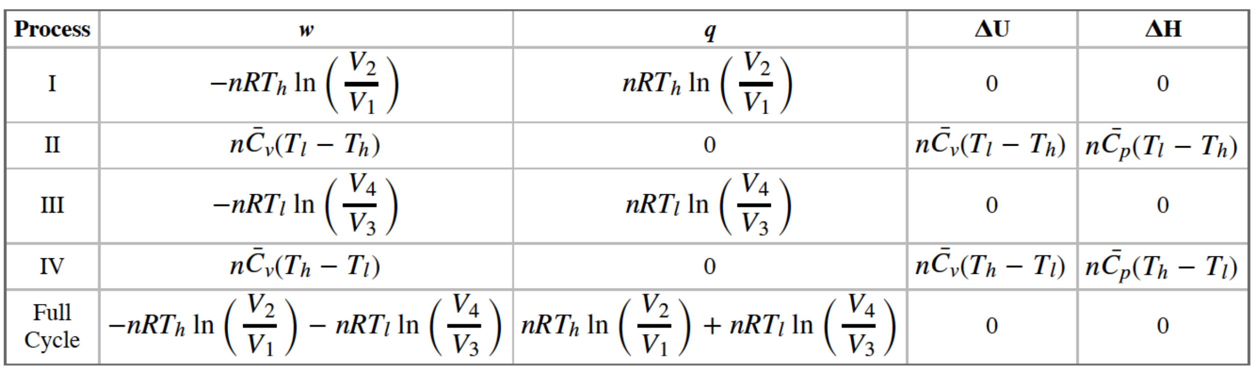

Process	w	q	ΔU	ΔH
I	$-nRT_h \ln\left(\frac{V_2}{V_1}\right)$	$nRT_h \ln\left(\frac{V_2}{V_1}\right)$	0	0
II	$n\bar{C}_v(T_l - T_h)$	0	$n\bar{C}_v(T_l - T_h)$	$n\bar{C}_p(T_l - T_h)$
III	$-nRT_l \ln\left(\frac{V_4}{V_3}\right)$	$nRT_l \ln\left(\frac{V_4}{V_3}\right)$	0	0
IV	$n\bar{C}_v(T_h - T_l)$	0	$n\bar{C}_v(T_h - T_l)$	$n\bar{C}_p(T_h - T_l)$
Full Cycle	$-nRT_h \ln\left(\frac{V_2}{V_1}\right) - nRT_l \ln\left(\frac{V_4}{V_3}\right)$	$nRT_h \ln\left(\frac{V_2}{V_1}\right) + nRT_l \ln\left(\frac{V_4}{V_3}\right)$	0	0

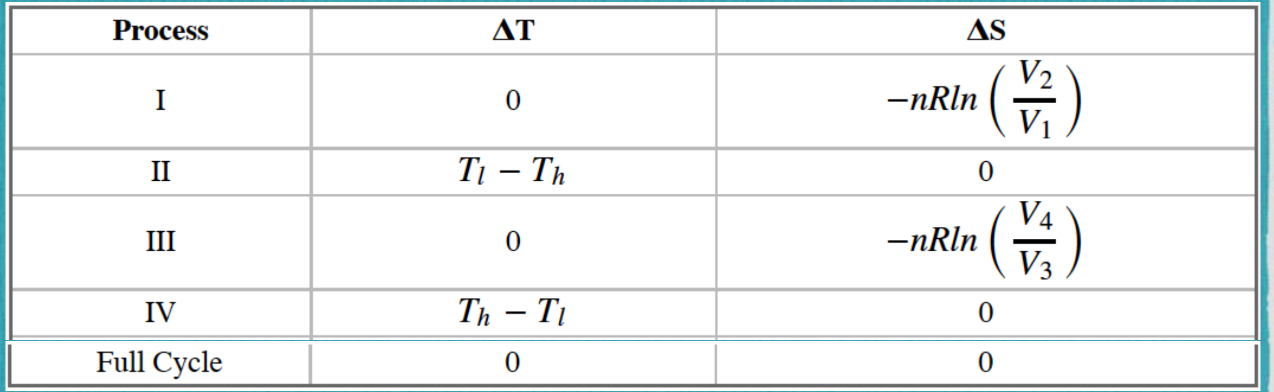

Process	ΔT	ΔS
I	0	$-nRln\left(\frac{V_2}{V_1}\right)$
II	$T_l - T_h$	0
III	0	$-nRln\left(\frac{V_4}{V_3}\right)$
IV	$T_h - T_l$	0
Full Cycle	0	0

http://chemwiki.ucdavis.edu/Physical_Chemistry/Thermodynamics/Thermodynamic_Cycles/Carnot_Cycle

Efficiency

efficiency = (work done) / (heat adsorbed)

$$\eta = \frac{nRT_h ln(\frac{V_2}{V_1}) + nRT_l ln(\frac{V_4}{V_3})}{nRT_h ln(\frac{V_2}{V_1})}$$

V3/V4 = V2/V1

$$\eta = \frac{T_h - T_l}{T_h}$$

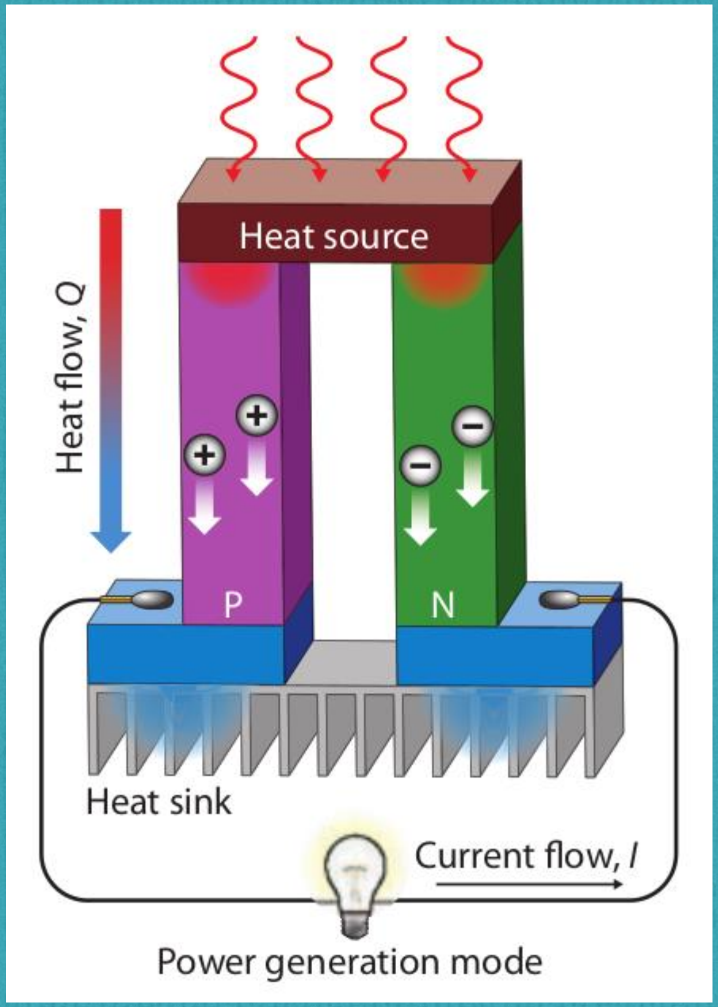

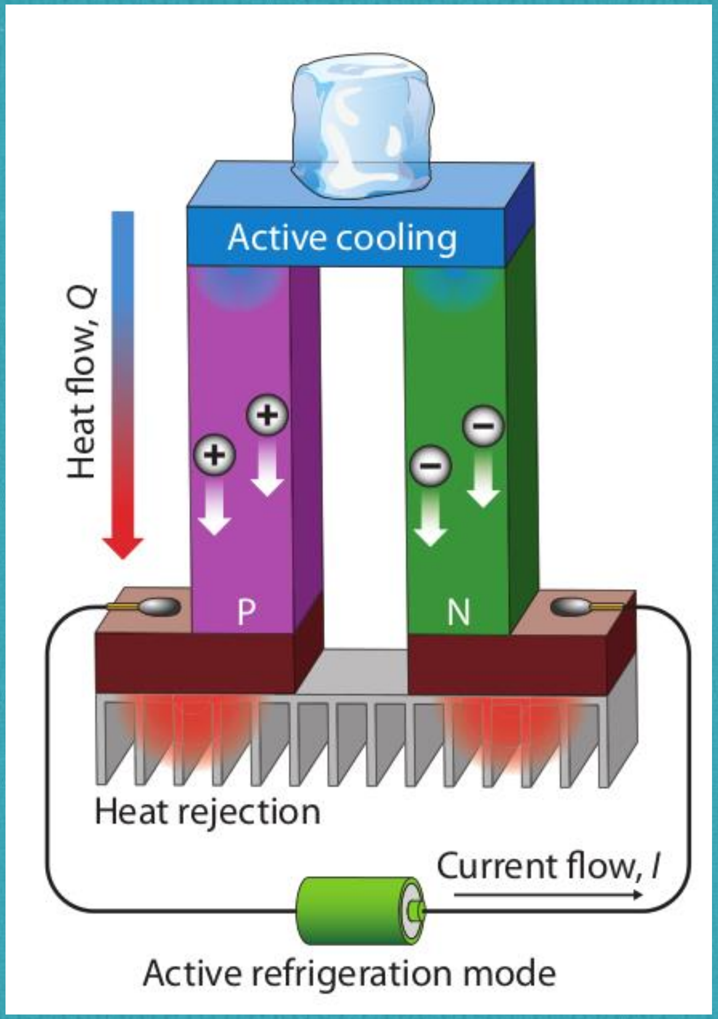

Images from: J-F Li, W-S Liu, L-D Zhao, M Zhou, High-performance nanostructured thermoelectric materials, *NPG Asia Mater.* 2 4 (2010) 152-158.

Seebeck Effect

- In 1821, Thomas Seebeck found that an electric current would flow continuously in a closed circuit made up of two dissimilar metals, if the junctions of the metals were maintained at two different temperatures.

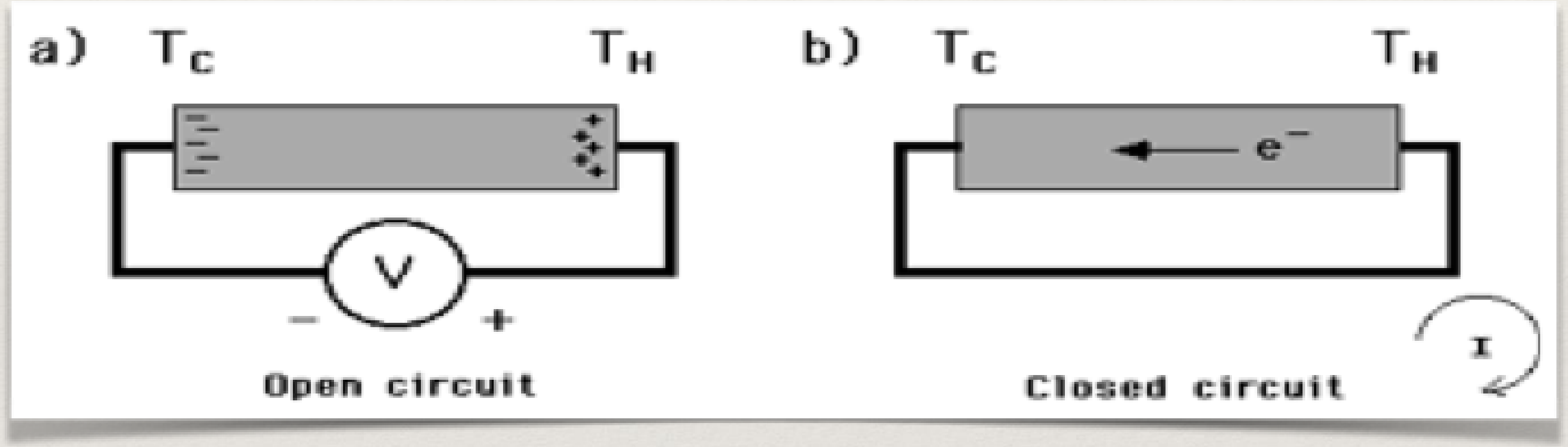

S= dV / dT;

S is the Seebeck Coefficient with units of Volts per Kelvin

S is positive when the direction of electric current is the same as the direction of thermal current

Peltier Effect

- In 1834, a French watchmaker and part time physicist, Jean Peltier found that an electrical current would produce a temperature gradient at the junction of two dissimilar metals.

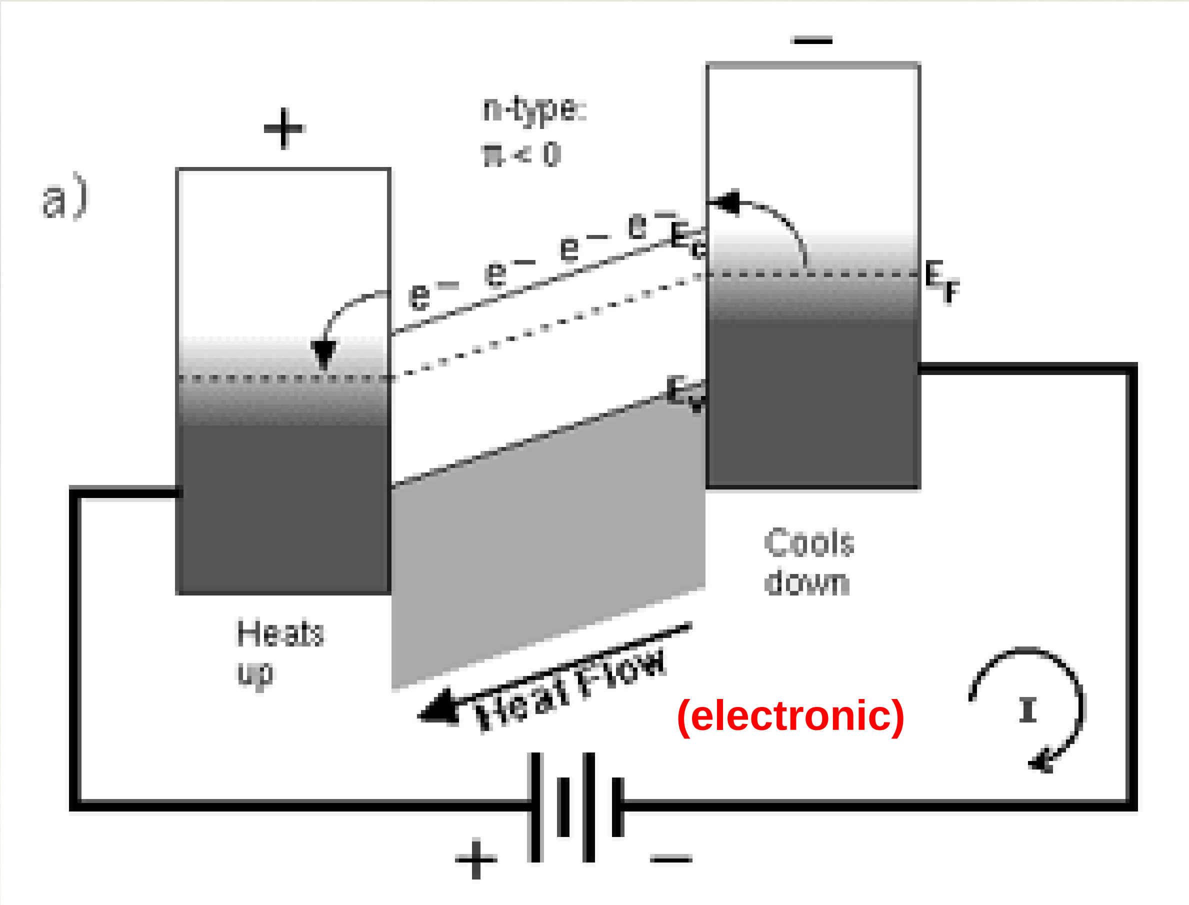

$\Pi < 0$; Negative Peltier coefficient

High energy electrons move from right to left.

Thermal current and electric current flow in opposite directions.

Peltier Cooling

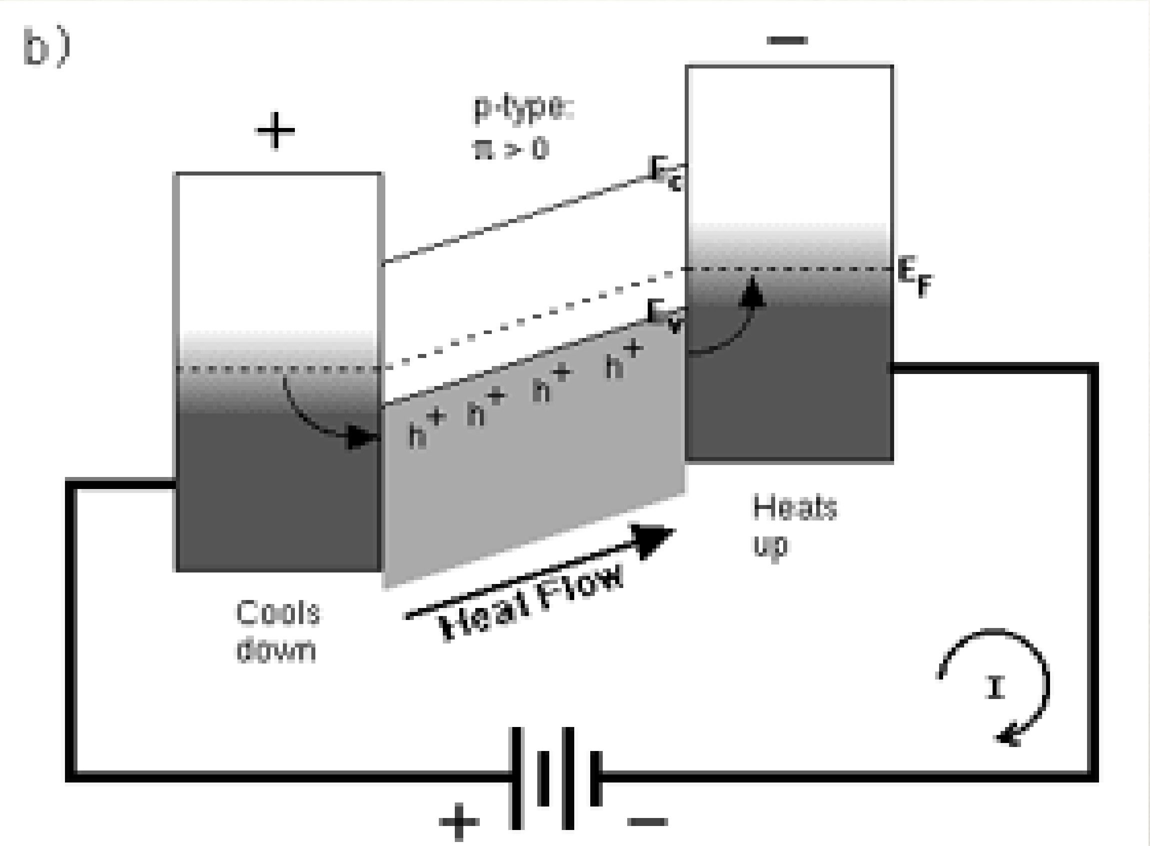

$\Pi > 0$; Positive Peltier coefficient

High energy holes move from left to right.

Thermal current and electric current flow in same direction.

$q=\Pi * j$, where q is thermal current density and j is electrical current density.

$\Pi = S*T$ (Volts) $S \sim 2.5\ k_B/e$ for typical TE materials

T is the Absolute Temperature

What material properties do we need to consider for a thermoelectric device?

What do we want this thermoelectric device to do?

To maximize output power or temperature gradient

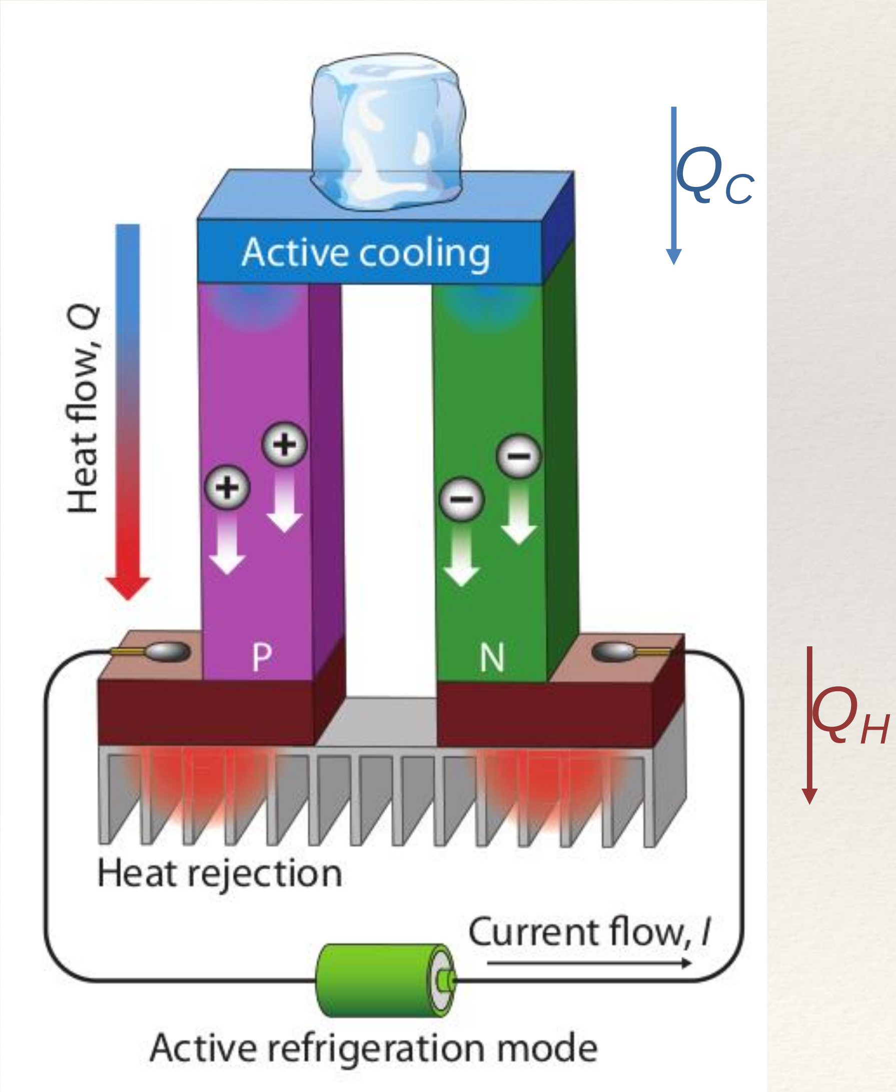

Q_C = *Peltier Cooling* – *Joule Heating* – *Thermal Diffusion*

$$= TS\frac{I}{A} - \frac{I^2 L}{2A^2\sigma} - \kappa\frac{dT}{dx}$$

$$\boxed{ZT = \frac{S^2\sigma}{\kappa}T}$$

Figure of Merit ZT

$$\boxed{ZT = \frac{S^2\sigma}{\kappa}T}$$

S is the Seebeck coefficient, σ is the electrical conductivity, T is the absolute temperature, and κ is the total thermal conductivity ($\kappa = \kappa_e + \kappa_L$, where κ_e and κ_L are the electronic and lattice contributions, respectively).

A *larger* ZT means a *better* TE

Figure of Merit

For conventional bulk materials the quantities S, σ, and κ are interrelated in such a way that it is very difficult to control these variables independently to increase the ZT value.

A high ZT value requires a combination of

- a large Seebeck coefficient, usually found in *insulators or intrinsic semiconductors*,
- a high electrical conductivity, which is characteristic of *metals*, and
- a low thermal conductivity, typical of *amorphous materials*.

Seebeck Coefficient

$$\alpha = \frac{8\pi^2 k_B^2}{3eh^2} m^* T \left(\frac{\pi}{3n}\right)^{2/3}$$

n: carrier concentration

$$1/\rho = \sigma = ne\mu$$

μ: carrier mobility
σ: conductivity
ρ: resistivity

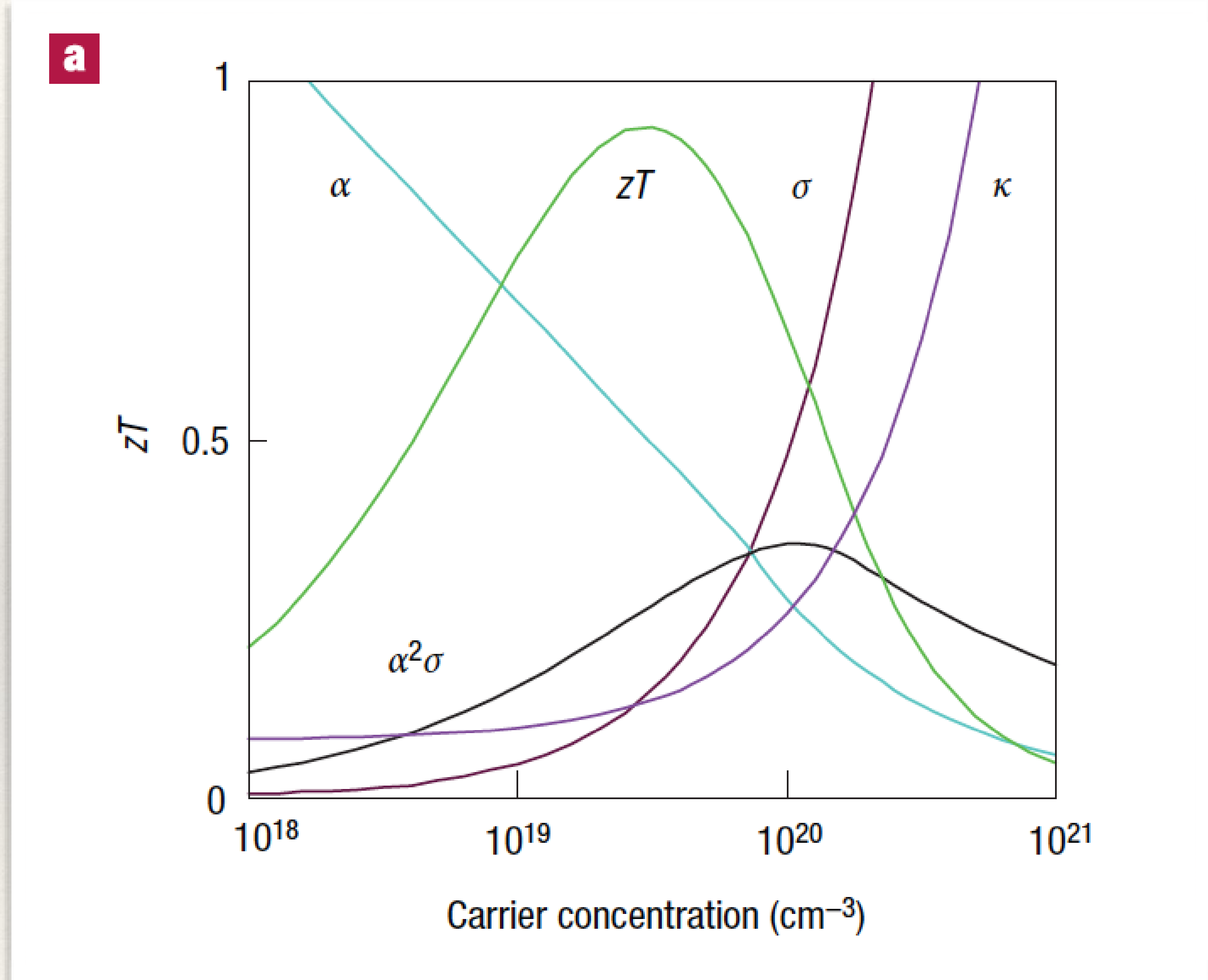

G. J. Snyder, E. S. Toberer, Nature Materials 7, 105 (2008).

Thermal Conductivity

$$zT = \frac{\alpha^2/L}{1 + \frac{\kappa_l}{\kappa_e}}$$

L: Lorenz factor 2.4 x 10^{-8} J^2 $K^{-2}C^{-2}$
κ_e: electron and holes thermal conductivity
κ_l: phonon thermal conductivity

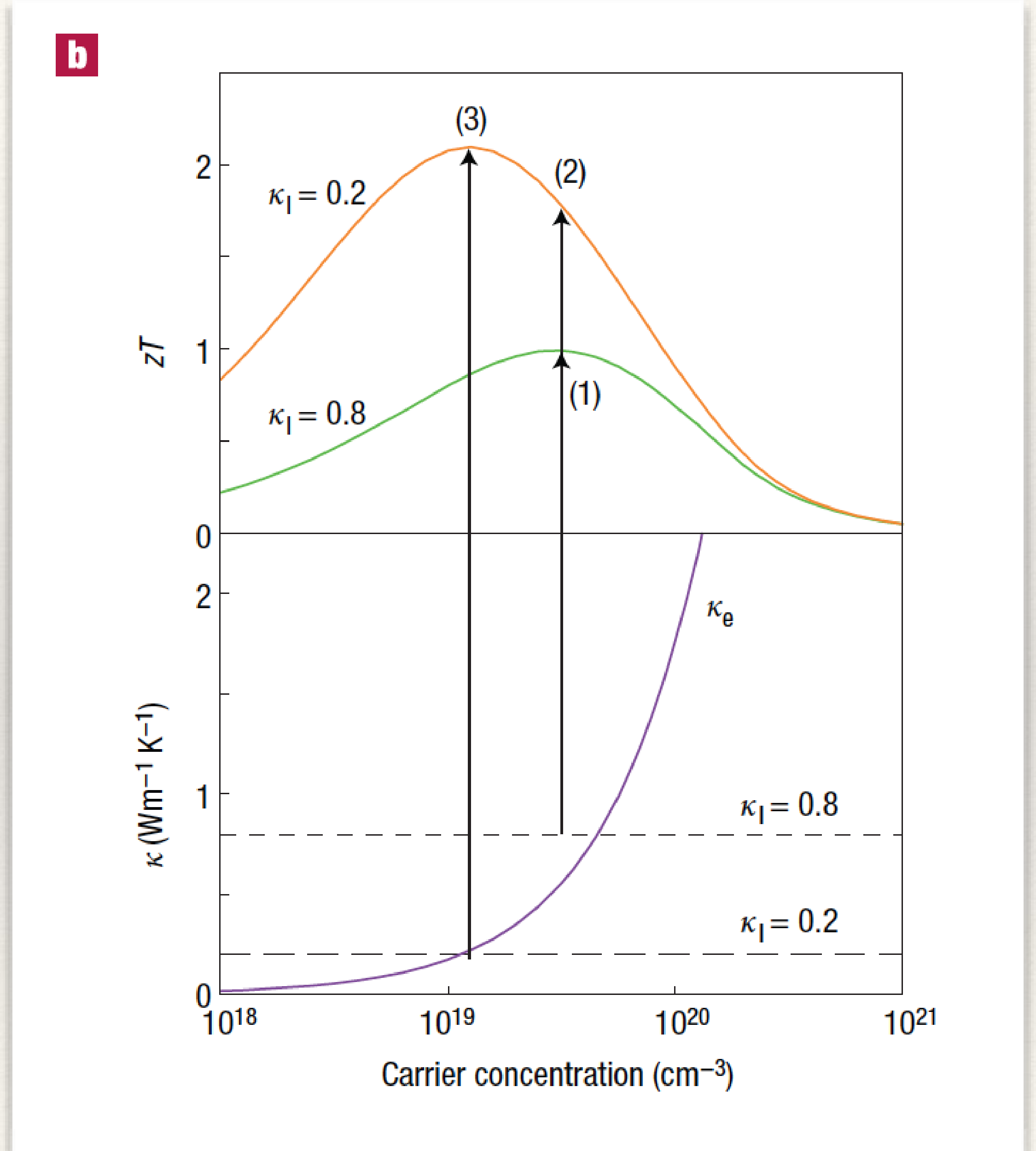

G. J. Snyder, E. S. Toberer, Nature Materials 7, 105 (2008).

Types of Materials

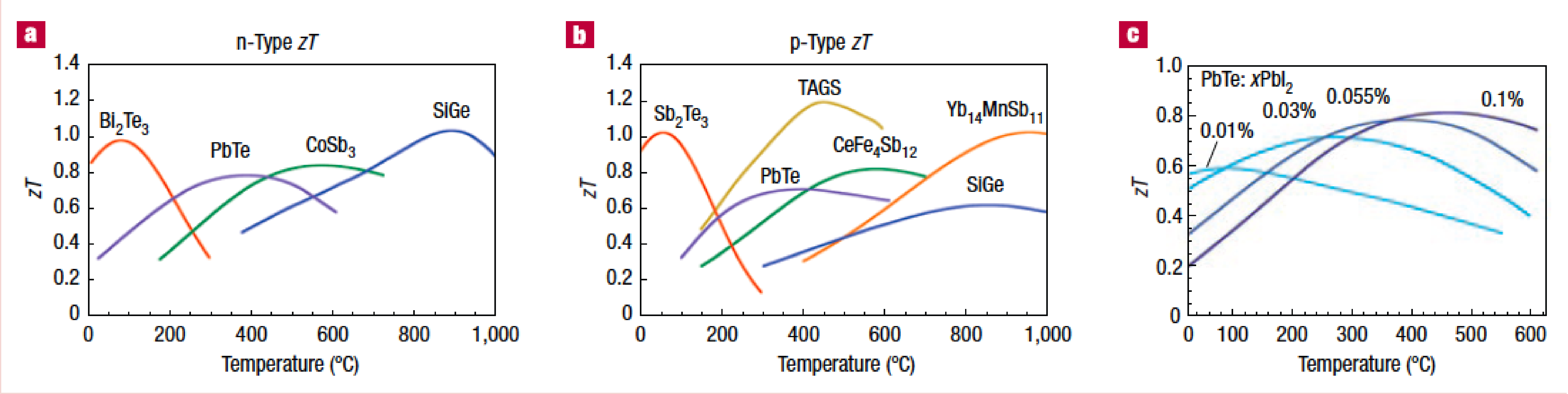

Figure-of-merit zT of some thermoelectrics.
a, p-type and b, n-type. Complex alloys with dopants; approximate compositions are shown.
c, Altering the dopant concentration changes not only the peak zT but also the temperature where the peak occurs.

As the dopant concentration in n-type PbTe increases (darker blue lines indicate higher doping) the zT peak increases in temperature.

G. J. Snyder, E. S. Toberer, nature materials, 7 (2008), 105-114

Types of Materials

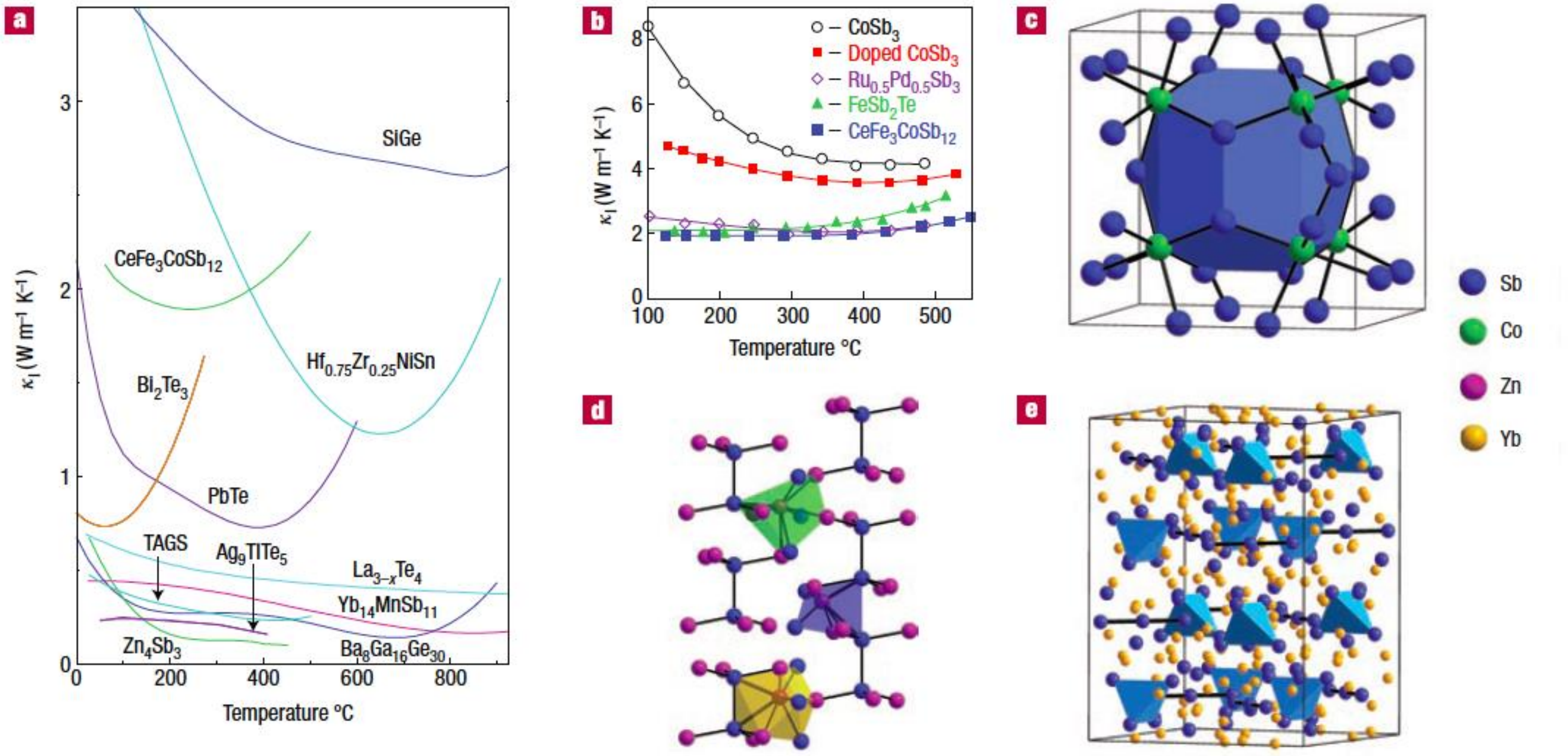

G. J. Snyder, E. S. Toberer, nature materials, 7 (2008), 105-114

Heusler Compounds
Intermetallics

Related to diamond & rocksalt

Tunable composition

Disorder

Half Heusler, XYZ
(e.g. TiCoSb)

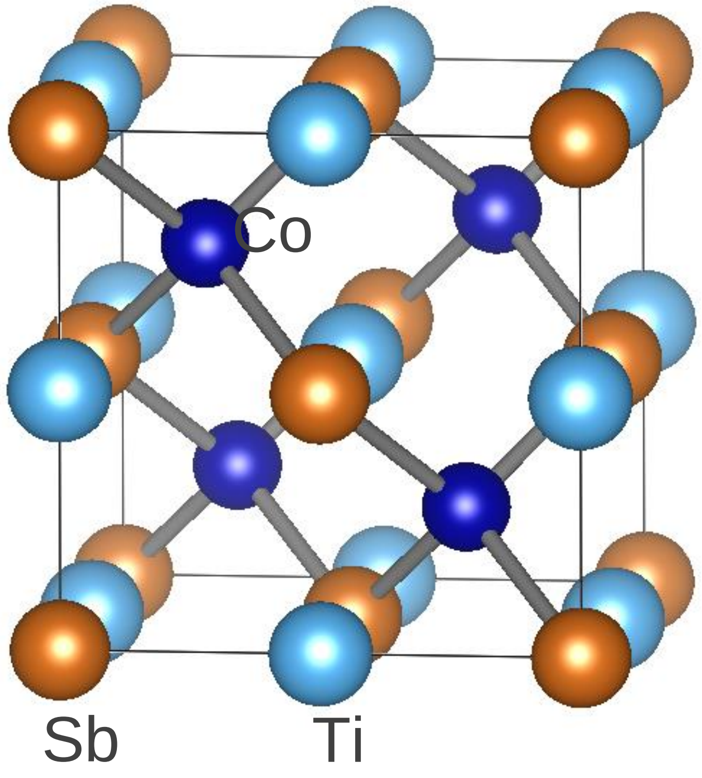

Full Heusler, XY_2Z
(e.g. $TiCo_2Sb$)

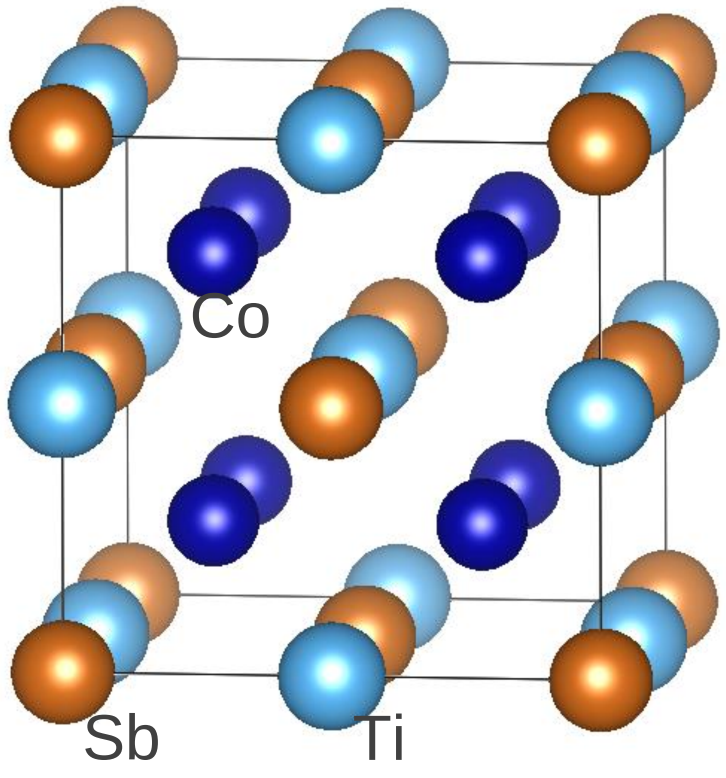

Valence precise half Heusler compounds can be semiconductors.

Example: TiCoSb

X: Ti → Ti^{4+} (Ar)

Y: Co → Co^{4-} (Ga)

Z: Sb → Sb

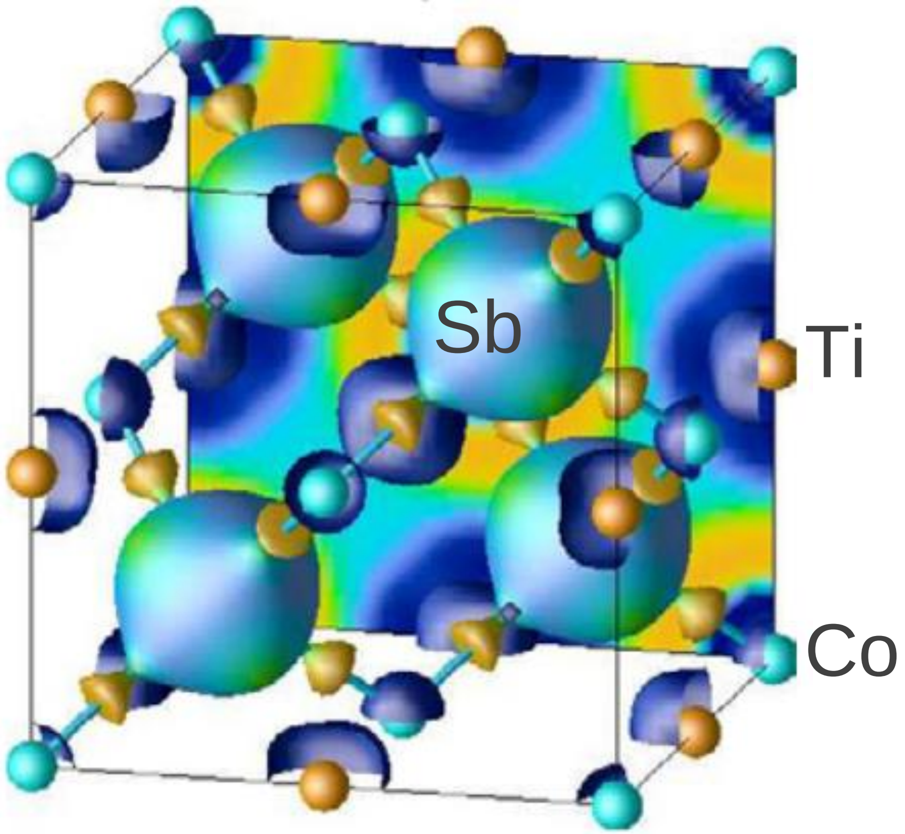

Image from: H.C. Kandpal, C. Fesler, R. Seshadri, Covalent bonding and the nature of band gaps in some half-Heusler compounds, *J. Phys. D* 39 (2006) 776-785.

X gives up its electrons and forms a covalent zinc-blende YZ sublattice.

18-electron half Heusler compounds are *electronically* identical to common III-V systems.

Atomic disorder can be used to scatter phonons by alloying on the X, Y, and Z sites.

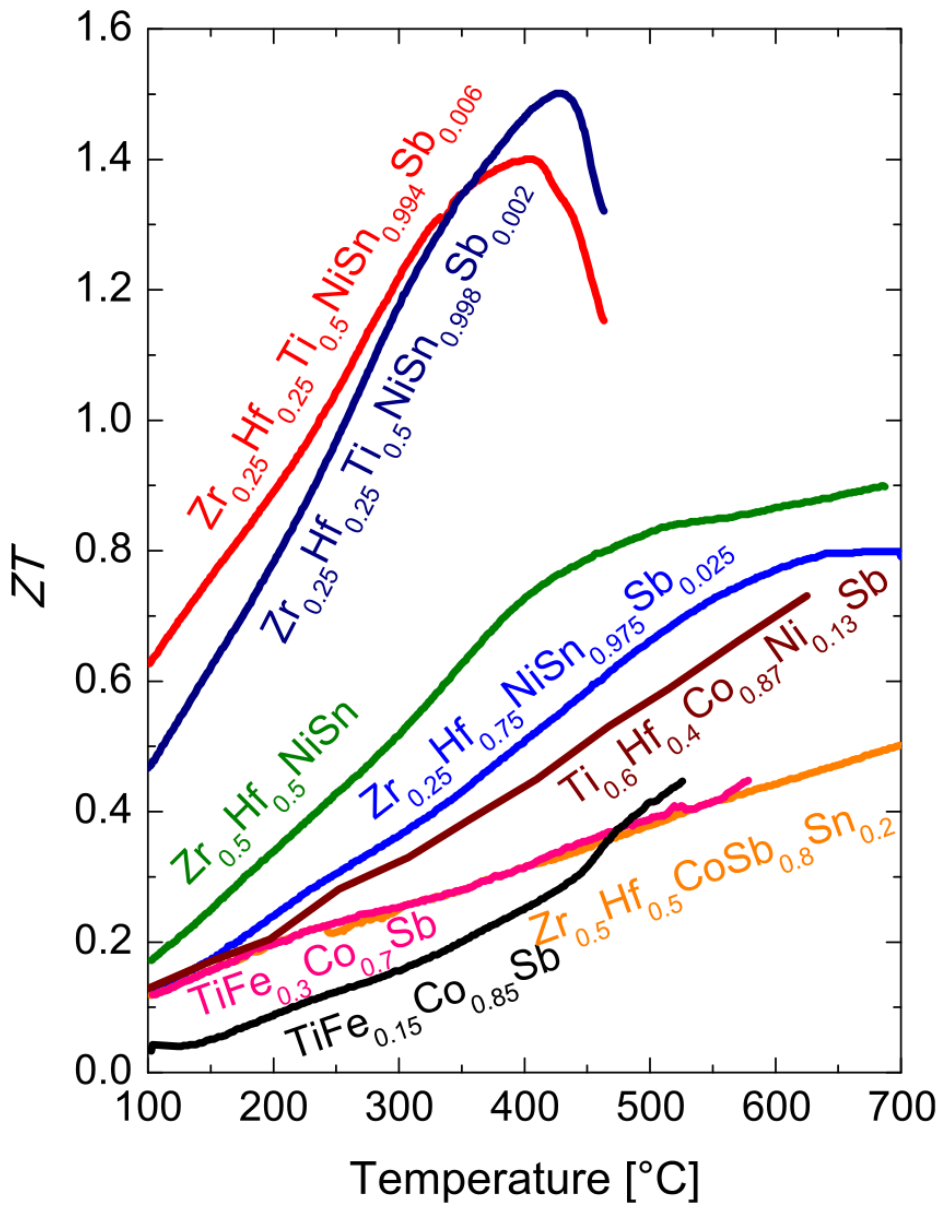

Heavily alloy X site
with large mass contrast (XX'NiSn)

X: $Ti \rightarrow Zr_xHf_yTi_{0.5}$

κ: 9.3 W/mK → 3-6 W/mK

Lightly dope on the Z site
to introduce carriers (XX'NiSn:Sb)

Z: $Sn \rightarrow Sn_{1-\delta}Sb_{\delta}$

σ: 100 S/cm → 1200 S/cm

Image from: T.Graf, C. Fesler, S.S.P. Parkin, Simple rules for the understanding of Heusler compounds, *Prog. Solid State Chem*. 39 (2011) 1-50.
Values from: H. Hohl, A.P. Ramirez, C. Goldmann, G. Ernst, B. Wolfing, E. Bucher, Efficient dopant for ZrNiSn-based thermoelectric materials, *J. Phys.: Condens. Matter* 11 (1999) 1697-1709.

However, phonons cover a wide range of wavelengths and require a multi-length scale scattering approach.

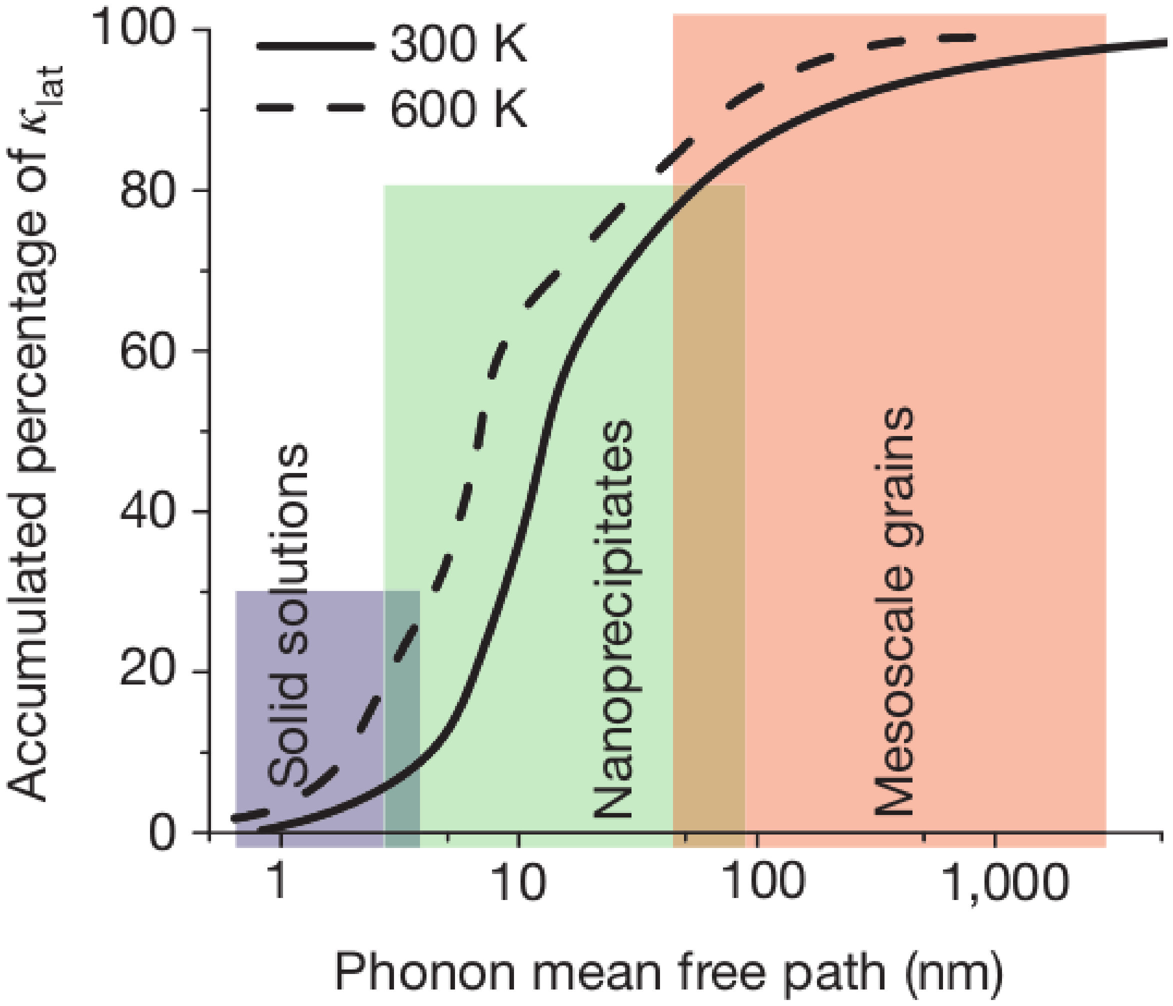

Image from: K. Biswas, J. He, I.D. Blum, C-I Wu, T.P. Hogan, D.N. Seidman, V.P. Dravid, M.G. Kanatzidis, High-performance bulk thermoelectrics with all-scale hierarchical architectures, *Nat. Lett.* 489 (2012) 414-418.

Nanoscale grain sizes impede mid-wavelength phonons, reduce thermal conductivity, and improve ZT.

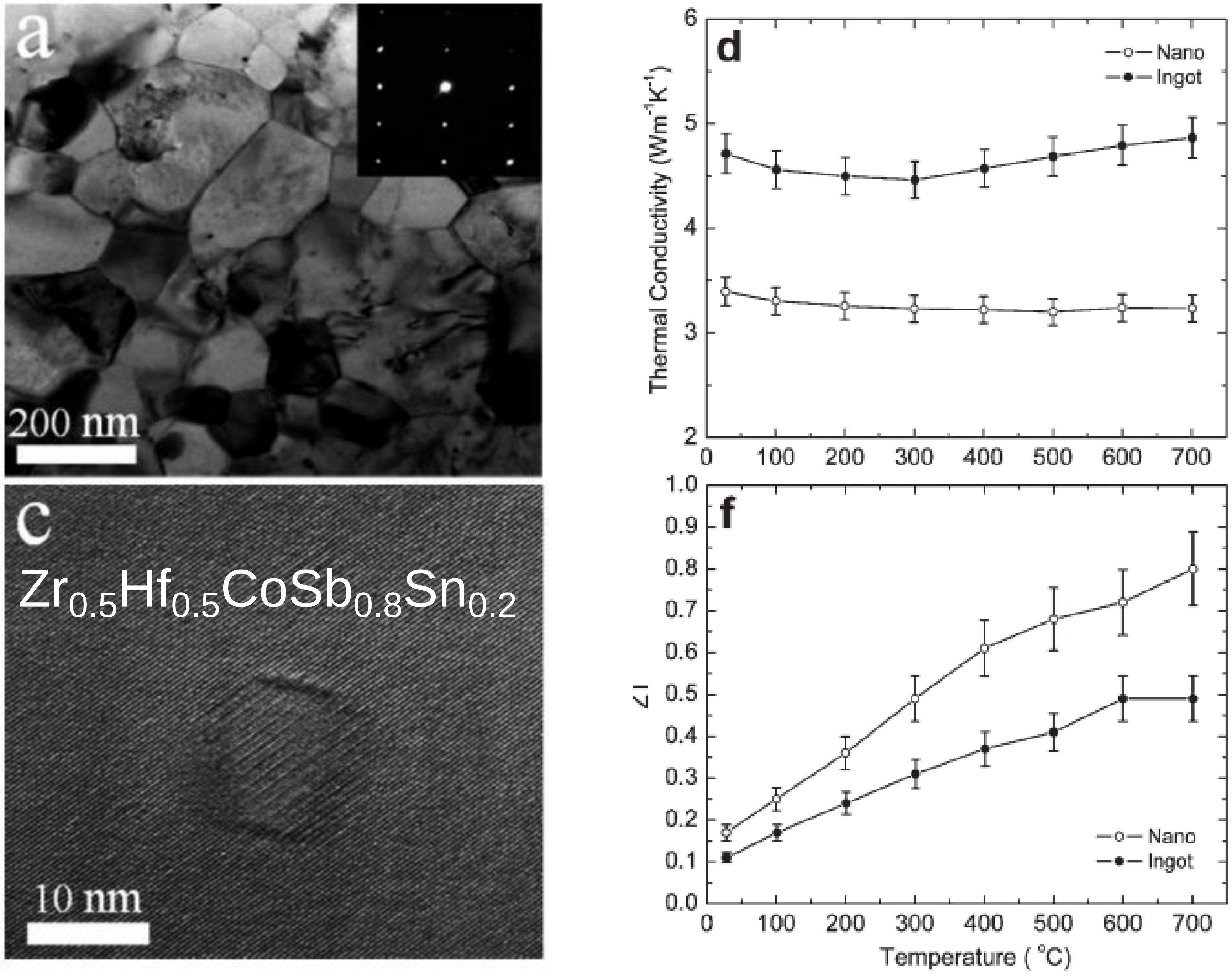

$Zr_{0.5}Hf_{0.5}CoSb_{0.8}Sn_{0.2}$

Images from: X. Yan, G. Joshi, W. Liu, Y. Lan, H. Wang, S. Lee, J.W. Simonson, S.J. Poon, T.M. Tritt, G. Chen, Z.F. Ren, Enhanced thermo-electric figure of merit of p-type half-heuslers, *Nano Lett.* 11 (2011) 556-560.

Half Heusler matrices with full Heusler nanoparticles also show reduced thermal conductivity and improved ZT.

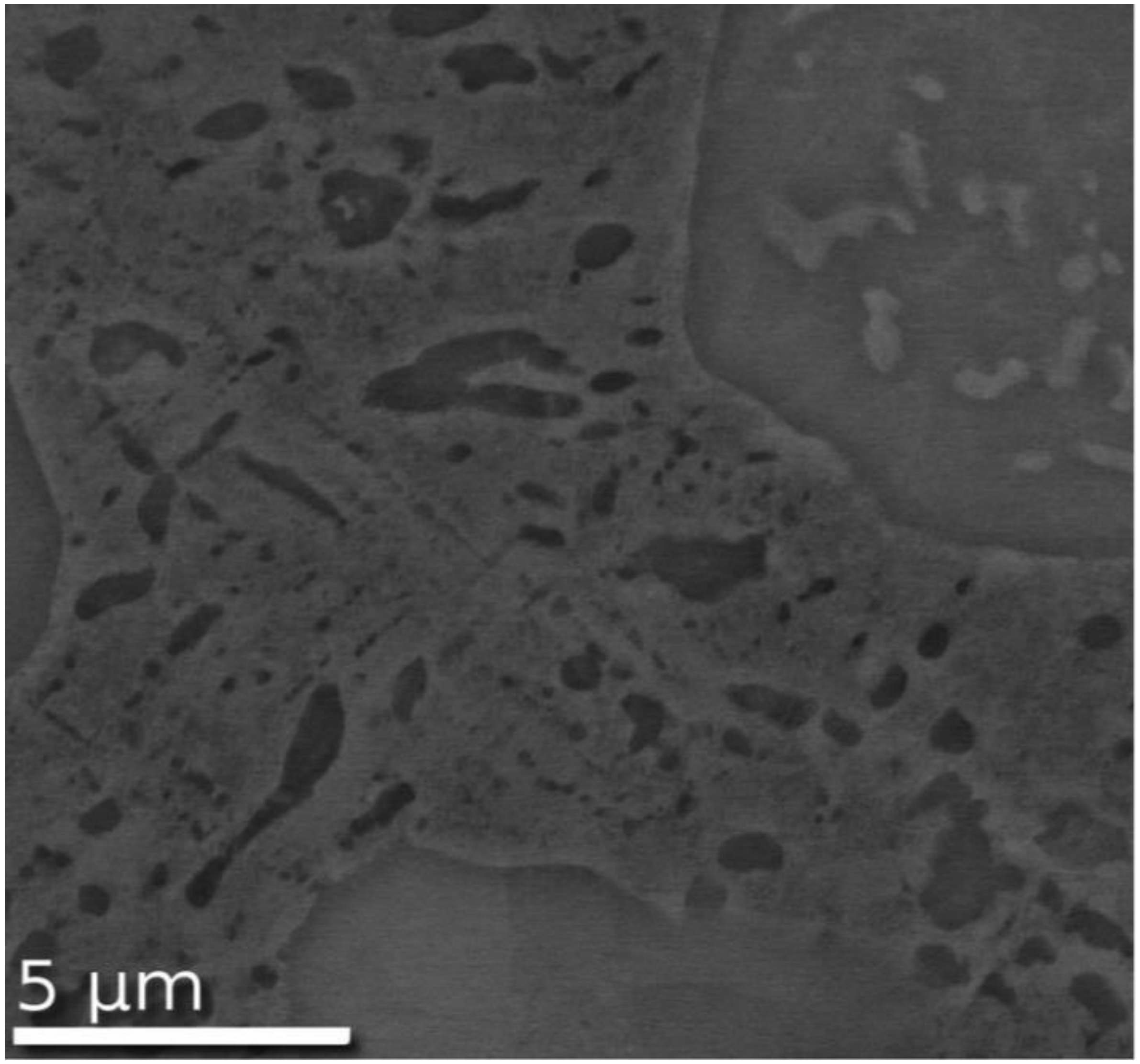

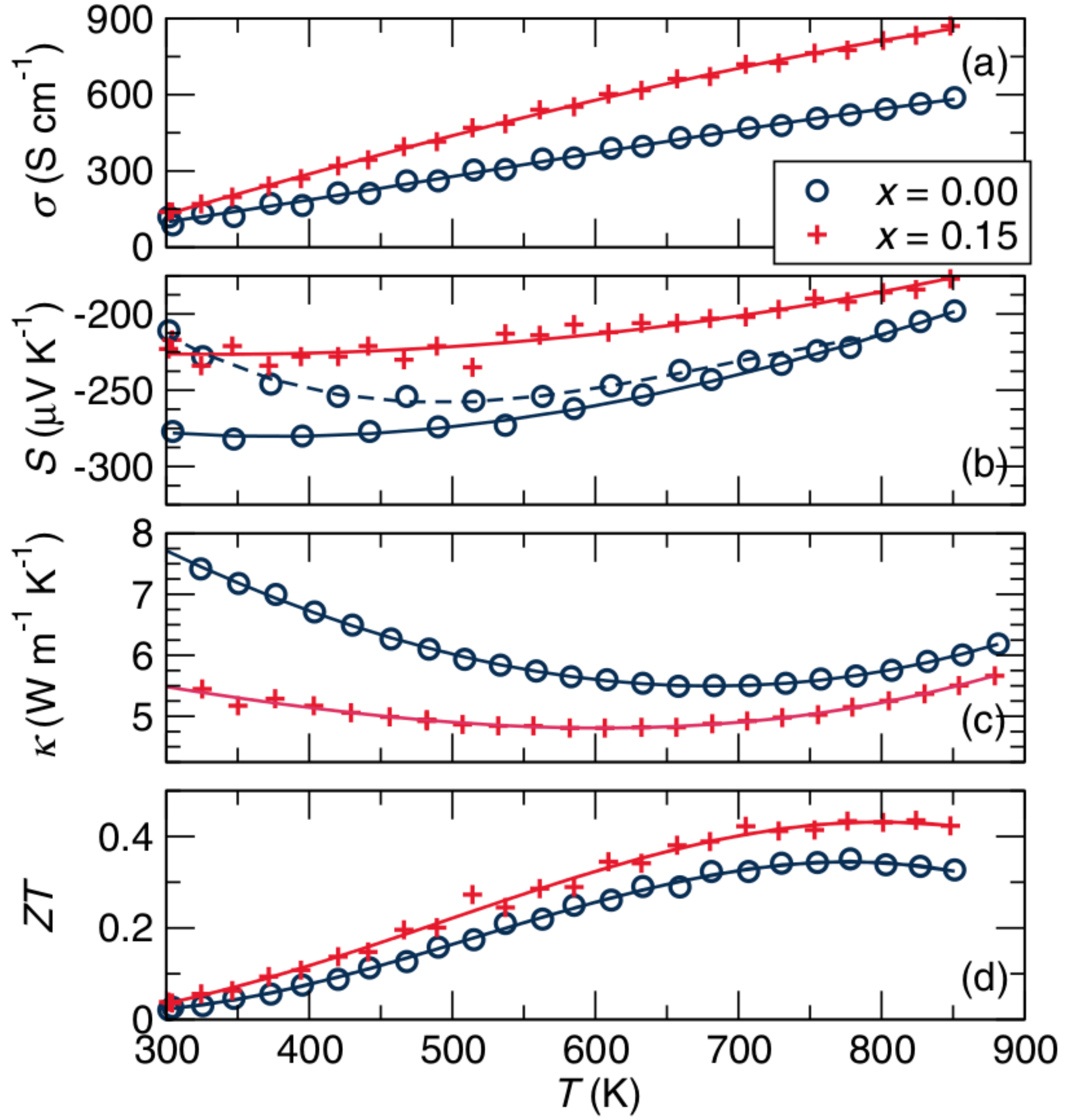

Image from: J.E. Douglas, C.S. Birkel, M-S Miao, C.J. Torbet, G.D. Stucky, T.M. Pollock, R. Seshadri, Enhanced thermoelectric properties of bulk TiNiSn via formation of a TiNi$_2$Sn second phase, *Appl. Phys. Lett.* 101 (2012) 183902.

High thermal conductivity still limits ZT in state-of-the-art Heulser thermoelectric compounds.

MATERIAL	**K** [W/mK]	ZT (Meas. Temp) [Ref.]
TiNiSn (n-type)	4-5	0.35 (740K) [1]
$Hf_{0.5}Zr_{0.5}NiSn$	3	0.9 (960 K) [2]
$Zr_{0.25}Hf_{0.25}Ti_{0.5}NiSn_{0.998}Sb_{0.002}$	3	1.4 (700 K) [2]
TiCoSb (p-type)	6-12	0.04 (780 K) [1]
$ZrCoSb_{0.9}Sn_{0.1}$	7-10	0.45 (958 K) [2]
$Zr_{0.5}Hf_{0.5}CoSb_{0.8}Sn_{0.2}$	3.6-4.1	0.8 (1000 K) [2]
SnSe	0.3 - 0.7	2.6 (932 K) [3]

Values from: [1] C.S. Birkel, W.G. Zeier, J.E. Douglas, B.R. Lettiere, C.E. Mills, G. Seward, A. Birkel, M.L. Snedaker, Y. Zhang, G.J. Snyder, T.M. Pollock, R. Seshadri, G.D. Stucky, Rapid microwave preparation of thermelectric TiNiSn and TiCoSb half-Heusler compounds, *Chem. Mater.* 24 (2013) 2558-2565. [2] T.Graf, C. Fesler, S.S.P. Parkin, Simple rules for the understanding of Heusler compounds, *Prog. Solid State Chem*. 39 (2011) 1-50. [3] L-D. Zhao, S-H Lo, Y. Zhang, H. Sun, G. Tan, C. Uher, C. Wolverton, V.P. Dravid, M.G. Kanatzidis, Ultralow thermal conductivity and high thermoelectric figure of merit in SnSe crystals, *Nat. Lett.* 508 (2014) 373-377.

Lead Chalcogenides PbX, X=S, Se, Te

- Promising class of thermoelectric materials
- Easily “tunable” into metals
- Thermal conductivity dominated by lattice part

A different approach to thermoelectrics is needed

K_L

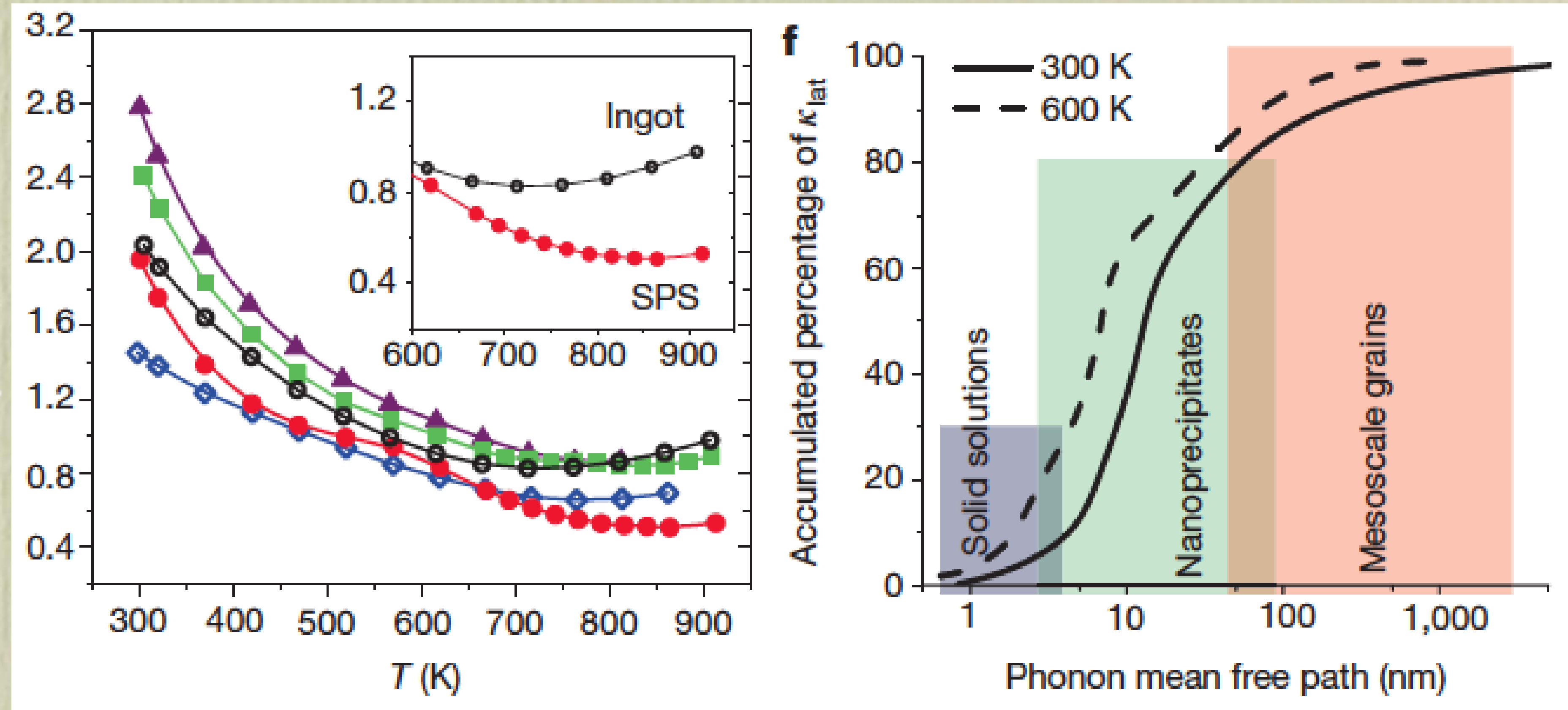

K. Biswas, M. Kanatzidis *et al.*, Nature 489, 414 (2012)
(figure from therein)

$$ZT = \frac{S^2\,T}{\boxed{\rho\,\kappa}}$$

ZT = Thermoelectric Figure of Merit, S = Seebeck Coefficient, T = Temperature

ρ = resistivity, κ = thermal conductivity

Time-Evolution of a System
Molecular Dynamics (MD)

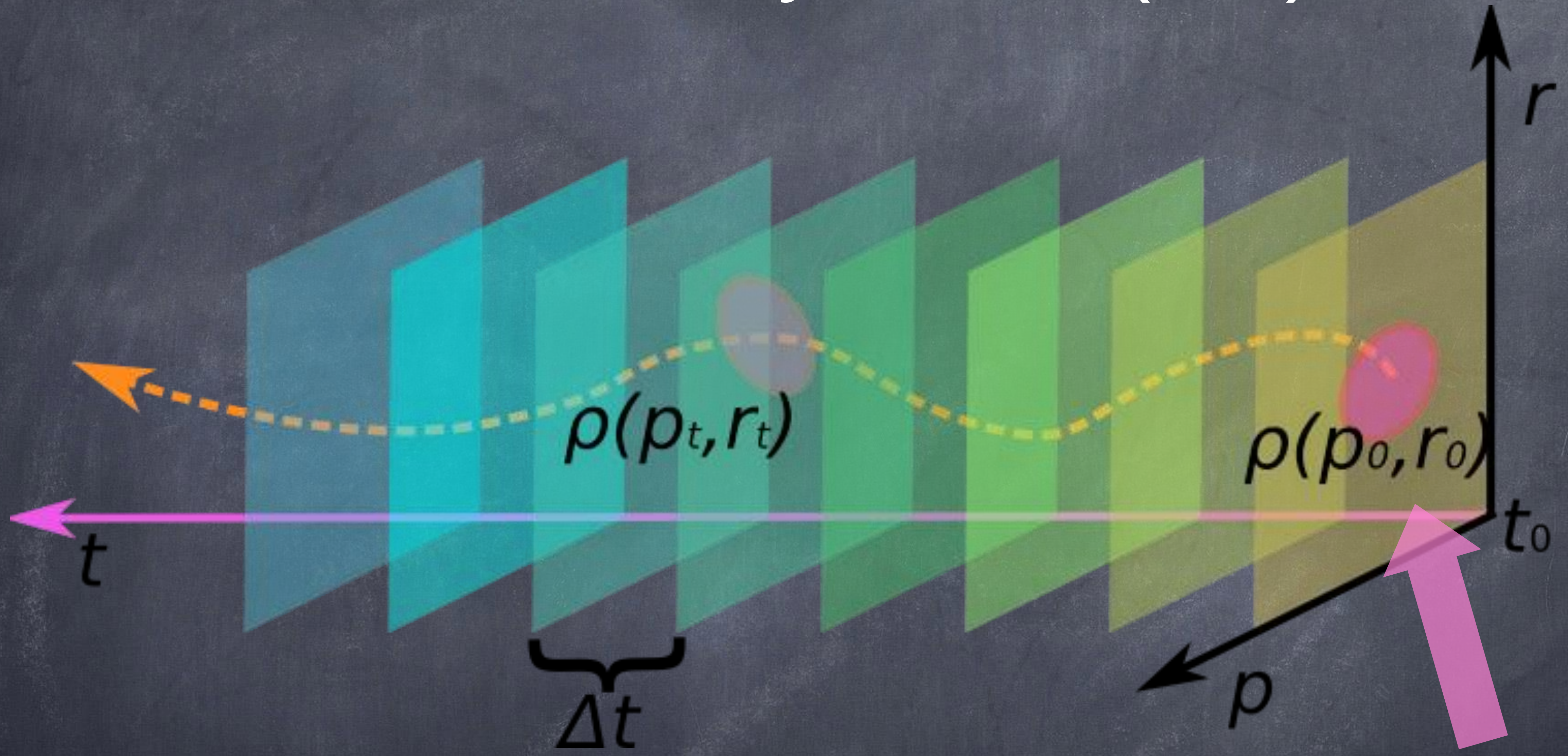

Initial configuration:
Specify positions and
velocitiy distribution
at temperature T.

Calculate forces on atoms and propagate in time

Fundamentals - Focus on nucleation

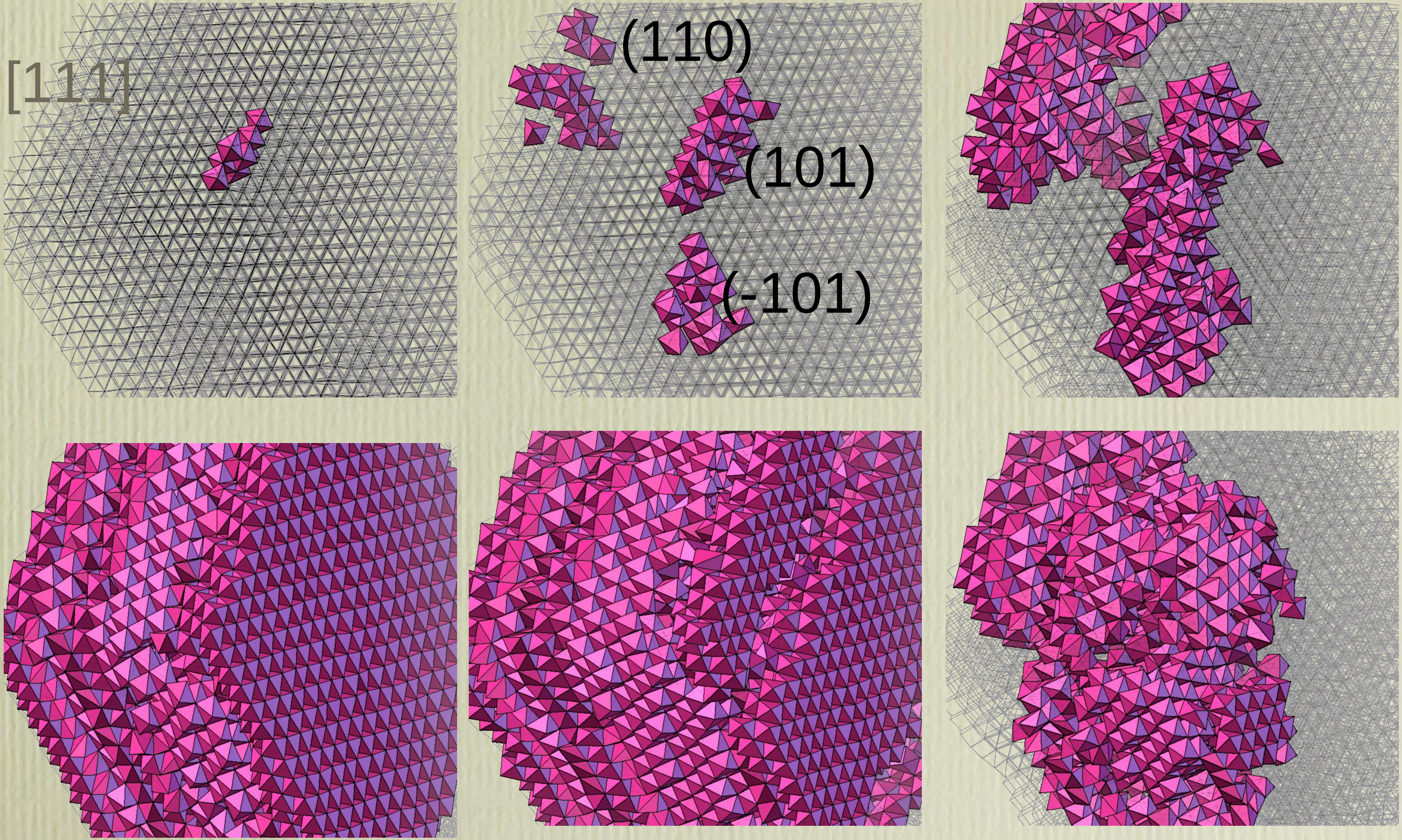

S. Leoni, R. Ramlau, K. Meier, M. Schmidt, U. Schwarz, PNAS 105, 19612 (2008)
S.Leoni, S. E. Boulfelfel, in “Modern Methods of Crystal Structure Predictions”, Wiley (2011)
S. Leoni, D. Selli, I. Baburin. D. Selli, Chemical Modelling Vol. 11, RCS Books (2015).
S. Jobbins, S.E. Boulfelfel, S. Leoni, Faraday Discussions (2019)

B1-B2 Phase Transition in PbSe

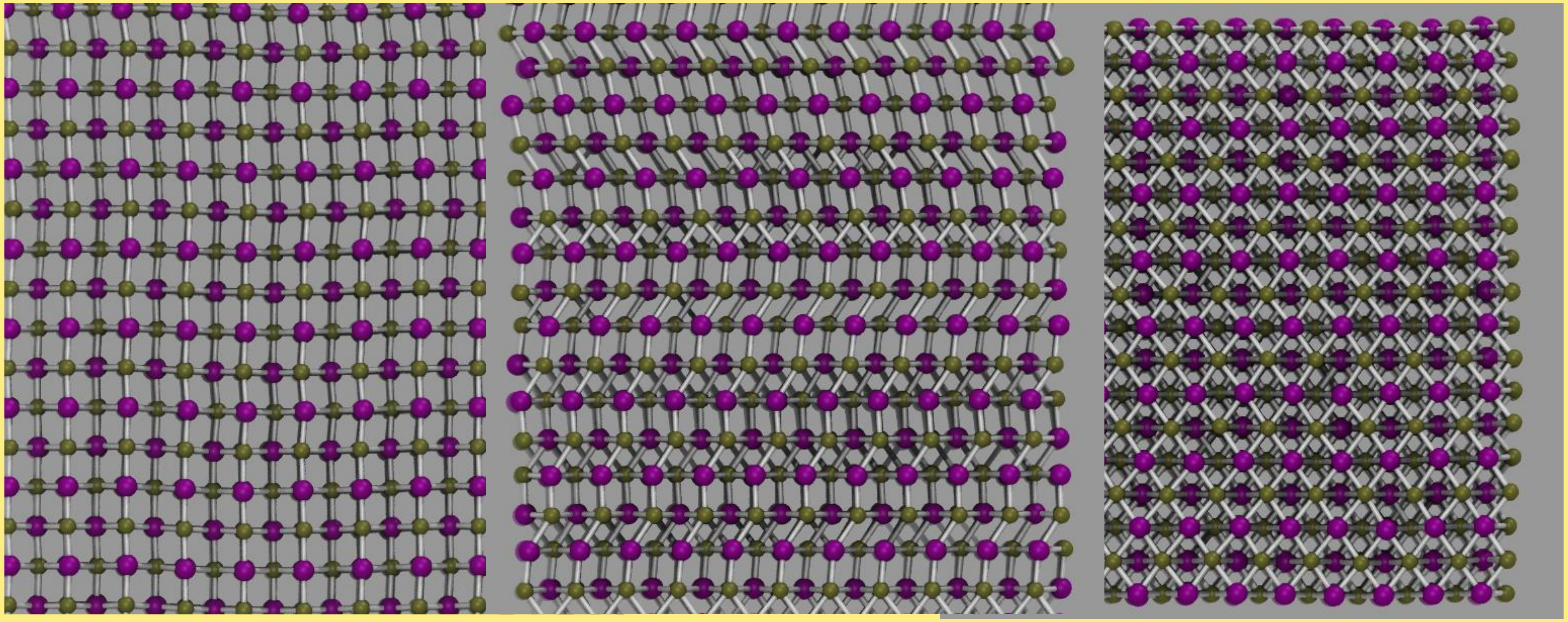

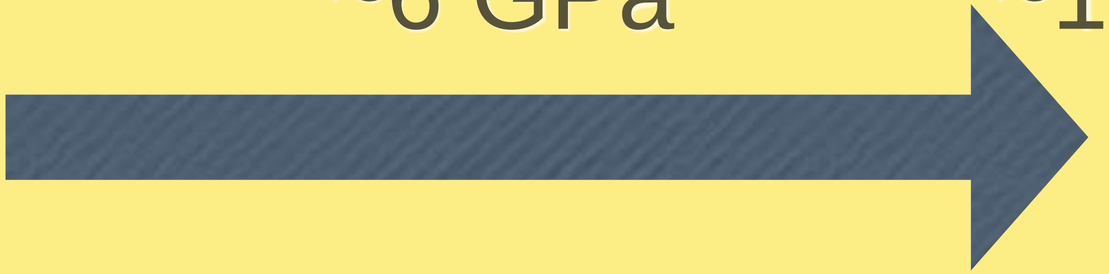

Intermediate (“B33”)

~6 GPa

~16 GPa

B1

B2

Pressure

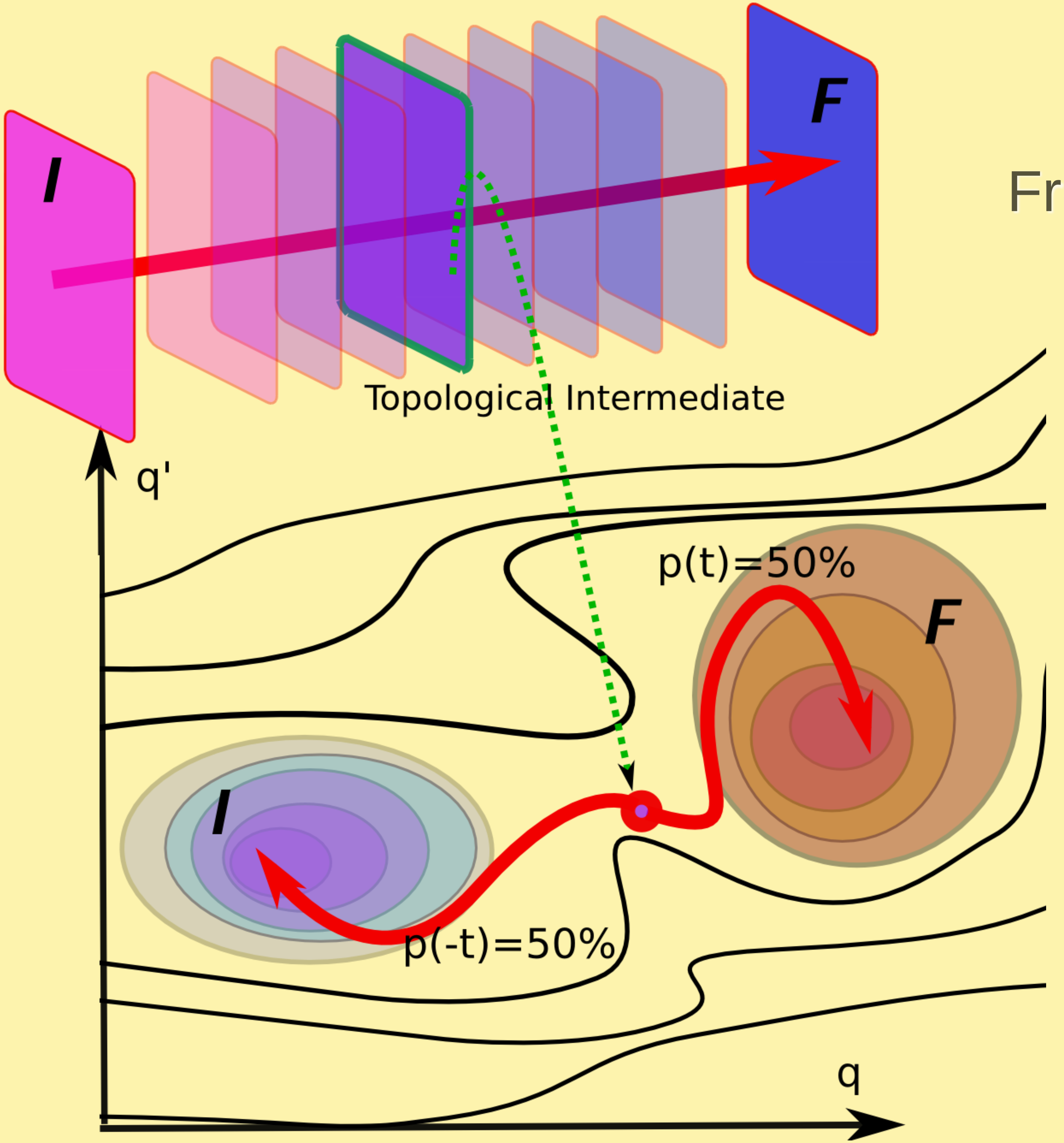

From a **Model**

To **MD**

A different picture: grains

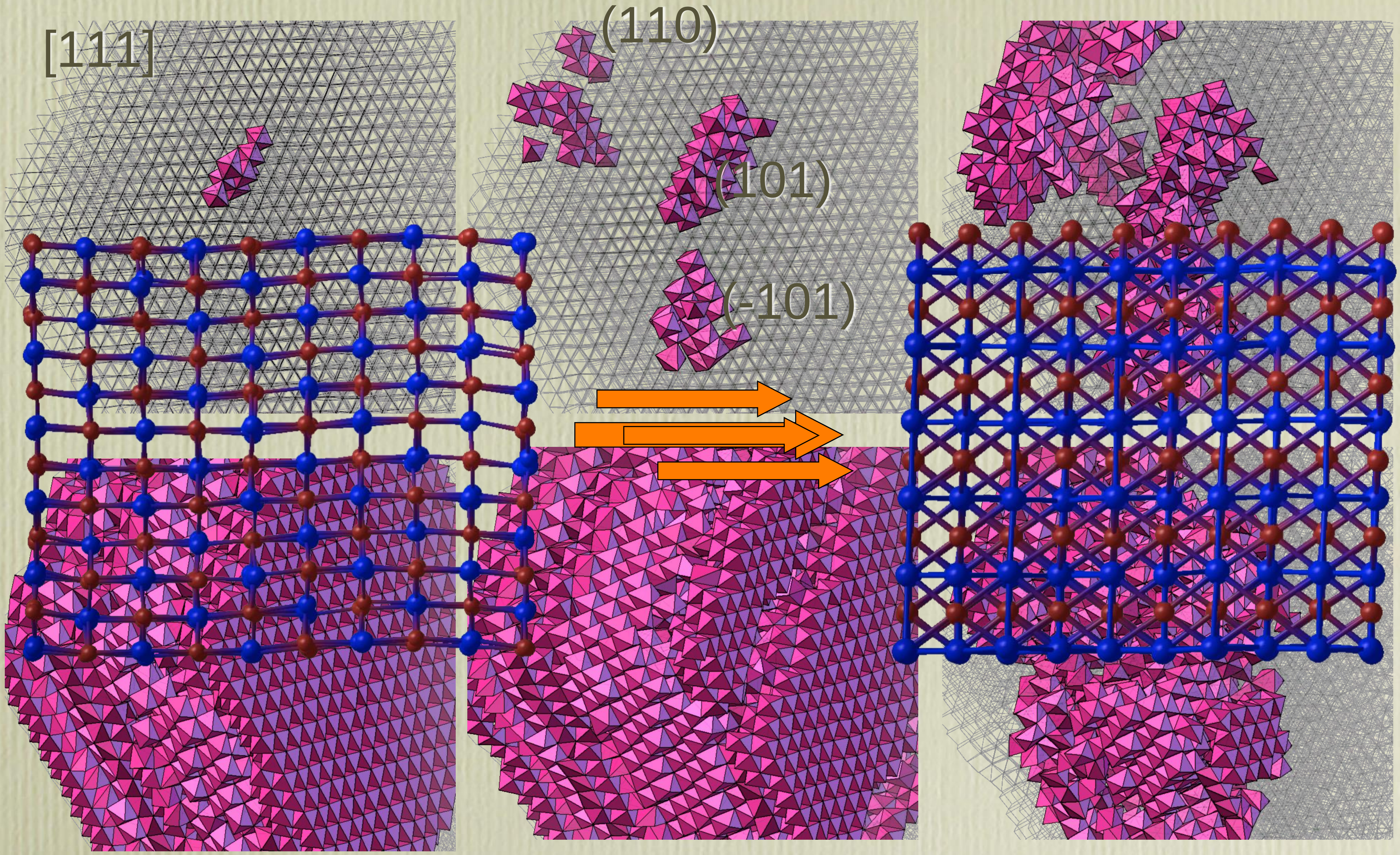

S. Leoni, R. Ramlau, K. Meier, M. Schmidt, U. Schwarz, PNAS 105, 19612 (2008)
S.Leoni, S. E. Boulfelfel, in “Modern Methods of Crystal Structure Predictions”, Wiley (2011)
S. Leoni, D. Selli, I. Baburin. D. Selli, Chemical Modelling Vol. 11, RCS Books (2015).
S. Jobbins, S.E. Boulfelfel, S. Leoni. Faraday Discussions (2019)

Obtaining Polycrystalline Materials

(ab initio)

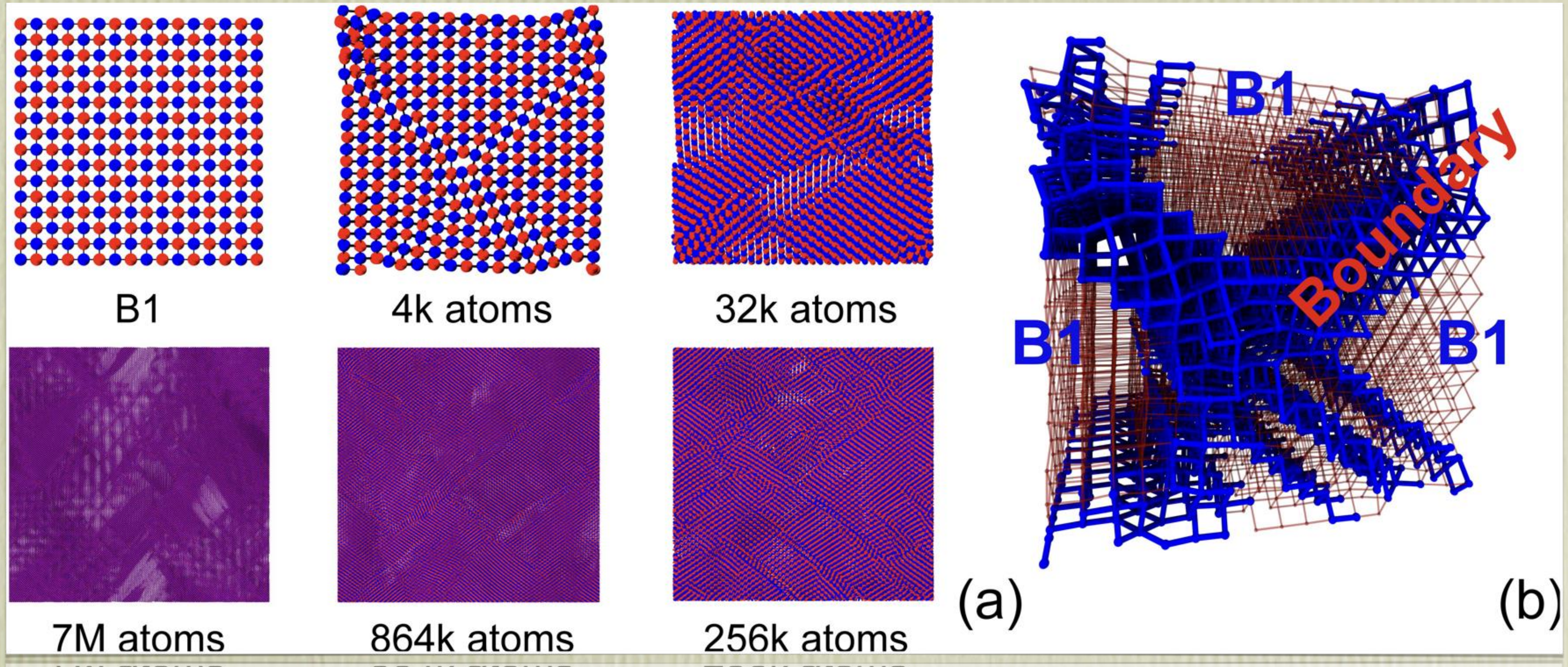

Computational protocol, which gives access to **features across length scales (!)**

D. Selli, S.E. Boulfelfel, P. Schapotschnikow, D. Donadio, S. Leoni, Nanoscale (2016)

PbSe: polycrystalline features

Grain Boundaries

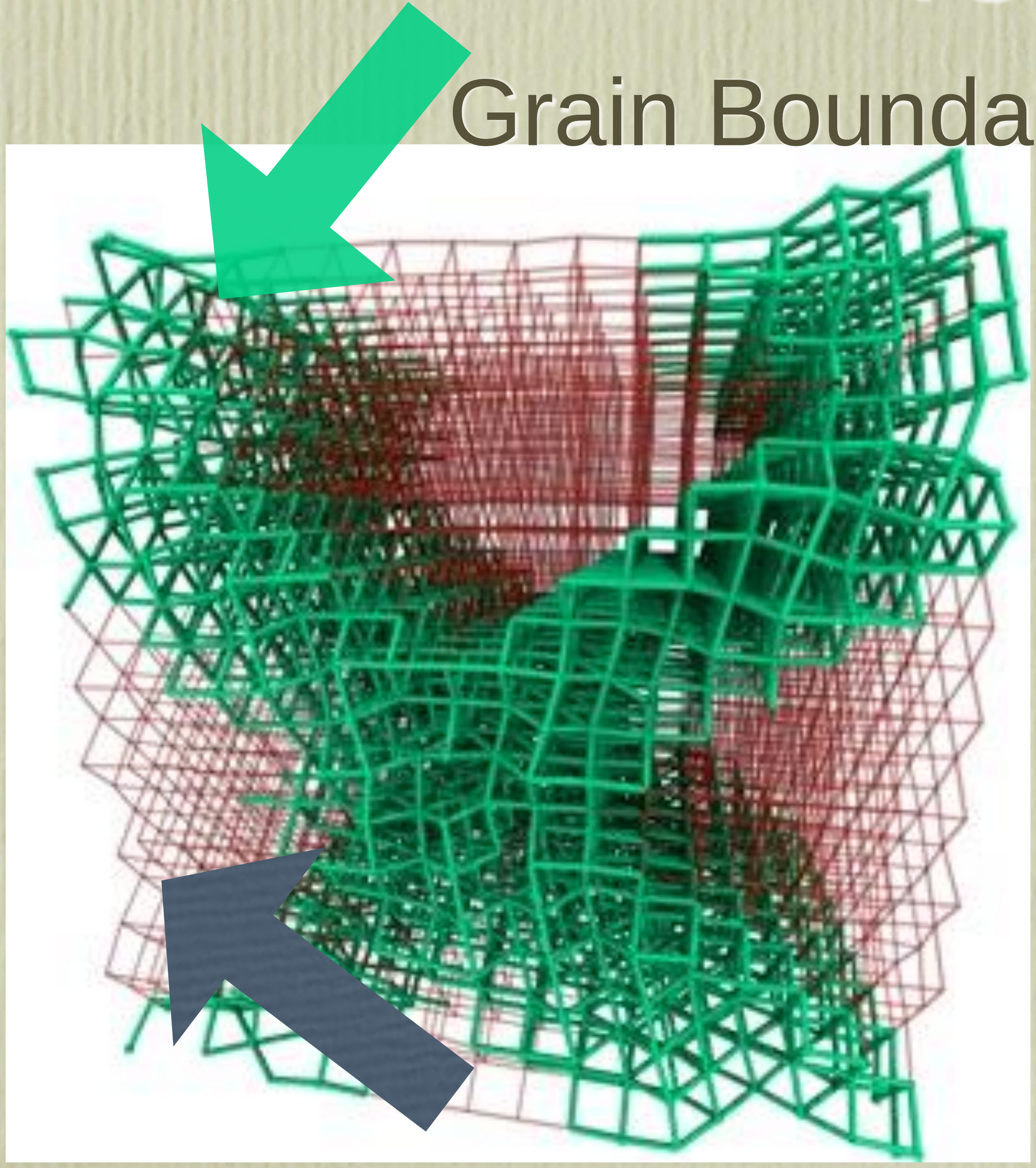

Grains: PbSe bulk

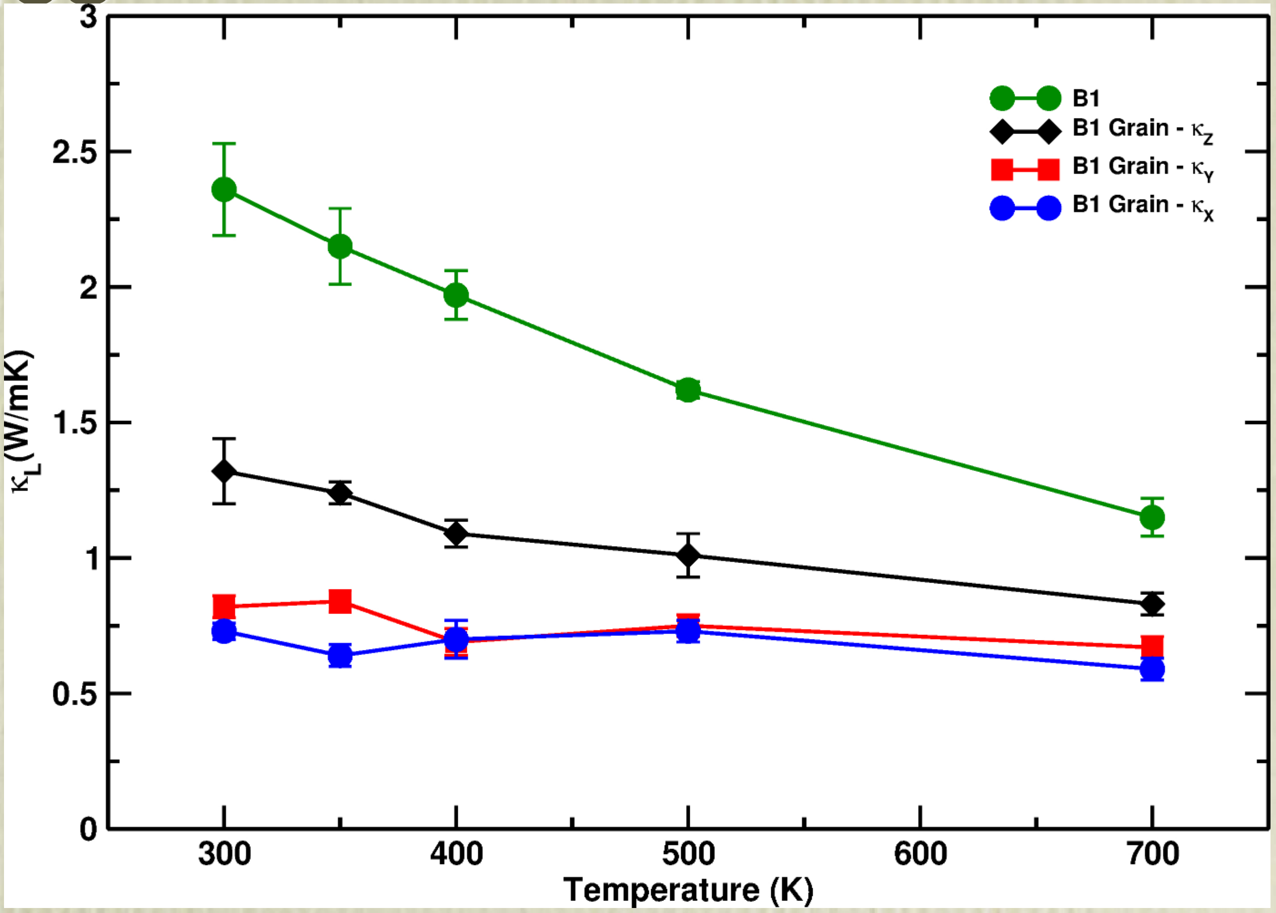

Selective lowering
of thermal conductivity

Thermal Transport

$$k_L = \frac{1}{3k_B T^2 V}\int_0^\infty \langle J(0)\cdot J(t)\rangle dt$$

Green-Kubo

$$J = \frac{1}{V}\left[\sum_i e_i \mathbf{v}_i + \frac{1}{2}\sum_{i<j}(\mathbf{f}_{ij}\cdot(\mathbf{v}_i + \mathbf{v}_j))\mathbf{x}_{ij}\right]$$

Heat Flux

EMD

Scalable Features - Grains

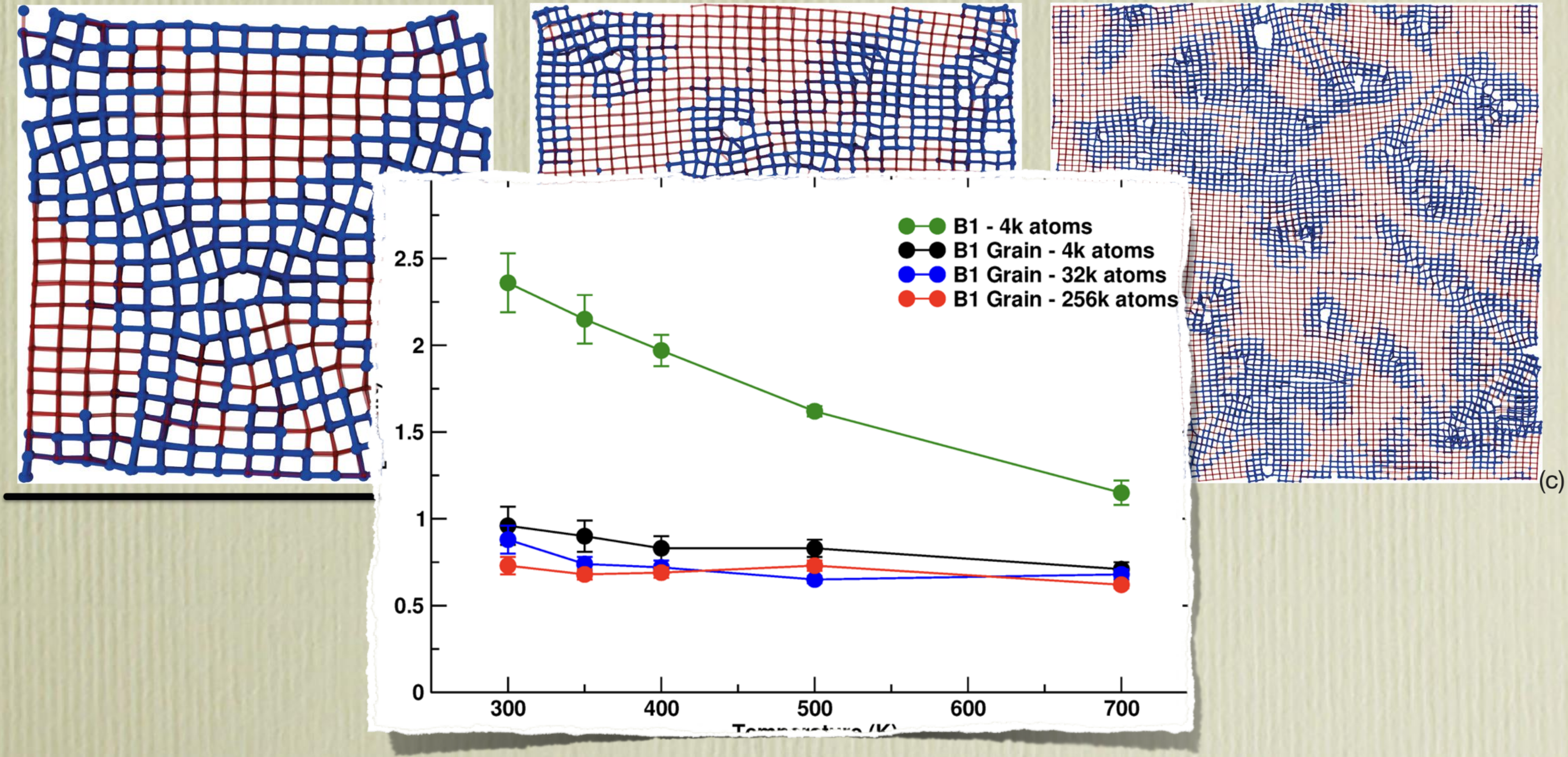

Phonon Scattering

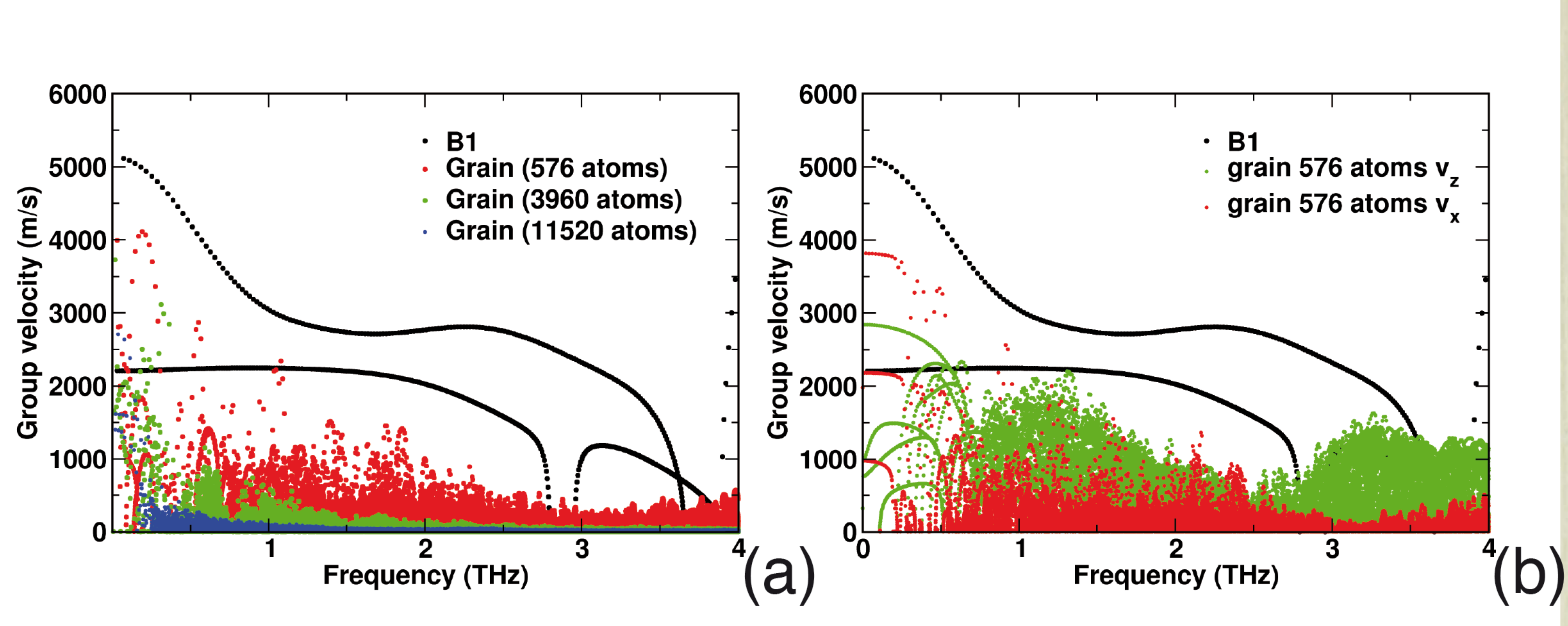

Phonon Scattering particularly efficient at lower frequencies - not possible on the nanoscale

D. Selli, S.E. Boulfelfel, P. Schapotschnikow, D. Donadio, S. Leoni, Nanoscale (2016)

Layered (2D) Materials

High Pressure Phases of Group V Elements

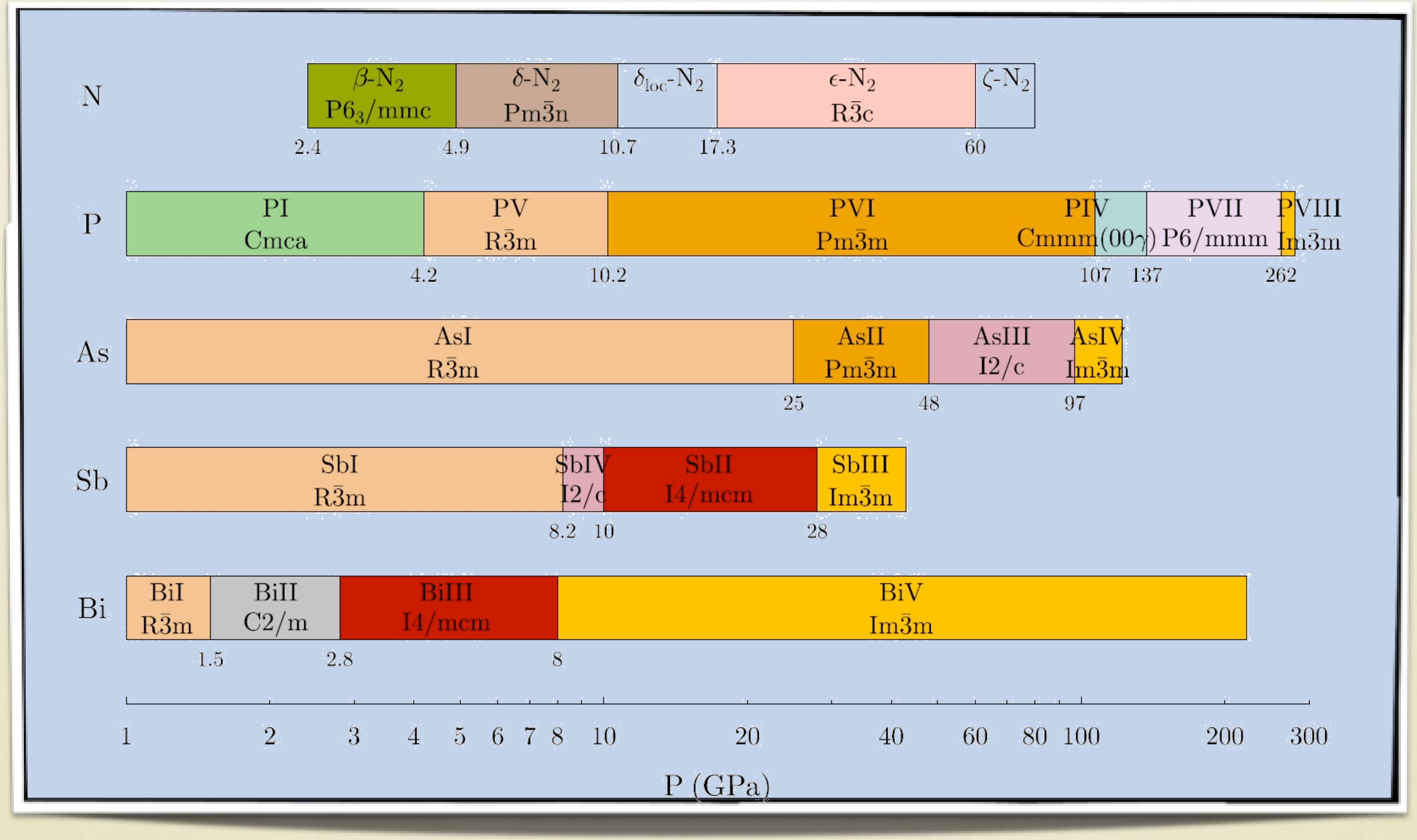

H. Katzke and P. Tolédano PRB 77, 024109 (2008)

Polymorphism of Phosphorus

Black P

α-As

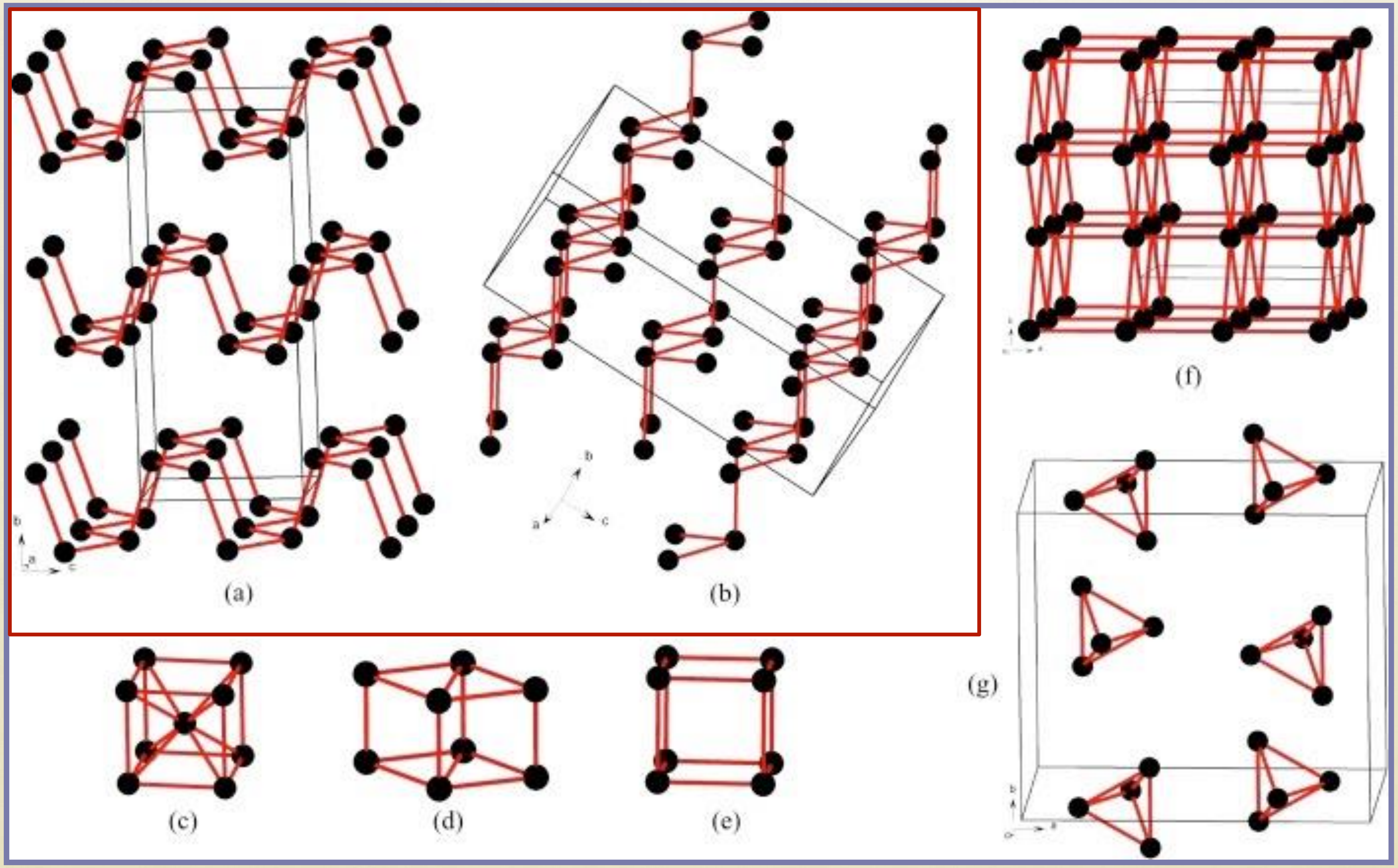

Resistivity under pressure

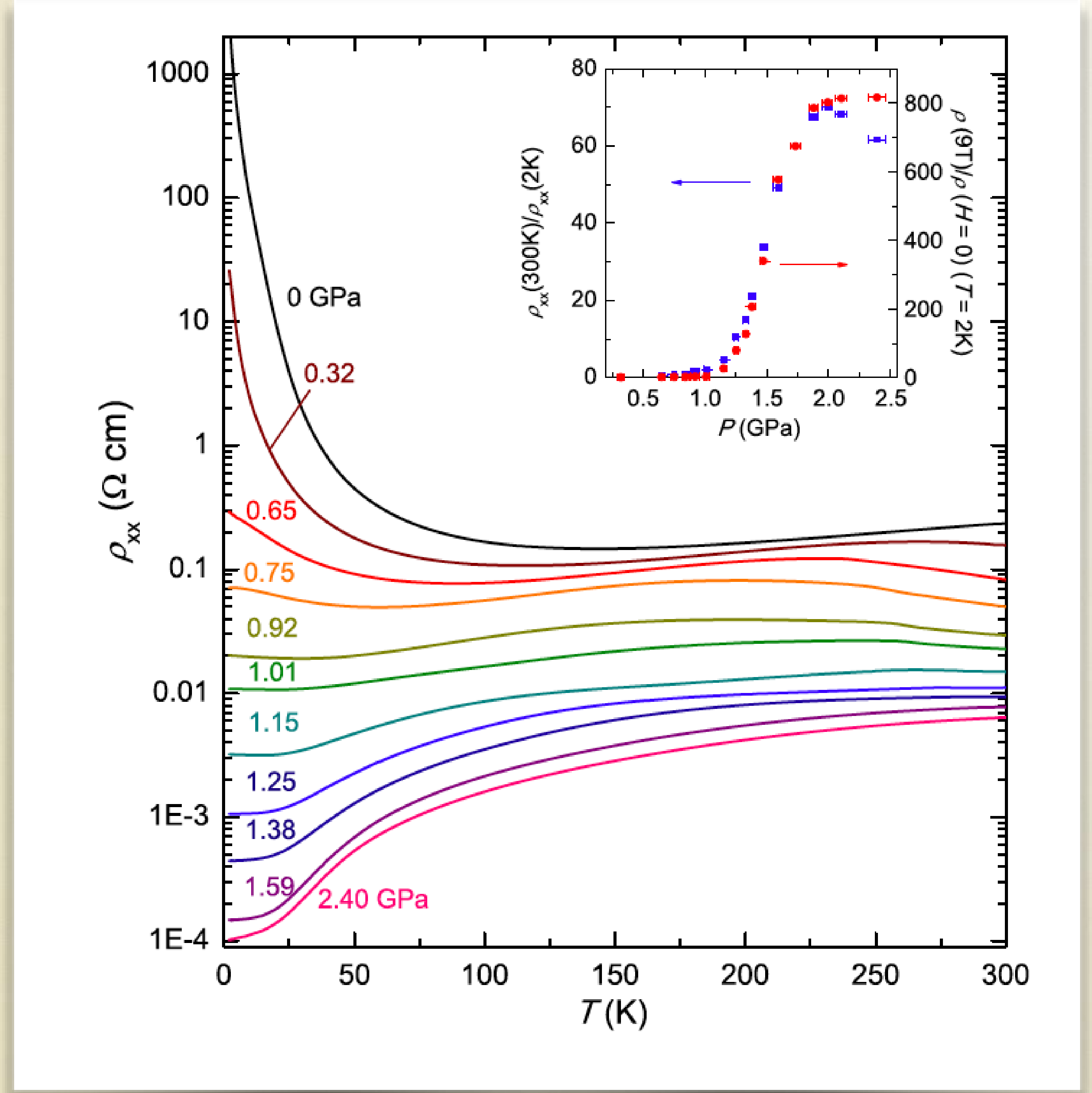

Longitudinal resistivity versus pressure for BP

Evolution into a semimetal (topological electronic phase transition)

ZJ Xiang *et al.*, PRL 115 186403 (2015)

DFTB

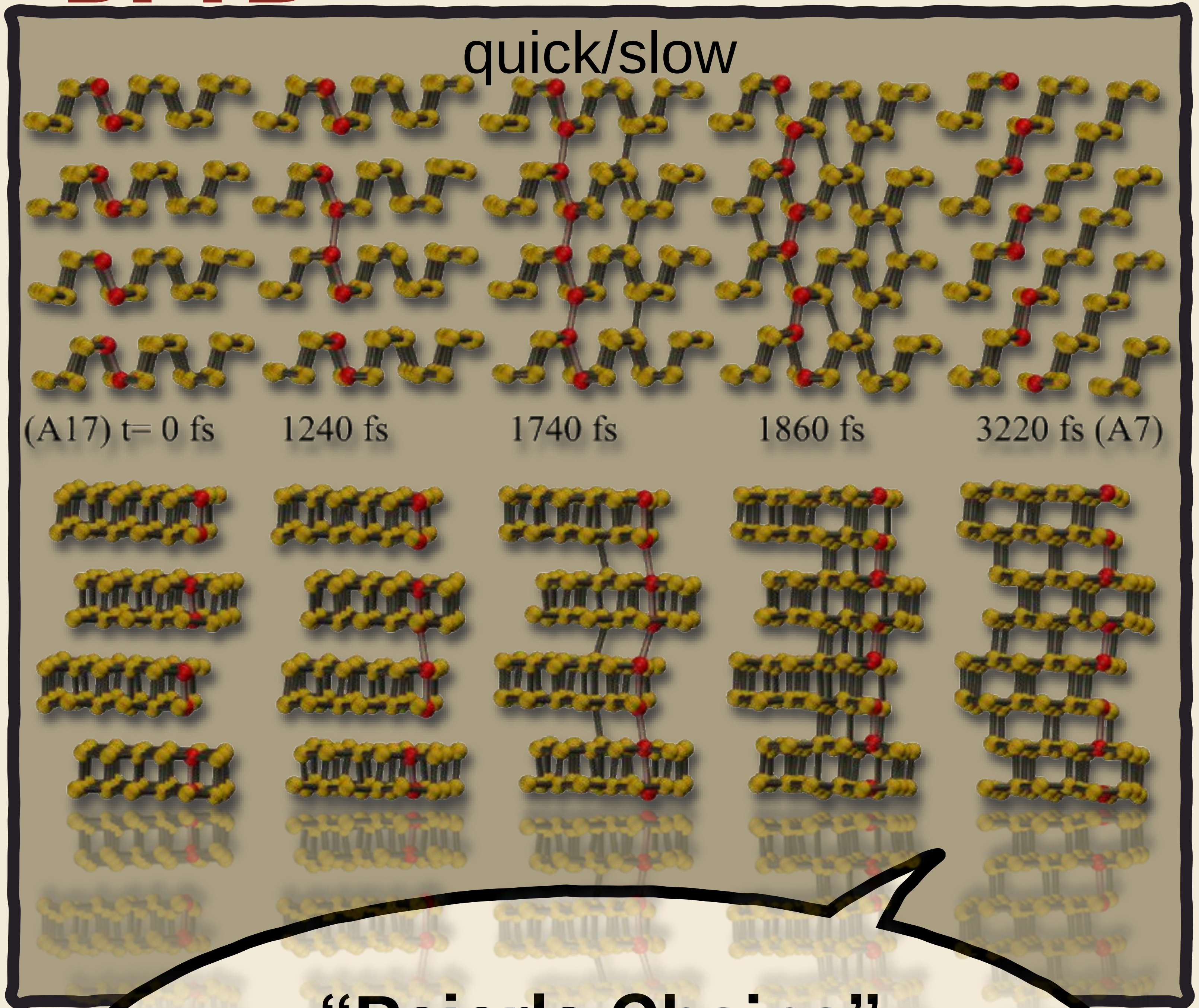

“Peierls Chains”
Bond-Density-Wave
(BDW)

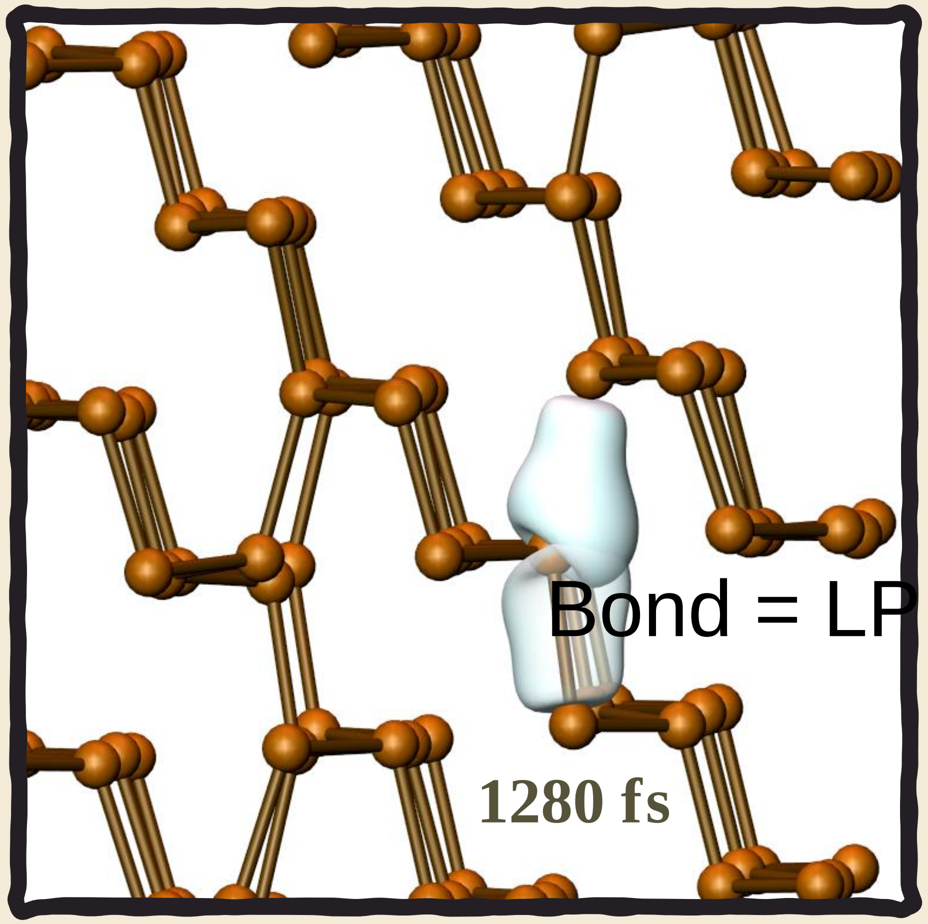

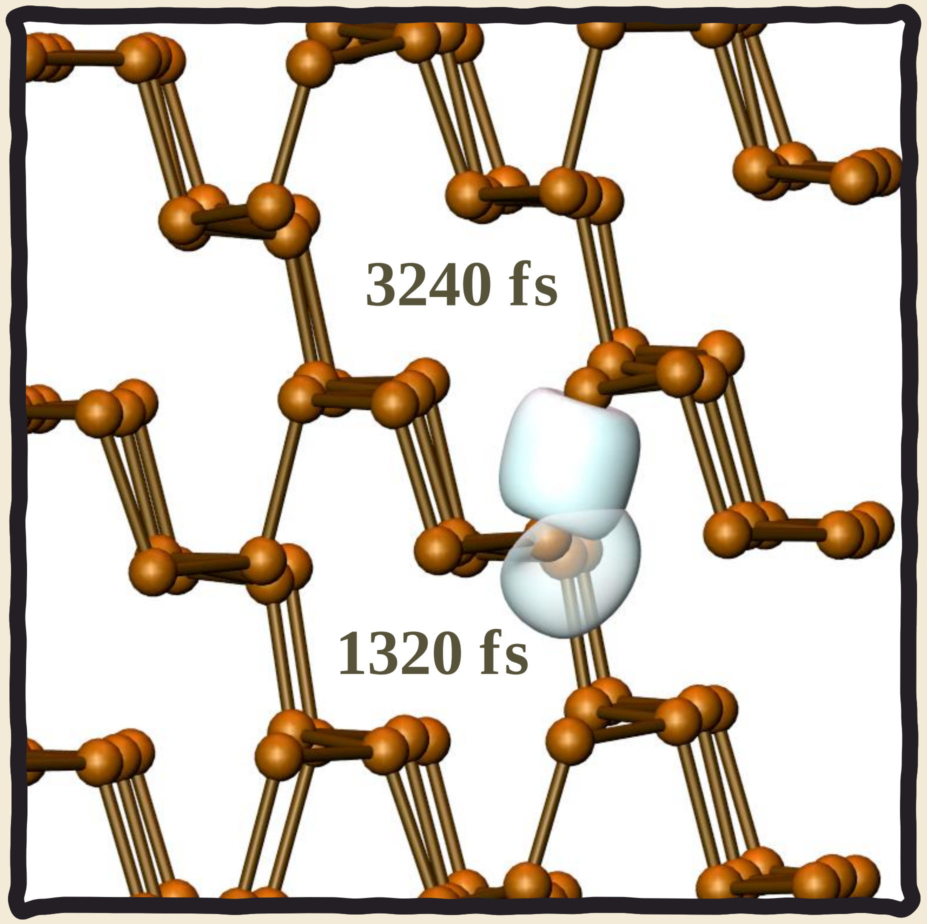

S.E. Boulfelfel, G. Seifert, Yu. Grin, S. Leoni, Phys. Rev B 85, 014110 (2012)

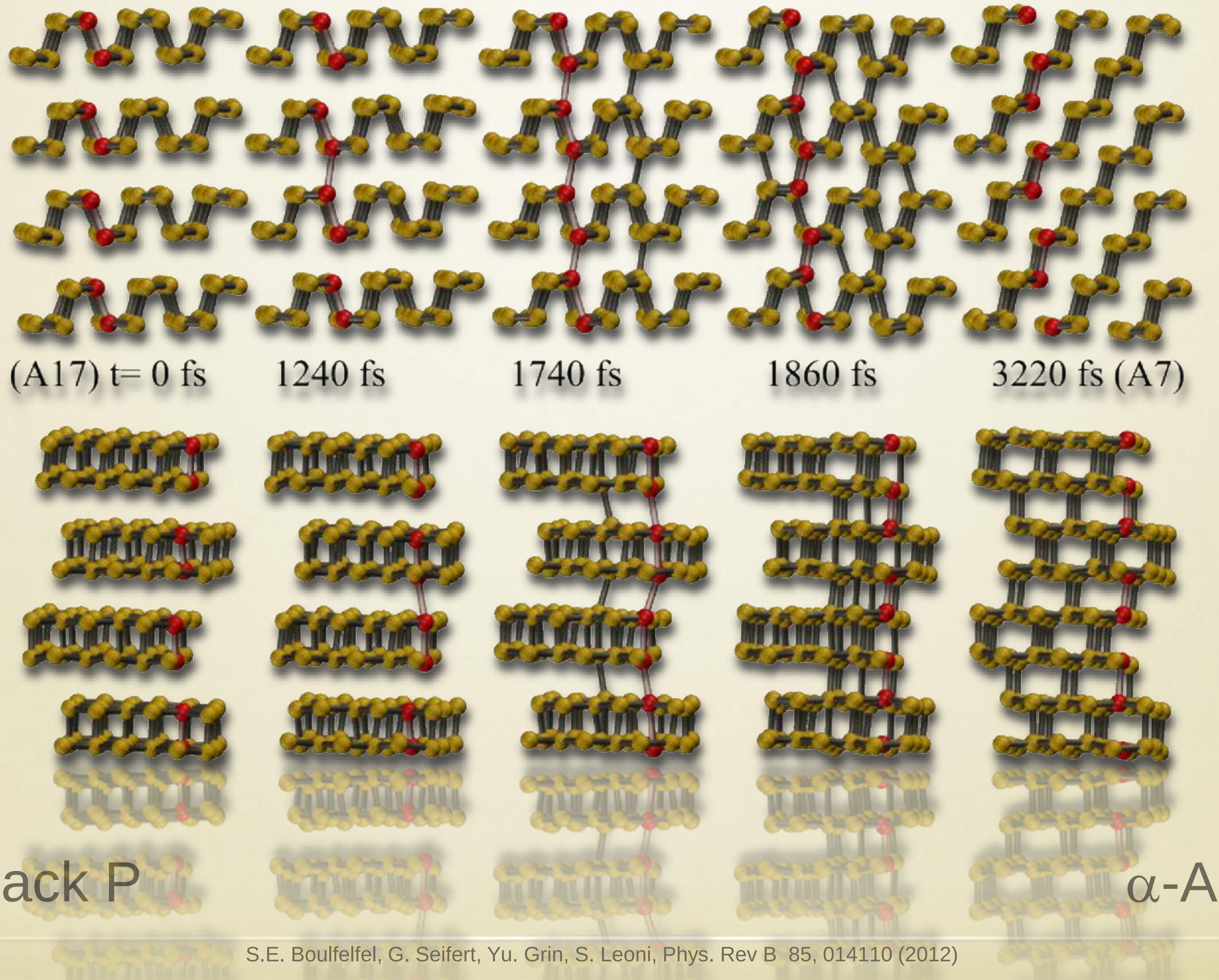

Black P

α-As

S.E. Boulfelfel, G. Seifert, Yu. Grin, S. Leoni, Phys. Rev B 85, 014110 (2012)

Localized „Orbitals“ (MLWF)

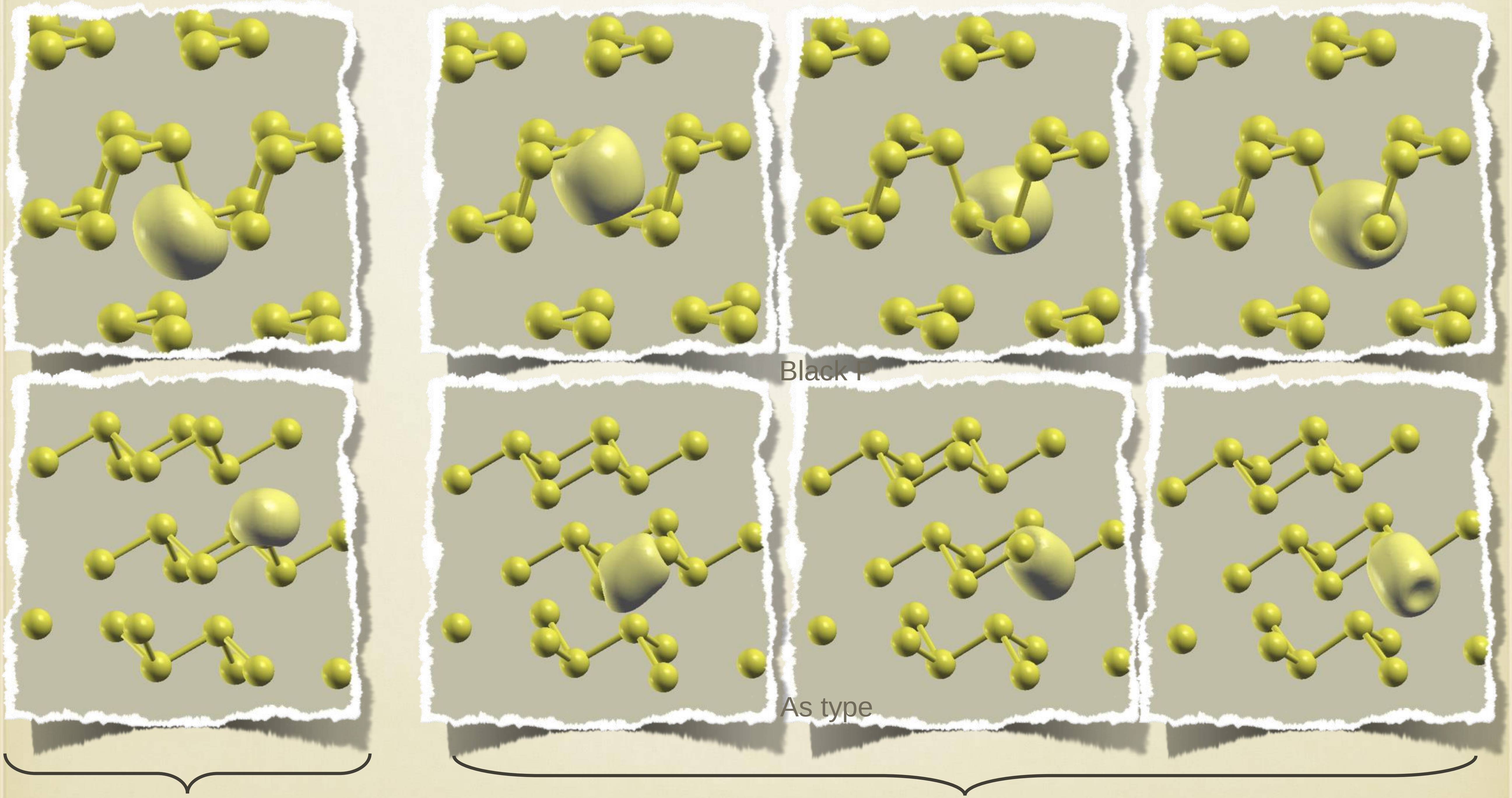

Structural variety & anisotropy

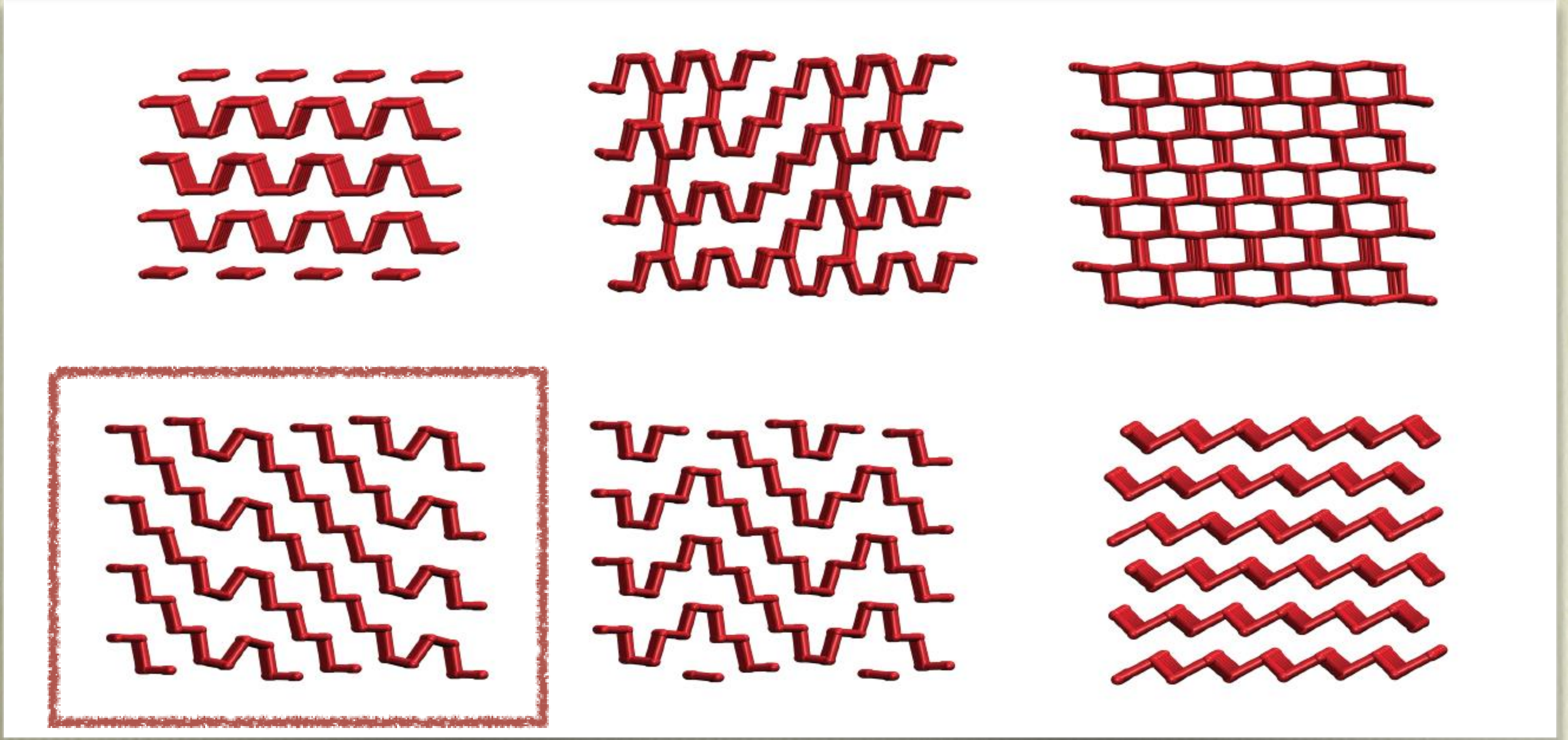

Co-existing structural features under pressure
(intermediate from TPS)

Transport Equations

$$[\boldsymbol{\sigma}]_{ij}(\mu, T) = e^2 \int_{-\infty}^{+\infty} dE \left(-\frac{\partial f(E, \mu, T)}{\partial E} \right) \Sigma_{ij}(E),$$

$$[\boldsymbol{\sigma}\mathbf{S}]_{ij}(\mu, T) = \frac{e}{T} \int_{-\infty}^{+\infty} dE \left(-\frac{\partial f(E, \mu, T)}{\partial E} \right) (E - \mu) \Sigma_{ij}(E),$$

$$[\mathbf{K}]_{ij}(\mu, T) = \frac{1}{T} \int_{-\infty}^{+\infty} dE \left(-\frac{\partial f(E, \mu, T)}{\partial E} \right) (E - \mu)^2 \Sigma_{ij}(E).$$

$$\Sigma_{ij}(E) = \frac{1}{V} \sum_{n,\mathbf{k}} v_i(n, \mathbf{k}) v_j(n, \mathbf{k}) \tau_{n\mathbf{k}} \delta(E - E_{n,\mathbf{k}}),$$

G. Pizzi et al., Computer Physics Communications 185, 422 (2014)

Resistivity as a function of “pressure” (Hubbard U)

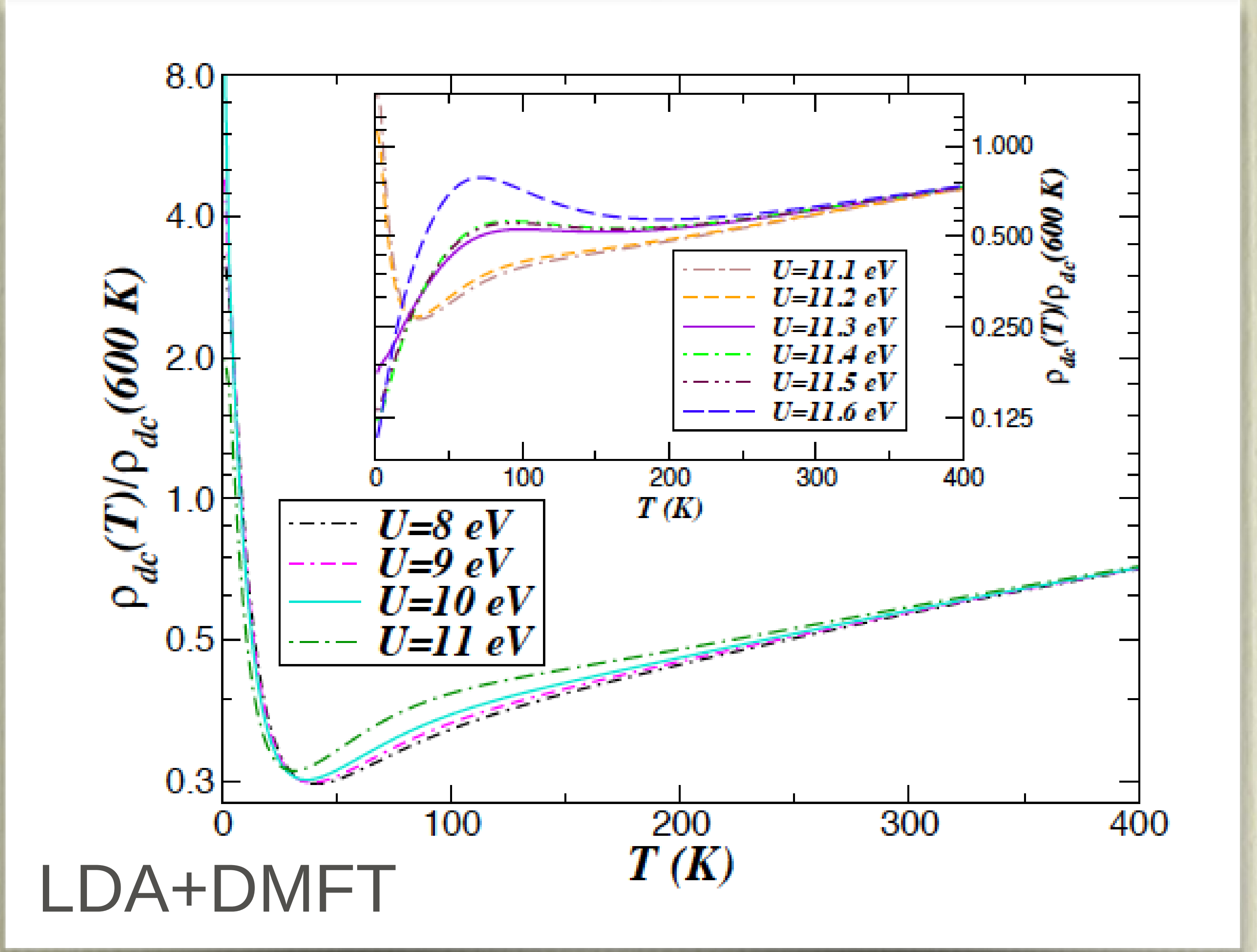

LDA+DMFT

L. Craco, S. Leoni, PRB (2017) 96, 075118

Figure of Merit ZT

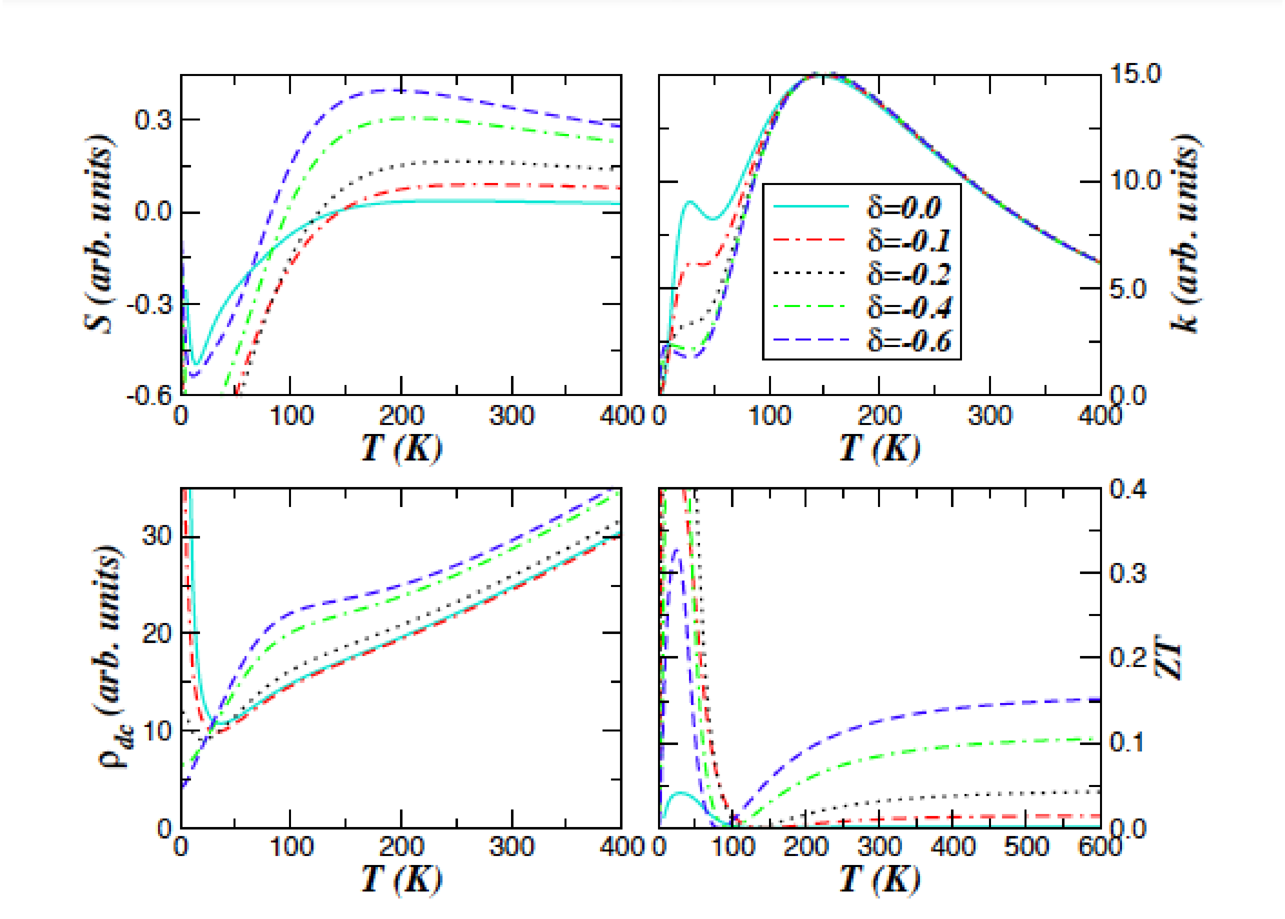

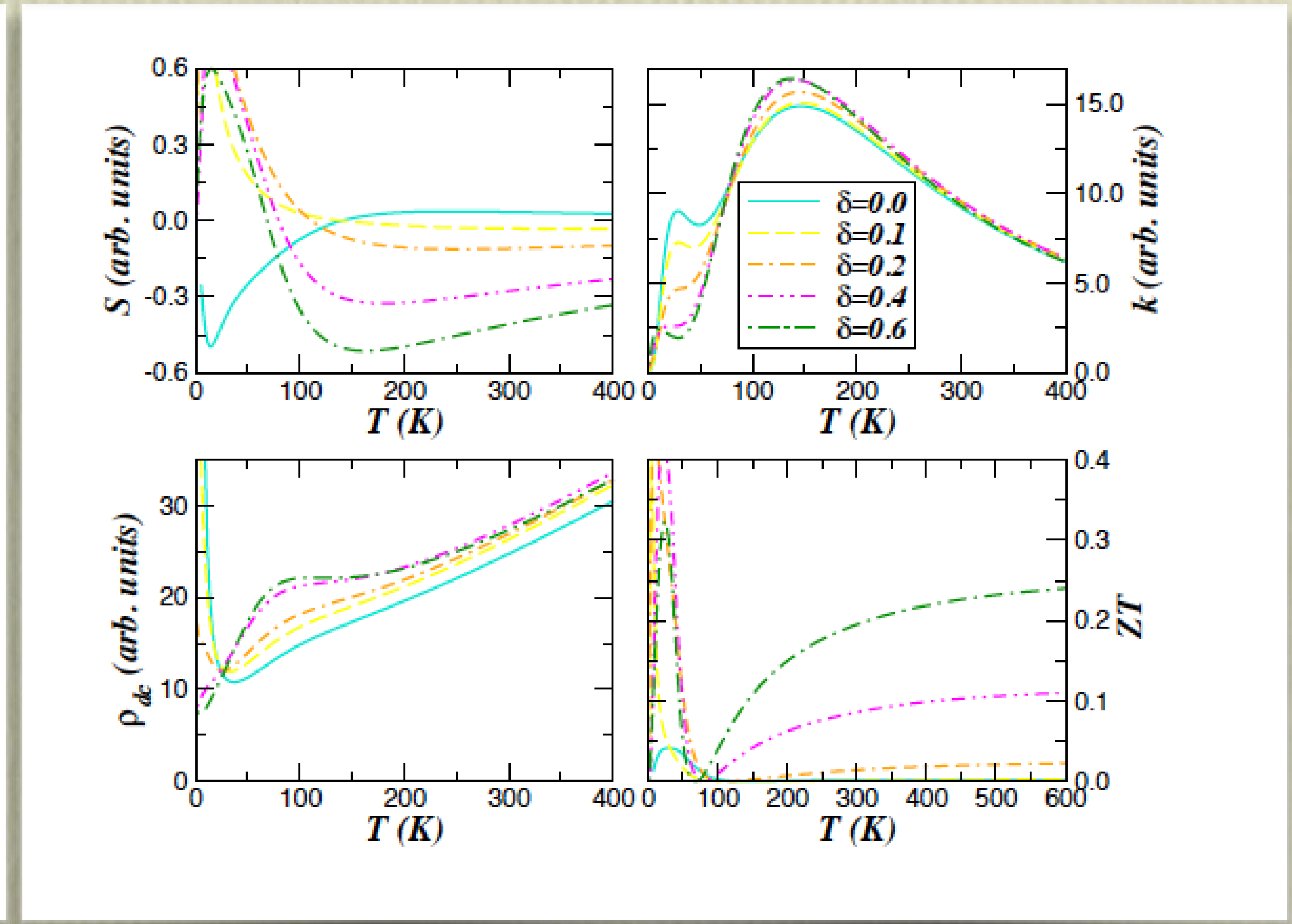

n-type p-type

L. Craco, S. Leoni, PRB (2017) 96, 075118

Pronounced Anisotropy

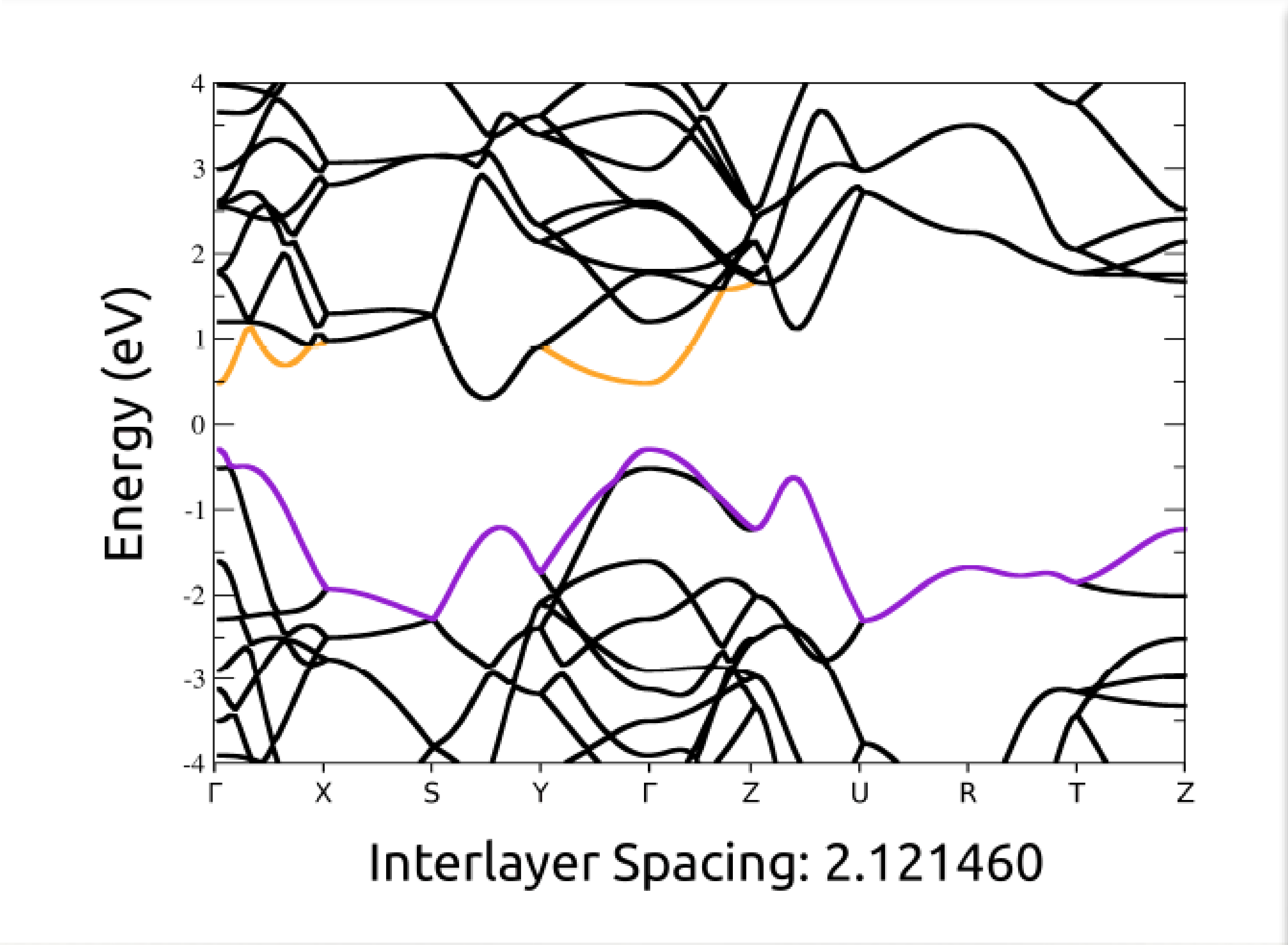

Interlayer Spacing: 2.121460

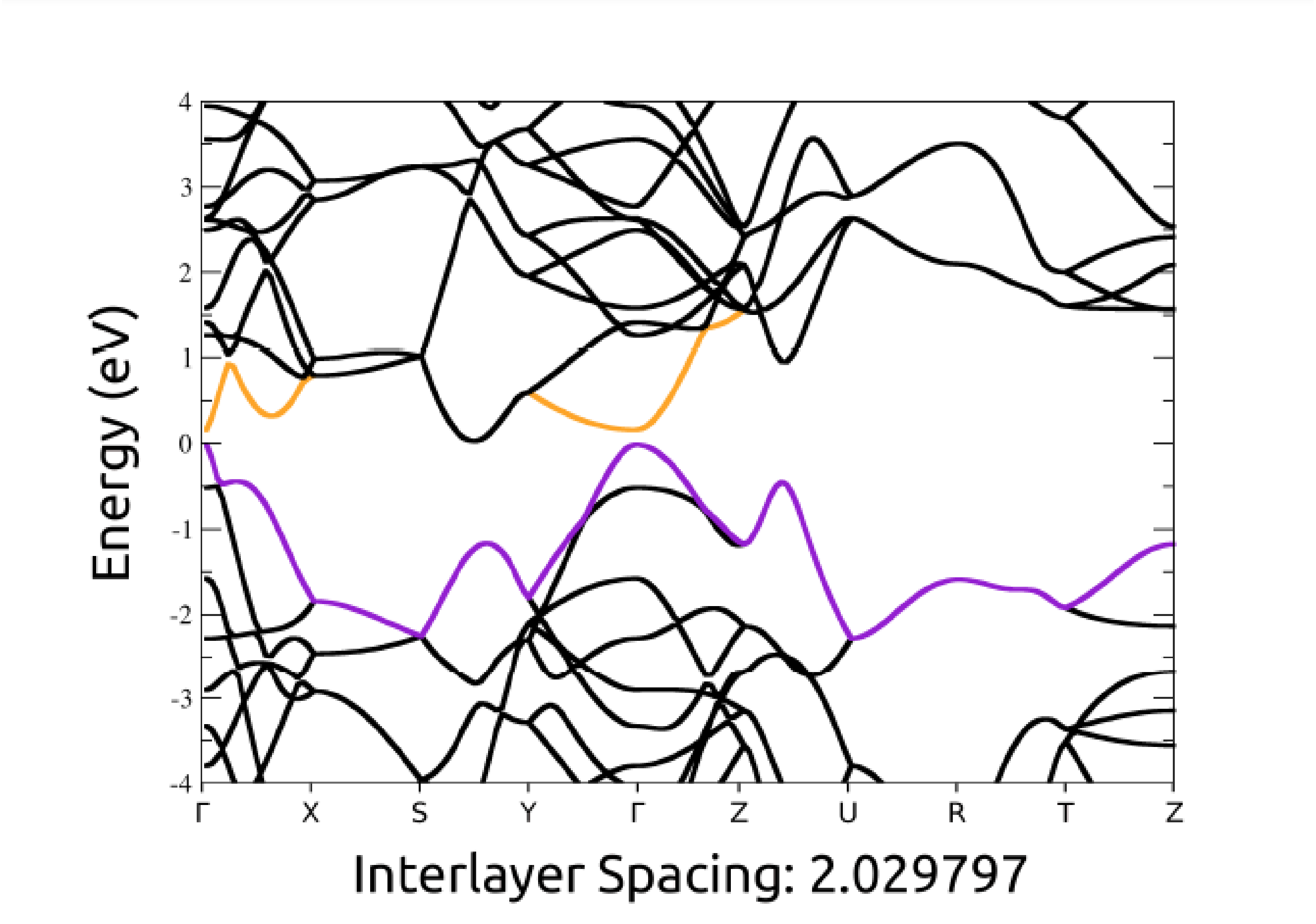

Interlayer Spacing: 2.029797

DFTB - band gap responds to compression/band kissing

D. Hardie, S. Leoni, unpublished

Structural variety & anisotropy

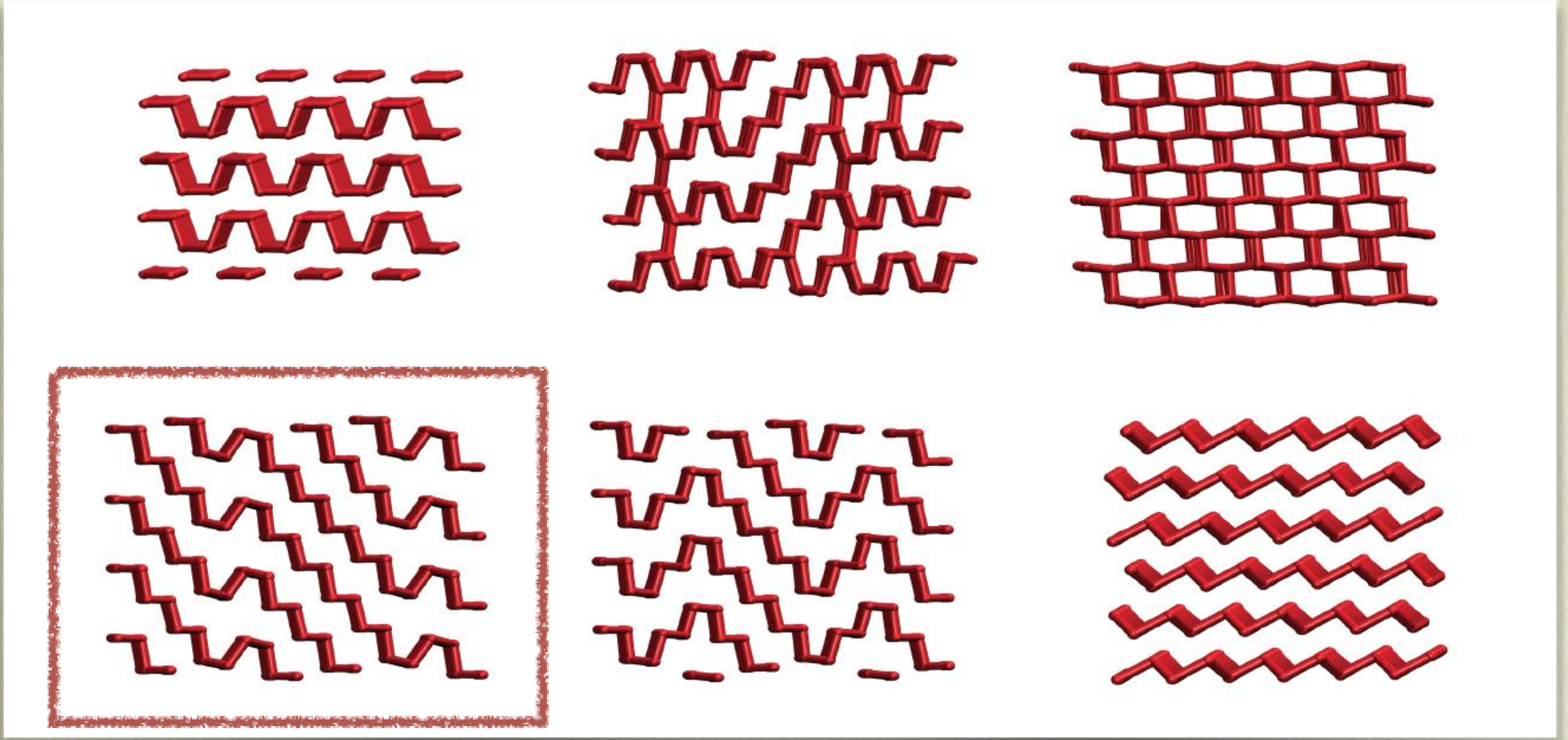

Co-existing structural features under pressure (intermediate from TPS)

Landauer-Büttiker

- Evaluate transmission as key quantity.

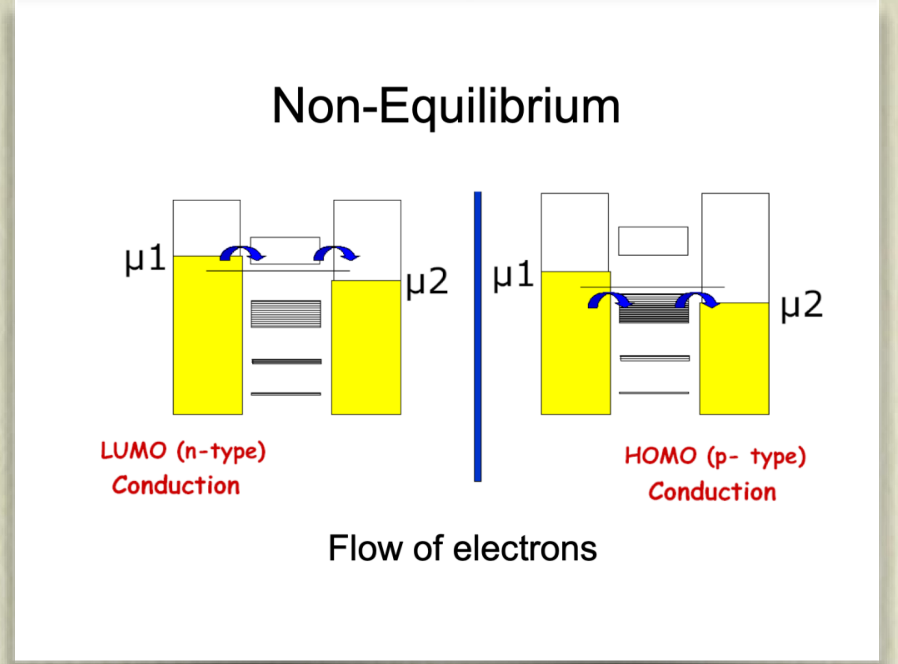

$$I = -\frac{2q}{h}\int_0^\infty d\varepsilon_k[f_0(\varepsilon_k - \mu_1) - f_0(\varepsilon_k - \mu_2)] = -\frac{2q}{h}T(E)[\mu_1 - \mu_2]$$

$$K_n = \frac{2}{h}\int dE\, T(E)\left(-\frac{\delta f}{\delta E}\right)(E-\mu)^n$$

T = Transmission!

$$\sigma = q^2 K_0$$

$$S = \frac{K_1}{qTK_0}$$

$$k_e = \frac{K_2 - \frac{K_1^2}{K_0}}{T}$$

Impact on Seebeck

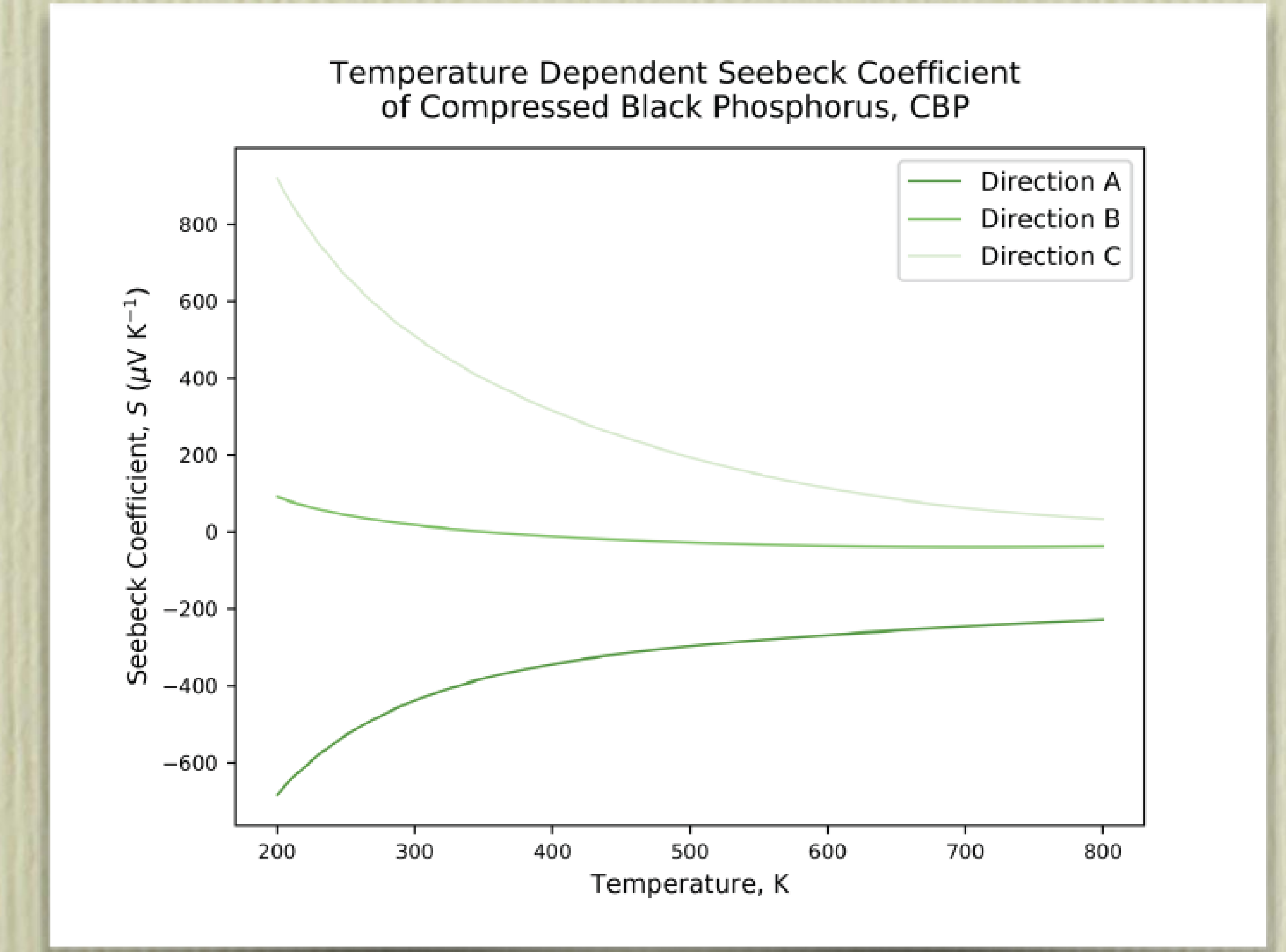

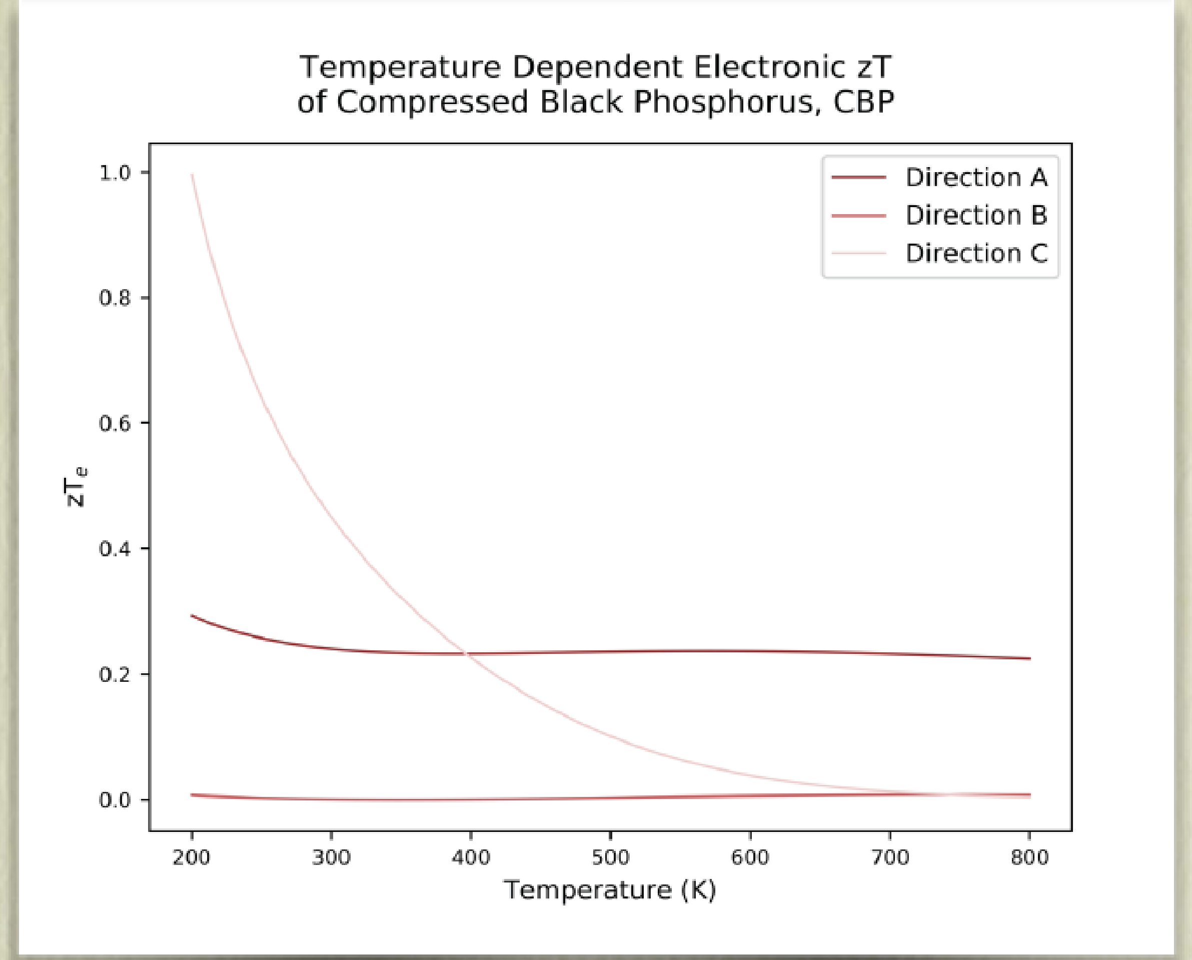

NEGF-DFTB

Co-existing p and n channels

Impact on Seebeck/ZT

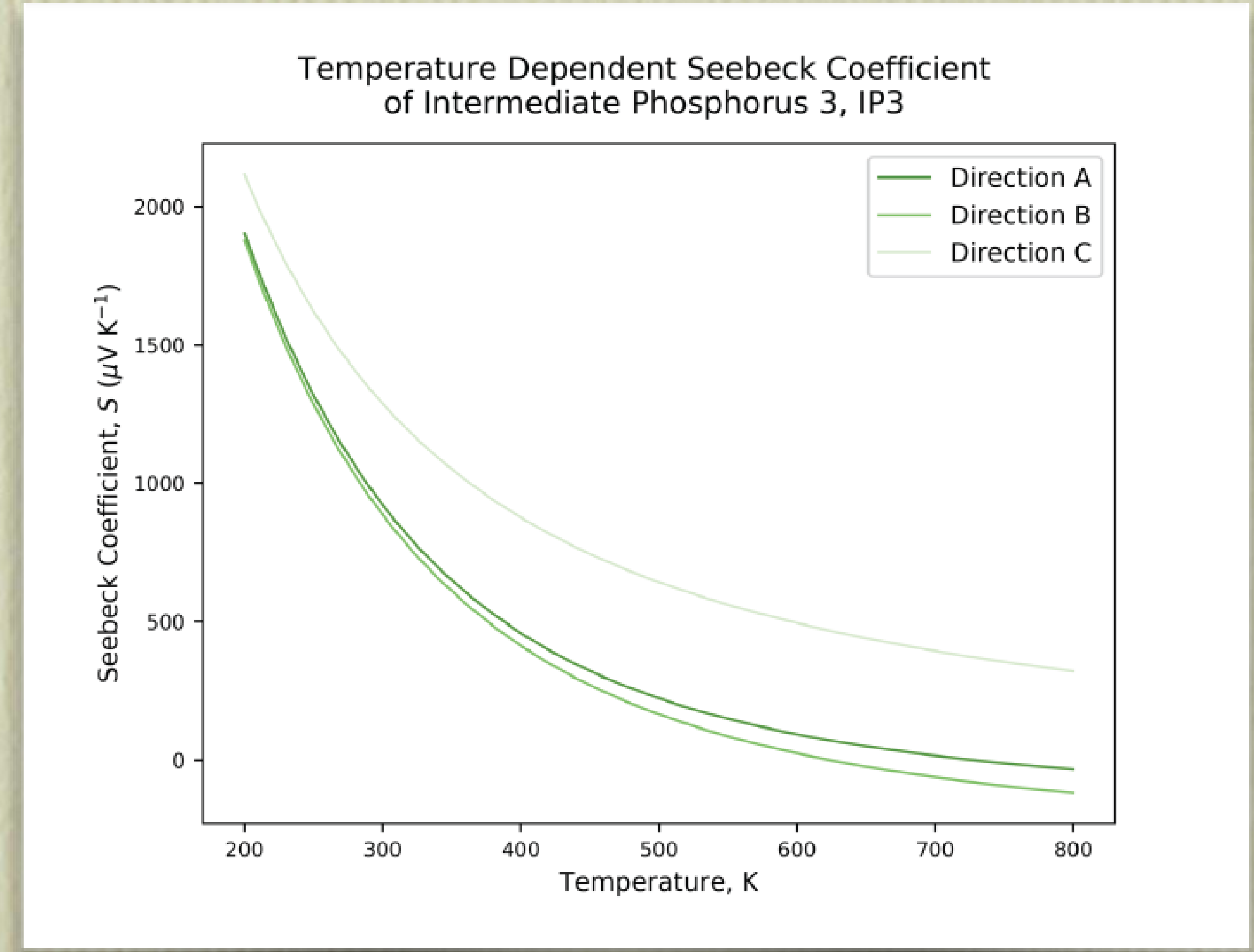
Temperature Dependent Seebeck Coefficient of Intermediate Phosphorus 3, IP3

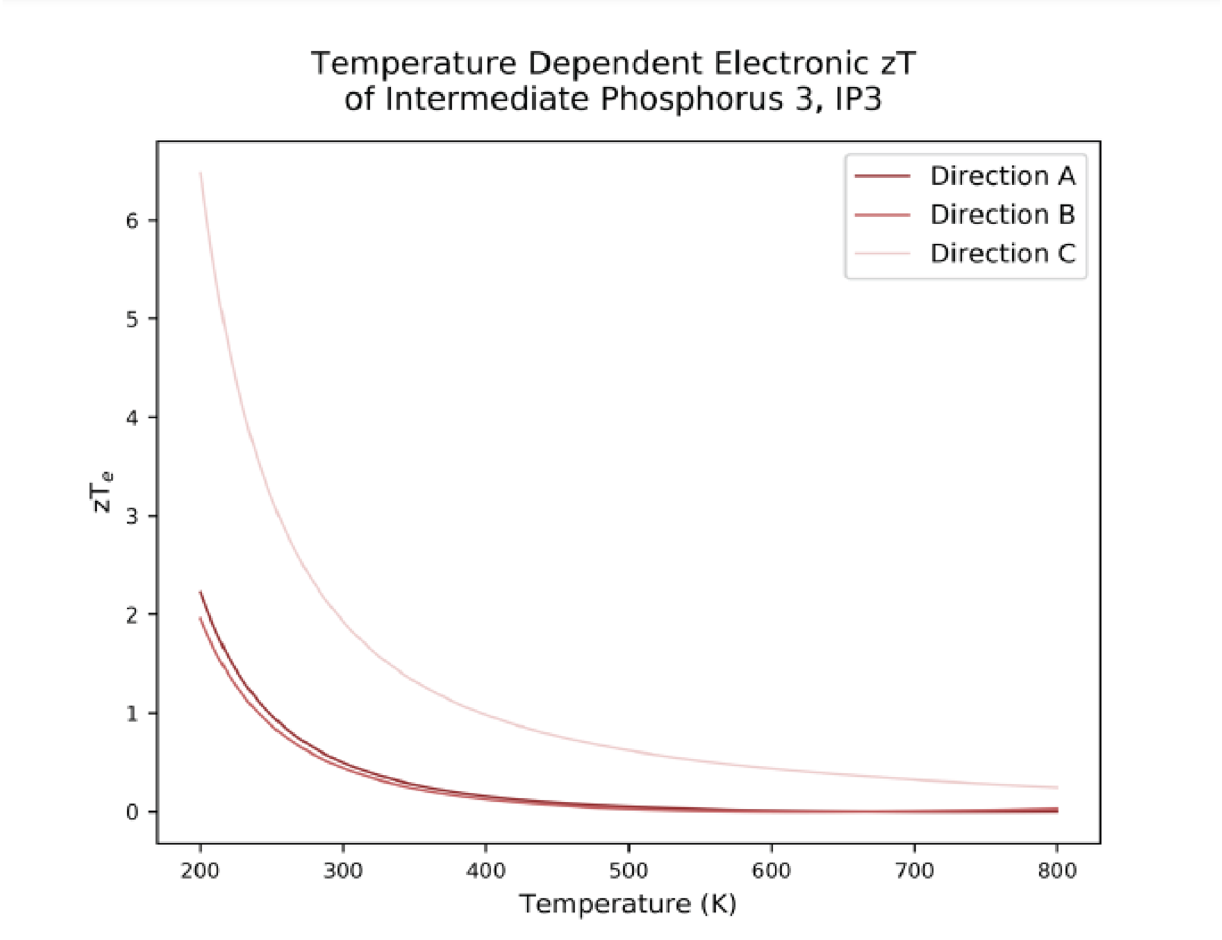
Temperature Dependent Electronic zT of Intermediate Phosphorus 3, IP3

Increase in Seebeck & ZT (electronic)

Less anisotropic under pressure

Strategies for competitive thermoelectric materials

SnS – case study

Stefano Leoni
Cardiff University

Motivation

- What makes a better thermoelectric materials?
- SnS 2D/ layered structure (and related IV-VI materials)
- Full characterisation (el, ph)
- Approaches to reduce ph heat transport
  - based on structural concepts
  - implementable as manufactory steps

Maximally Localized Wannier Functions

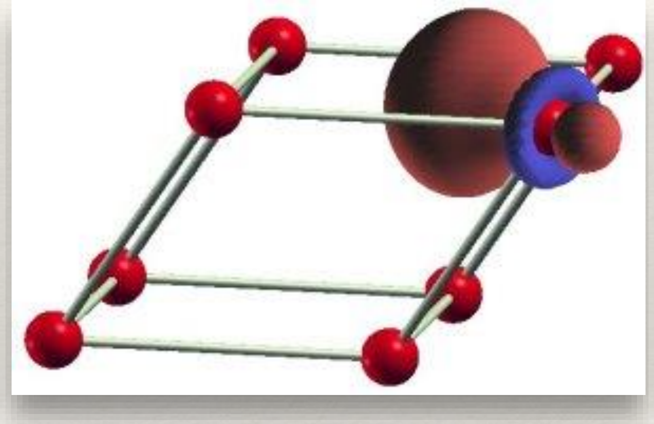

Fe (sp^3d^2)

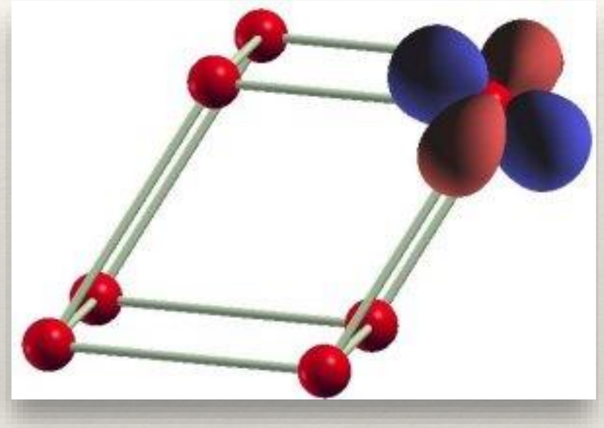

Fe (d_{xy})

- MLWF: defined in terms of a unitary transformation of occupied Bloch functions

$$\psi_{n\mathbf{k}}(\mathbf{r}) \;=\; e^{i\phi_n(\mathbf{k})}\, u_{n\mathbf{k}}(\mathbf{r})\, e^{i\mathbf{k}\cdot\mathbf{r}}$$

- Uniqueness MLWFs resolved by requiring that the total spread of the WF be minimized in real space.

MLWF Analysis based on:

- Shape
- Spread
- Center

G. H. Wannier Phys. Rev. 52, 191 (1937)

N. Marzari and N. Vanderbilt PRB 56, 12847 (1997)

A. A. Mostofi et al., Comput. Phys. Commun. 178, 685 (2008)

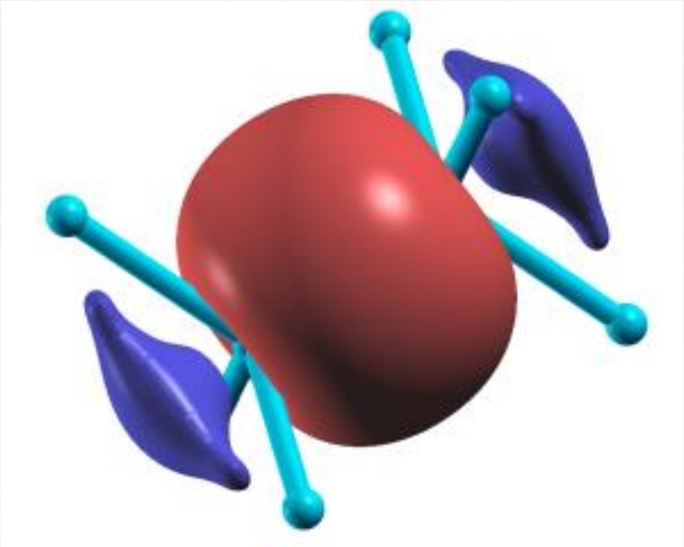

Si

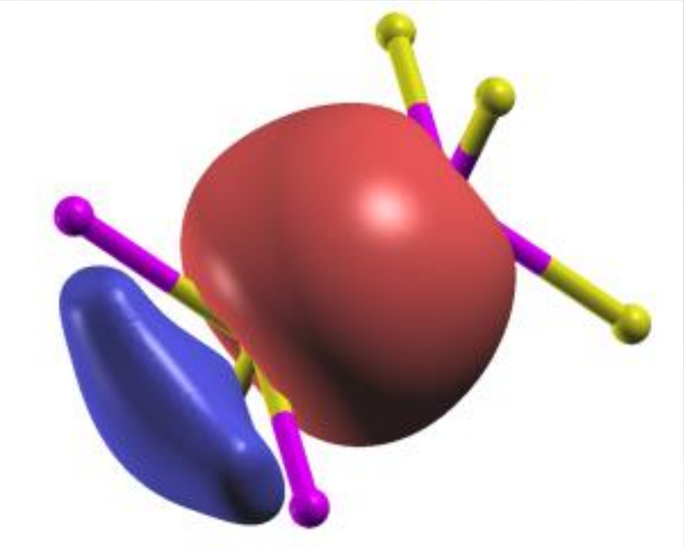

GaAs

Localized „Orbitals“ (MLWF)

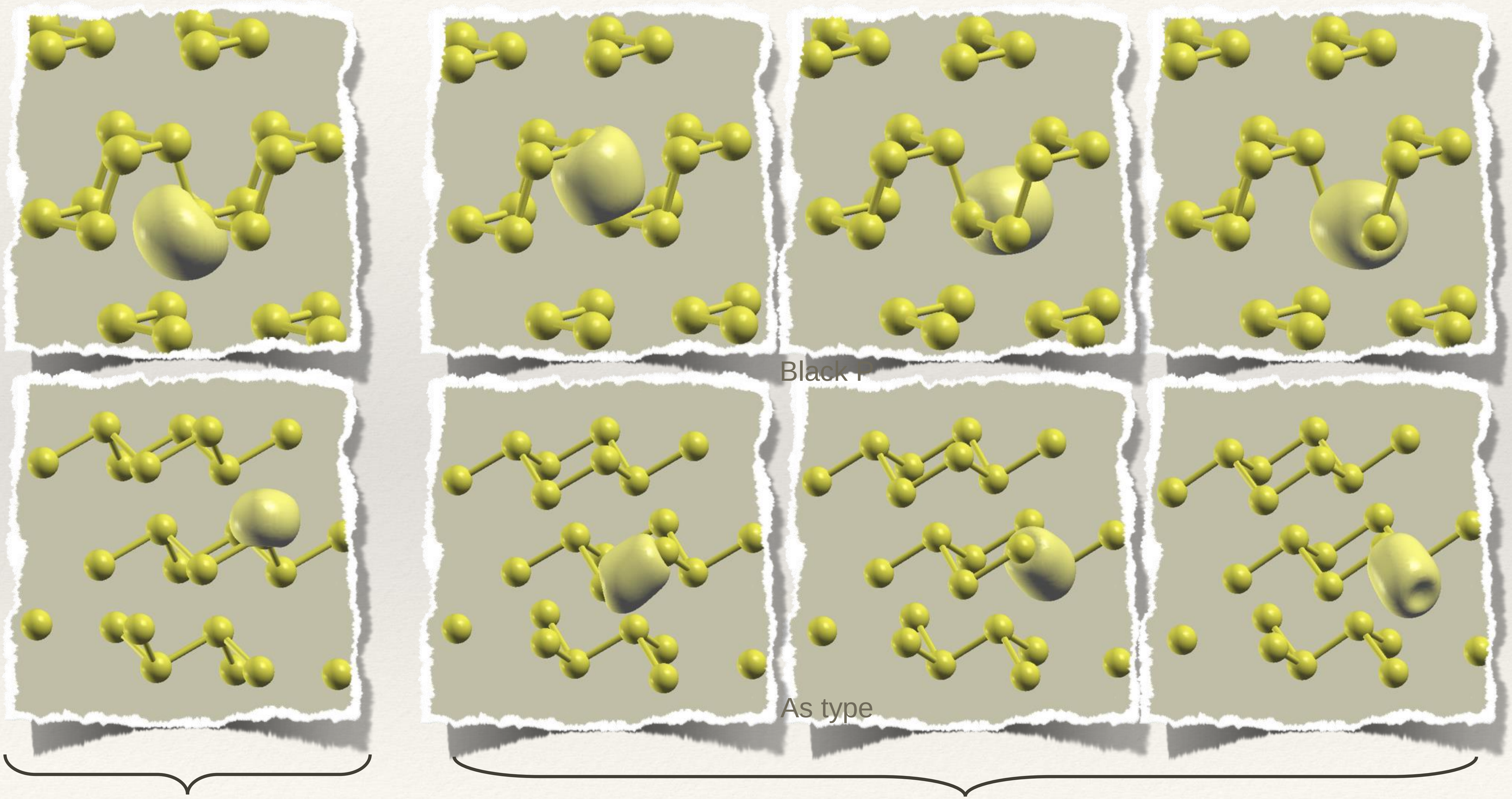

Lone Pairs

P-P σ Bonds

Wannier Function - Definition

$$| \mathbf{R}n \rangle = \frac{V}{(2\pi)^3} \int_{BZ} \sum_{m=1}^{N} U_{mn}^{(\mathbf{k})} \, | \psi_{m\mathbf{k}} \rangle \, e^{-i\mathbf{k}\cdot\mathbf{R}} \, d\mathbf{k}$$

$$\Omega = \sum_{n} \left[\langle \mathbf{0}n \, | \, r^2 \, | \, \mathbf{0}n \rangle - \langle \mathbf{0}n \, | \, \mathbf{r} \, | \, \mathbf{0}n \rangle^2 \right] = \sum_{n} \left[\langle r^2 \rangle_n - \bar{\mathbf{r}}_n^2 \right]$$

Choose the unitary transformation *U* such that the spread Ω is minimized!

https://cfm.ehu.es/ivo/publications/marzari-psik03.pdf

SnS - Band Structures (WF)

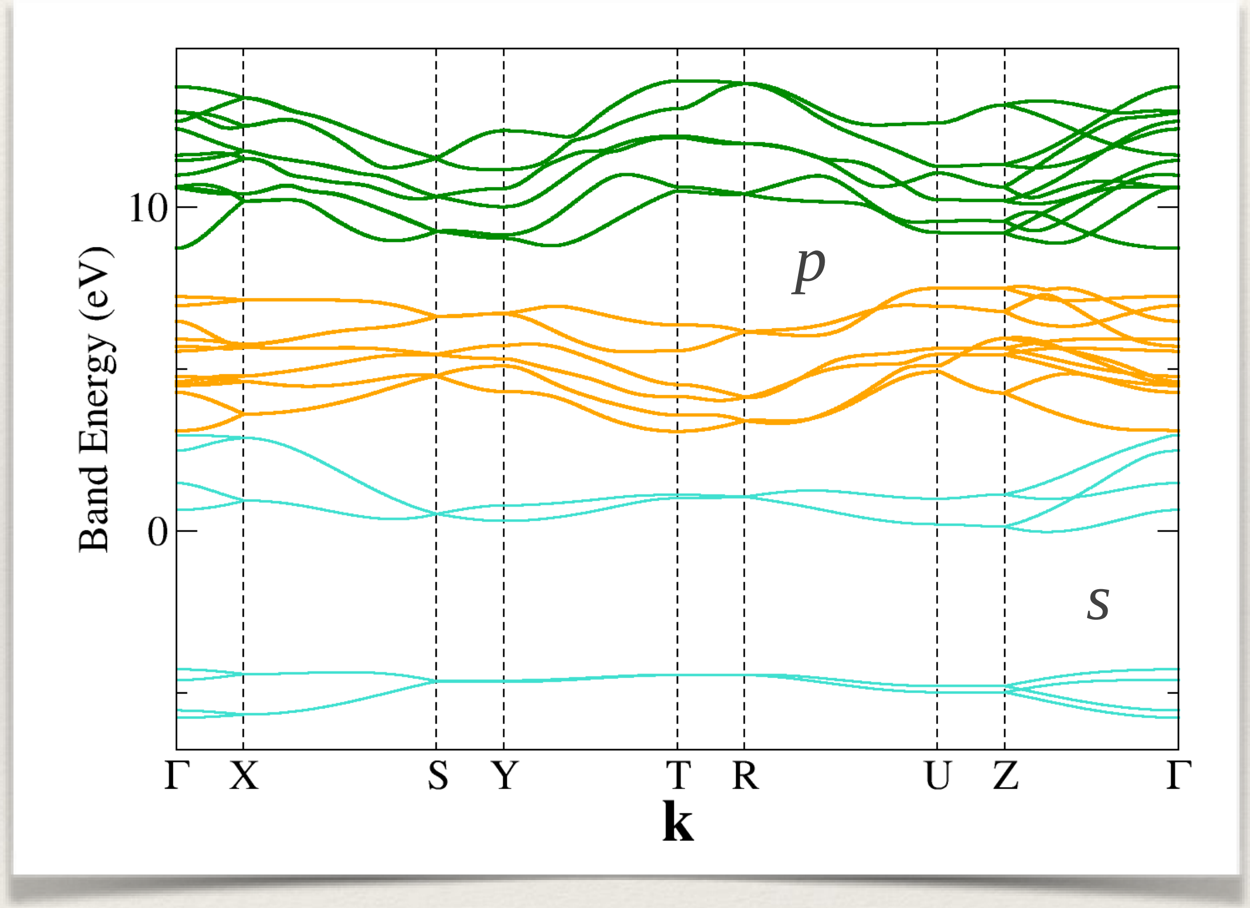

32 WFs

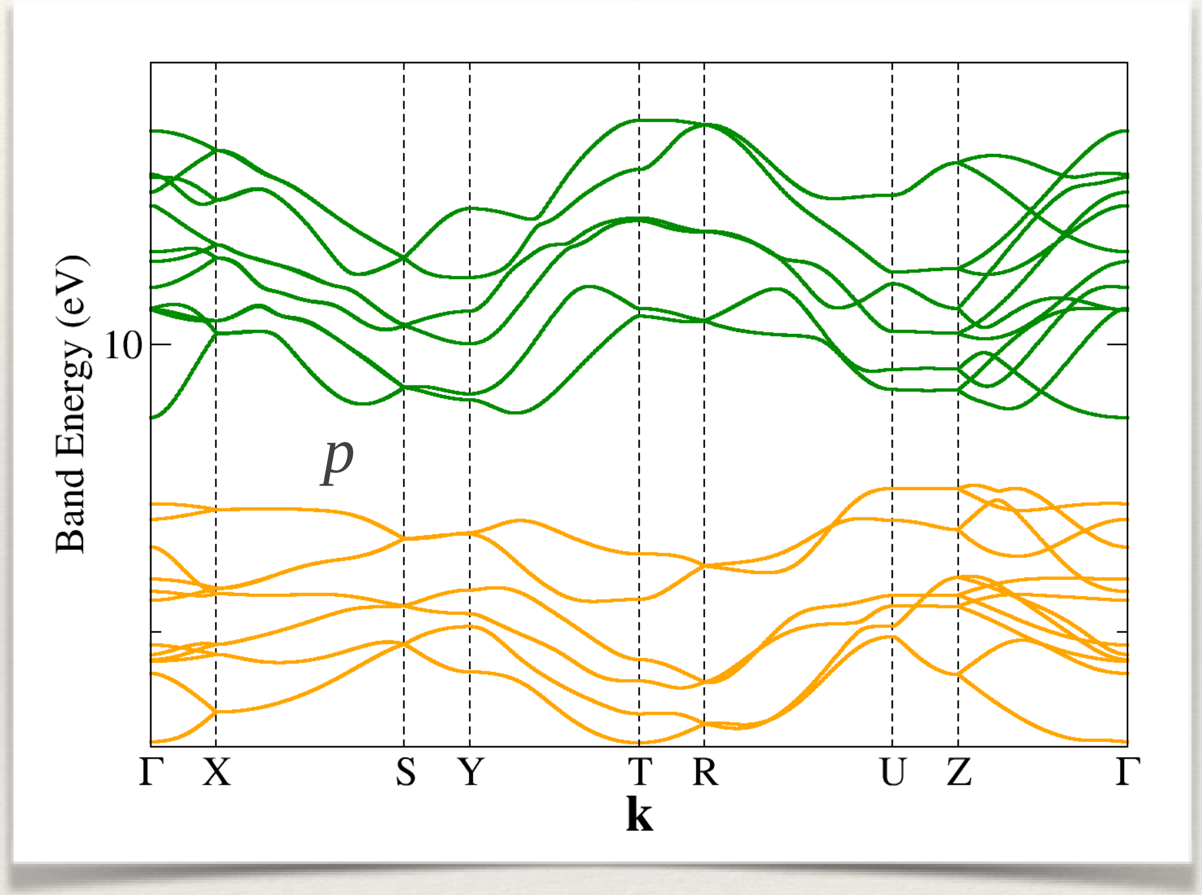

24 WFs

QE, wannier90
GGA (PBE)

SnS - Band Structures (WF)

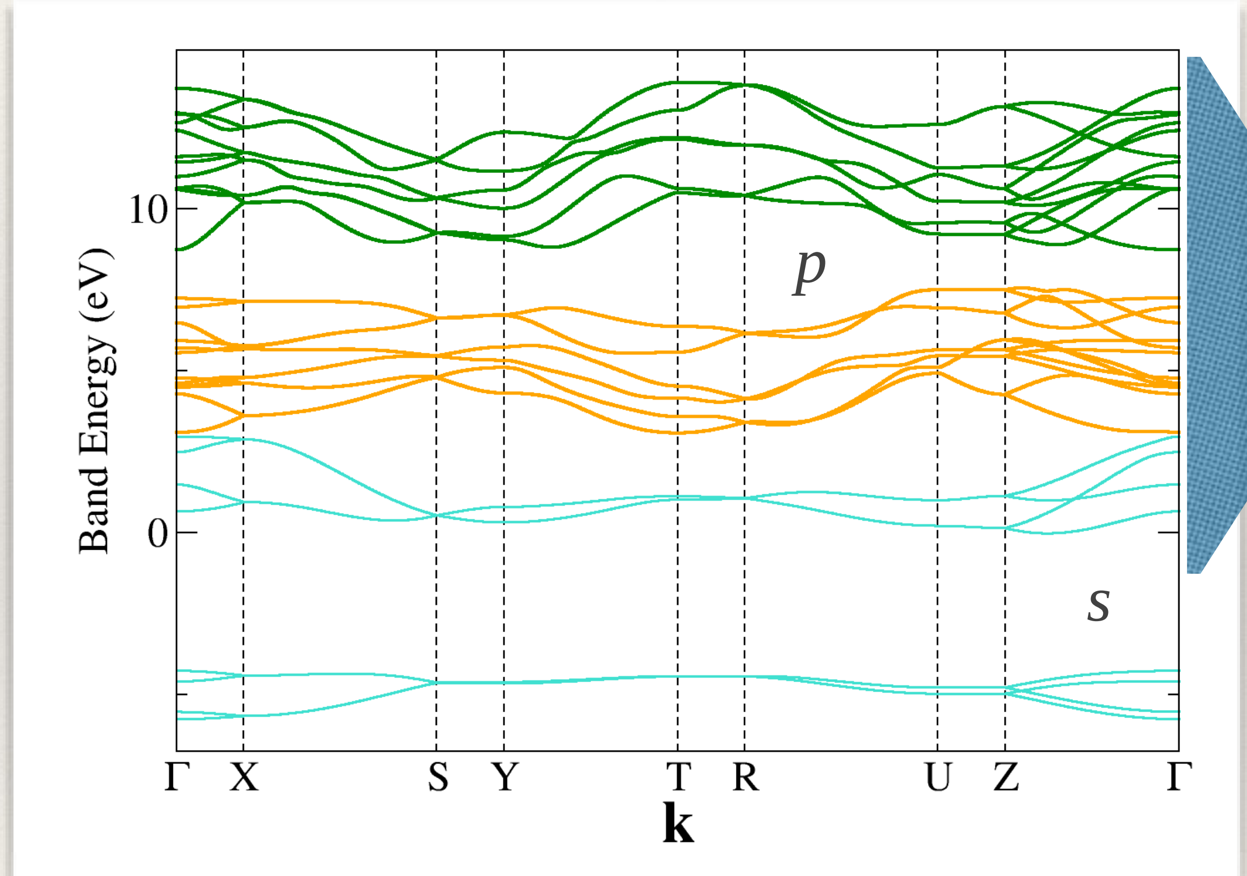

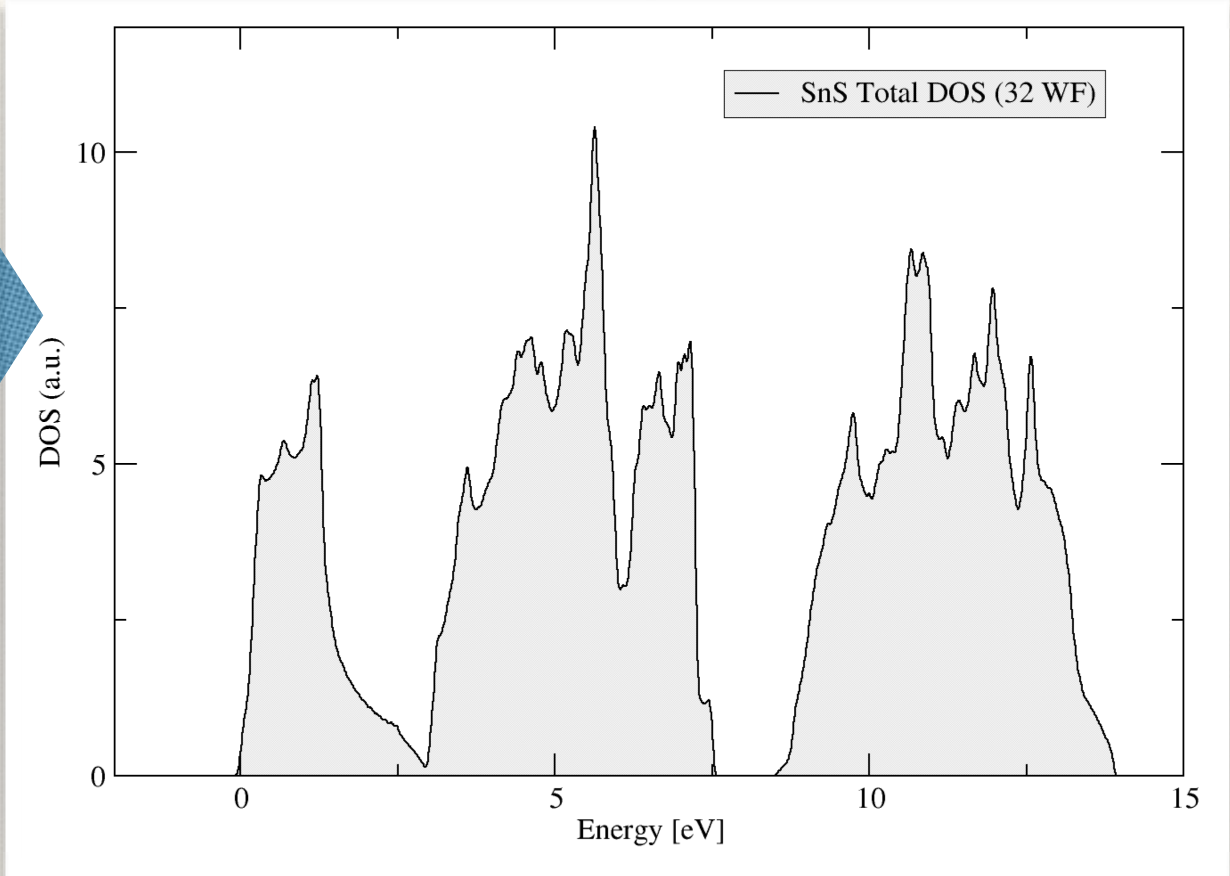

32 WFs

band gap: 0.97 eV
GGA (PBE)
(1.11 HSE06[1])

---

[1] L. A. Burton et al., Chem. Mater. 2013, 25 (4908)

Transport Equations

$$[\boldsymbol{\sigma}]_{ij}(\mu, T) = e^2 \int_{-\infty}^{+\infty} dE \left(-\frac{\partial f(E, \mu, T)}{\partial E} \right) \Sigma_{ij}(E),$$

$$[\boldsymbol{\sigma}\mathbf{S}]_{ij}(\mu, T) = \frac{e}{T} \int_{-\infty}^{+\infty} dE \left(-\frac{\partial f(E, \mu, T)}{\partial E} \right) (E - \mu) \Sigma_{ij}(E),$$

$$[\mathbf{K}]_{ij}(\mu, T) = \frac{1}{T} \int_{-\infty}^{+\infty} dE \left(-\frac{\partial f(E, \mu, T)}{\partial E} \right) (E - \mu)^2 \Sigma_{ij}(E).$$

$$\Sigma_{ij}(E) = \frac{1}{V} \sum_{n,\mathbf{k}} v_i(n, \mathbf{k}) v_j(n, \mathbf{k}) \tau_{n\mathbf{k}} \delta(E - E_{n,\mathbf{k}}),$$

Band velocities

$$\Sigma_{ij}(E) = \frac{1}{V}\sum_{n,\mathbf{k}} v_i(n,\mathbf{k})\, v_j(n,\mathbf{k})\, \tau_{n\mathbf{k}}\, \delta(E - E_{n,\mathbf{k}}),$$

$$v_i(n,\mathbf{k}) = \frac{1}{\hbar}\frac{\partial E_{n,\mathbf{k}}}{\partial k_i}.$$

Band velocities necessary for transport calculations
May be imprecise using a dense grid of ***k*** points
Wannier functions (WF) improve smoothness.
(Cons: WF defined up to a phase, must be ***localised***)

Seebeck & el. cond.

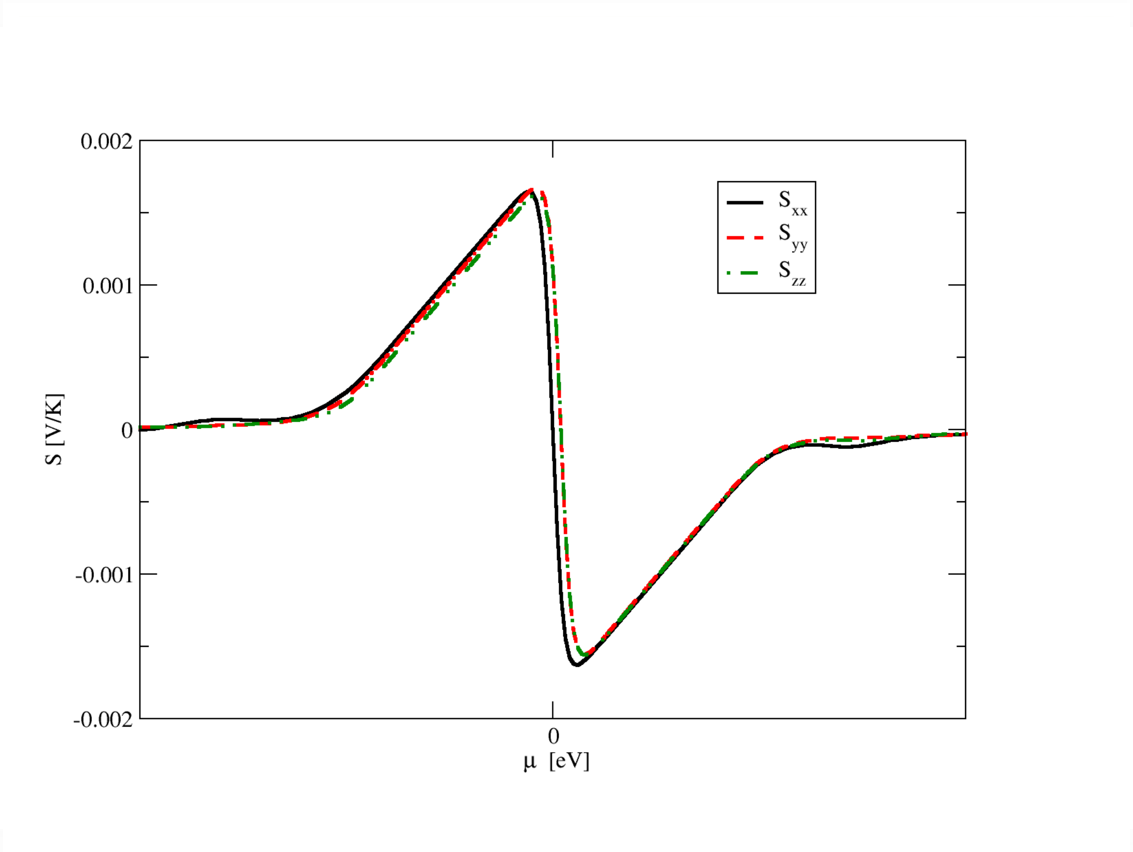

QE, 32 WFs, 6x6x6 *MP* grid
QE/ wannier90
Boltzmann TE

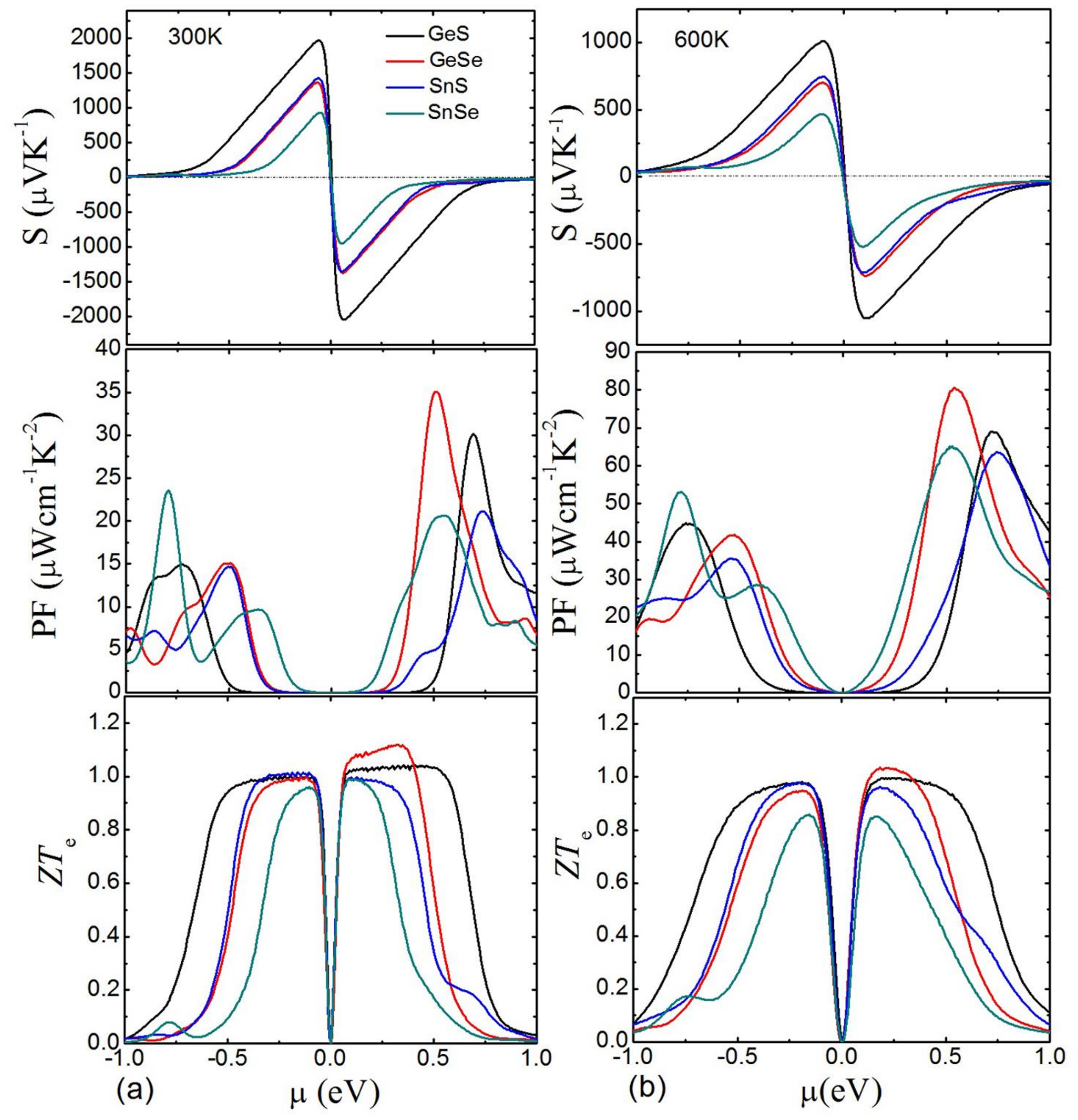

Guangqian Ding *et al.*, Sci. Rep. 5, 9567 (2015)

Transport Channels (Transmission)

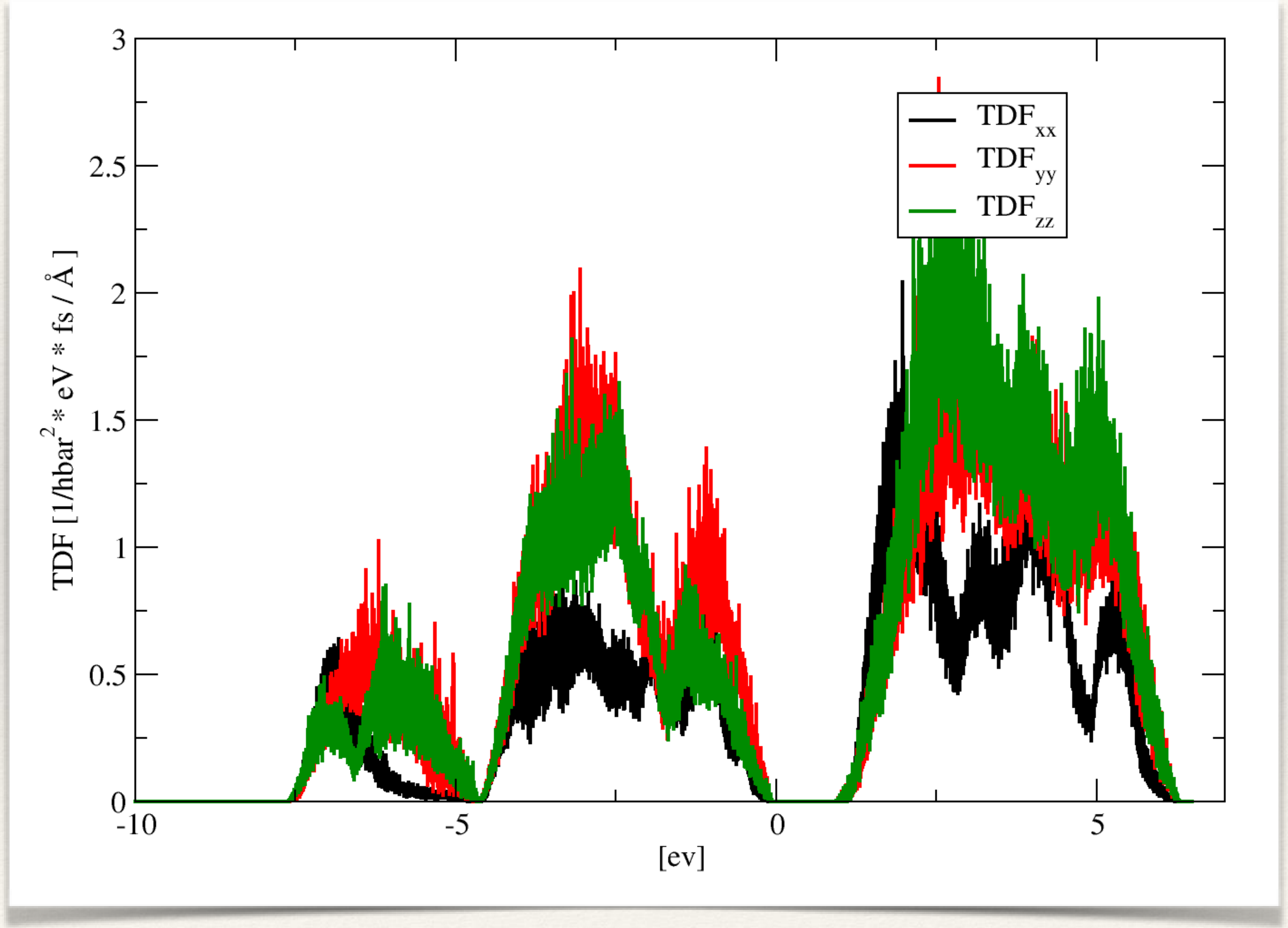

Thermal Conductivity

From phonon dispersions/spectra

$$k_{ij} = \frac{1}{NV_0} \sum_{\mathbf{q},s} C_V(\mathbf{q}s)\nu_i(\mathbf{q}s)\nu_j(\mathbf{q}s)\tau(\mathbf{q}s)$$

$$C_V(\mathbf{q}s) = \frac{\hbar^2\omega^2(\mathbf{q}s)}{k_B T^2}\bar{n}(\mathbf{q}s)[\bar{n}(\mathbf{q}s) + 1]$$

K_{ij} is the ij element of the thermal conductivity tensor, N is number of unit cells, V_0 is UC volume, C_v is the specific heat capacity, { are phonon group velocities, **q** is a ***given*** displacement vector (frozen phonon), s is a (phonon) band, τ is a relaxation time, ω is a frequency, n(bar) is the Bose-Einstein distribution.

Relaxation time, τ

$$\tau^{-1} = \tau_{BS}^{-1} + \tau_{MD}^{-1} + \tau_{3PP}^{-1}$$

τ^{-1} : Inverse of relaxation time, scattering rate.

Calculation of scattering poses the largest problems, especially within ab-initio/frozen phonons approaches. This has mainly to do with the complexity of the scattering problem than limitation in principle. One of the main constraintsis actually the use of a single relaxation time for every mode.

Sources of scattering: Boundaries, Mass and Interphonon (3-phonon here) scattering

ph scattering

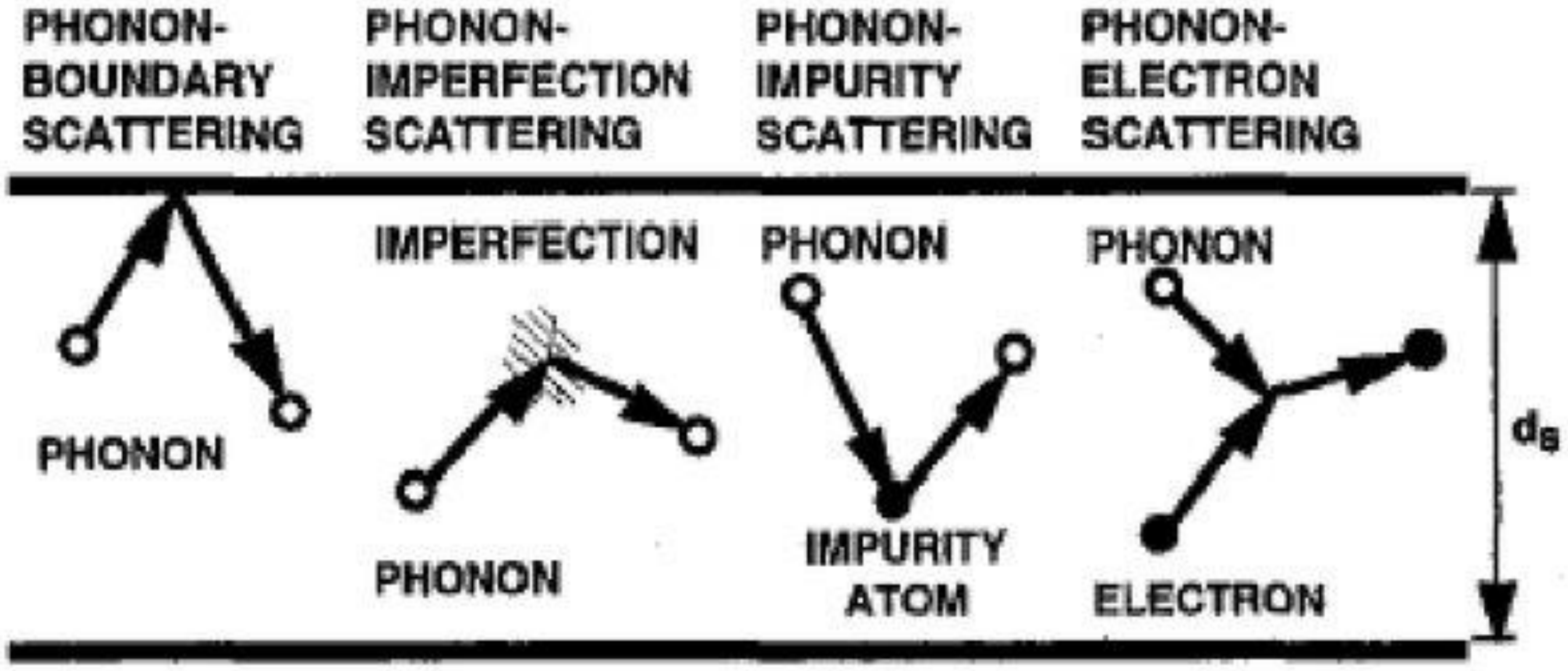

https://www.researchgate.net/publication/234108456_ECST_Vasileska/figures?lo=1

^{3}pp

Dependency of ^{3}pp over T – low and high-T regime:

$$\tau^{-1} \propto \omega^2 T^3$$

longitudinal ph

Low T

$$\tau^{-1} \propto \omega T^4$$

transverse ph

$$\tau^{-1} \propto T^{-1}$$

High T

$$\alpha = \frac{\gamma c_v}{3B}$$

α Thermal expansion coefficient
γ Grüneisen parameter
B bulk modulus

Phonon frequencies change with unit cell volume

Ashcroft/ Mermin, SSP

Transverse/longitudinal

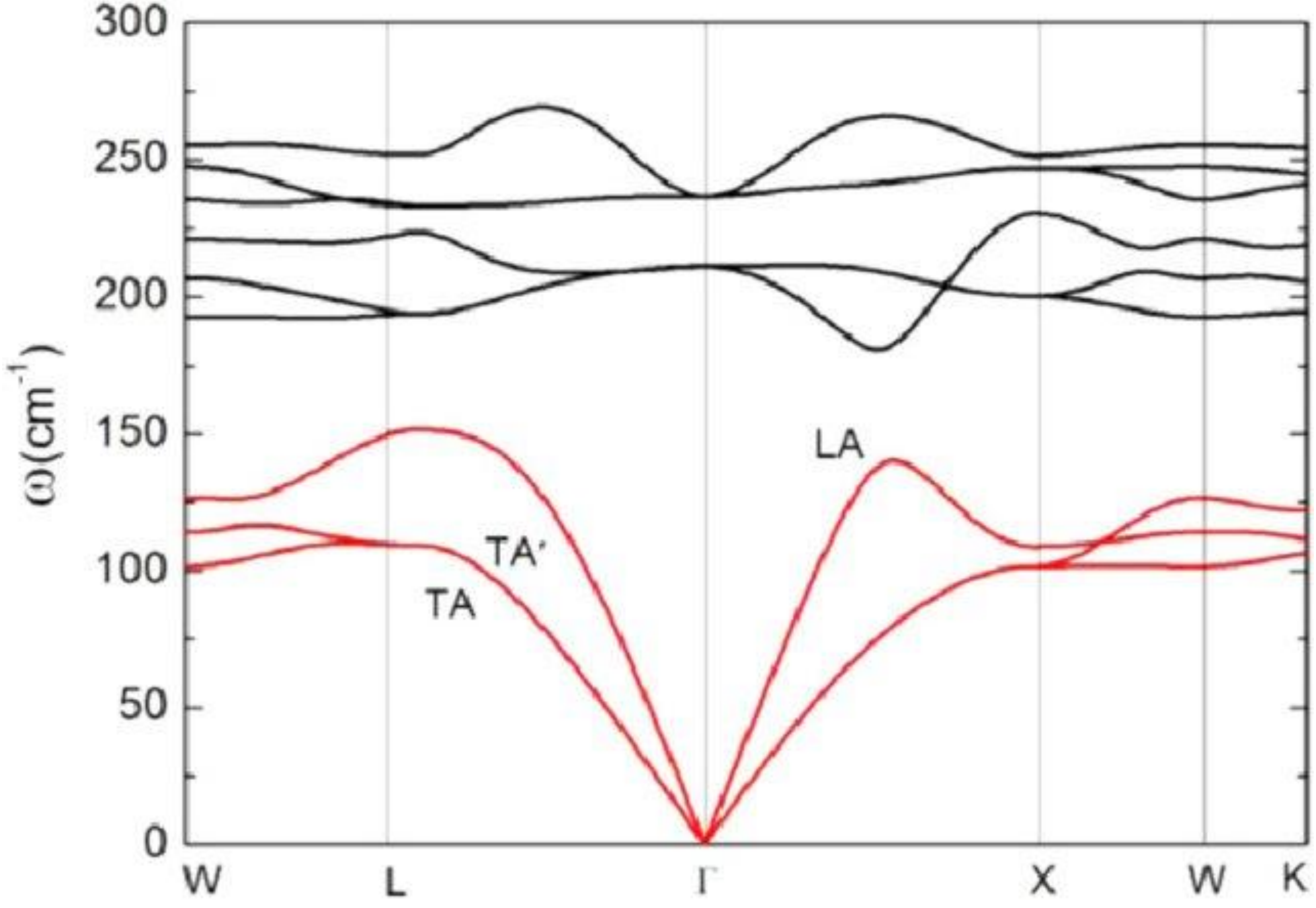

https://www.researchgate.net/publication/276279237_Examining_the_thermal_conductivity_of_half-Heusler_alloy_TiNiSn_by_first-principles_calculations/figures?lo=1

^{3}pp

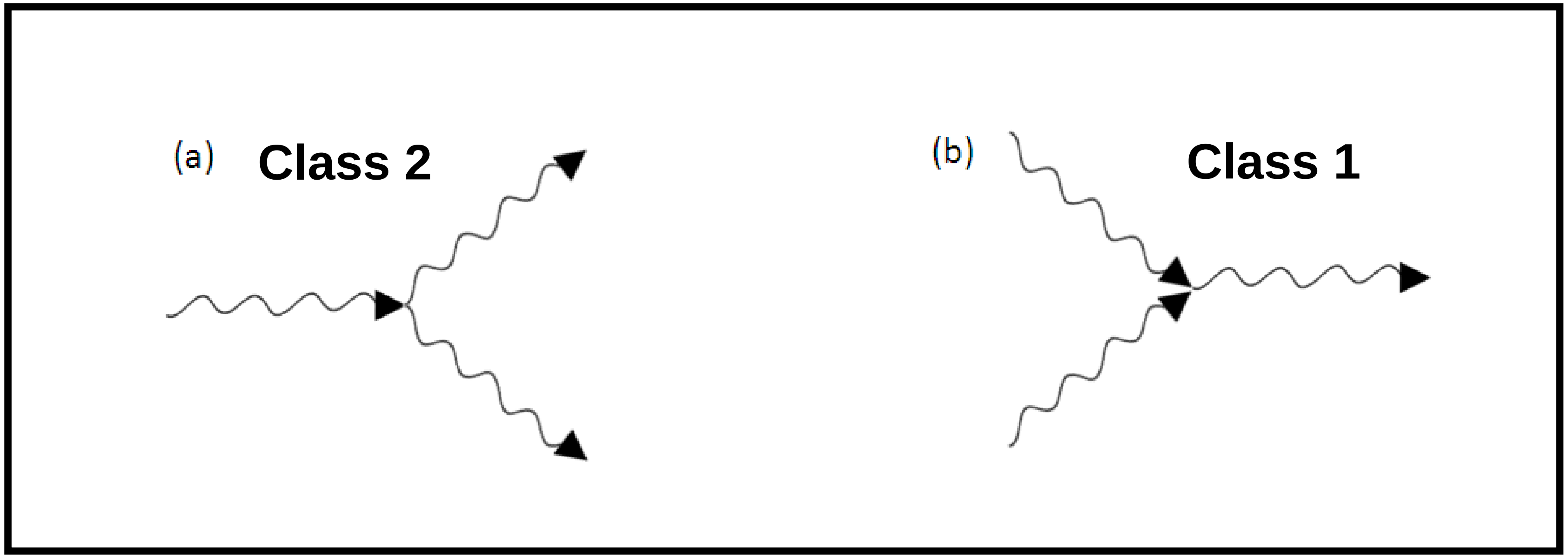

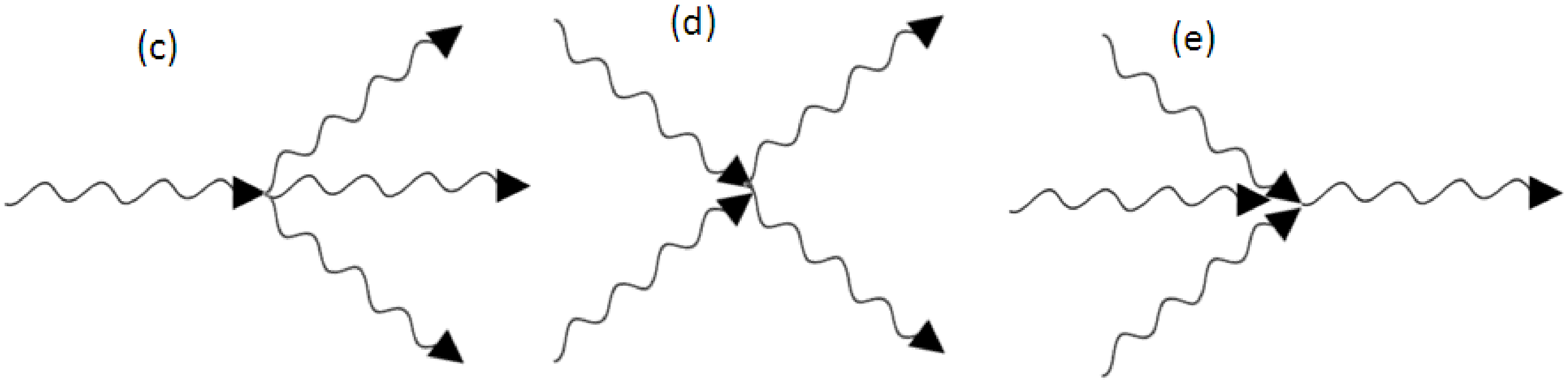

https://www2.physics.ox.ac.uk/sites/default/files/CrystalStructure_Handout9_2.pdf

Phonons

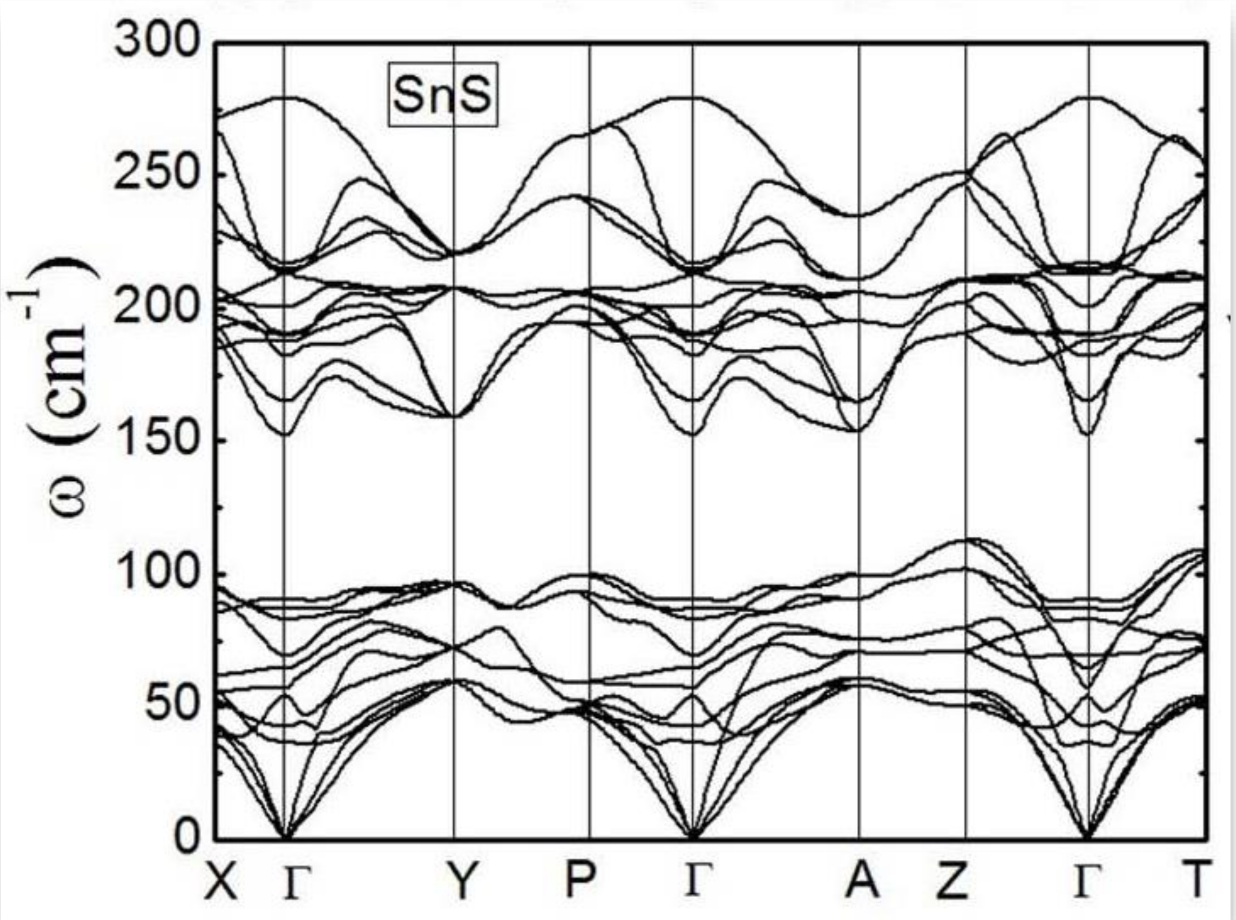

lower limit of lattice conductivity
(Debye model of lattice vibrations)
consider acoustic modes only (3),
- constant phonon lifetime -

$$K_{L,min} = \left(\frac{\pi}{6}\right)^{1/3} k_B n^{2/3} \sum_i v_i \left(\frac{T}{\Theta_i}\right)^2 \int_0^{\Theta_i/T} \frac{x^3 e^x}{(e^x - 1)^2} dx$$

$$\Theta_i = v_i \frac{\hbar}{k_B} (6\pi^2 n)^{1/3}$$

	v_{TA} [ms^{-1}]	$v_{TA'}$	v_{LA}	$k_{L,min}$ [Wm^{-1}K^{-1}]
SnS	1537	2343	3368	0.45
SnSe				0.32

$$v_i = \frac{\partial \omega_i(k)}{\partial k}$$

Vibrational Modes

$$C_{I\nu;J\mu} = \left. \frac{\partial^2 E(\mathbf{R})}{\partial R_{I\nu} \partial R_{J\mu}} \right|_{\mathbf{R}=\mathbf{R}0}$$

Dynamic Matrix
(interatomic force constants)

$$\mathbf{Q}_I = \mathbf{R}_I(t) - \mathbf{R}_I^0 = \mathbf{Q}_I e^{i\omega t}$$

Harmonic Approximation (HA)

time-dependent displacement

Finite Displacements

$$M_I \frac{\partial^2 \mathbf{R}_I}{\partial t^2} = \mathbf{F}_I(\mathbf{R}) = -\frac{\partial E(\mathbf{R})}{\partial \mathbf{R}_I}$$

Newton Equation of Motion

a) Standard

$$-\omega^2 M_I Q_{I\nu} = -\sum_{J\mu} C_{I\nu;J\mu}\, Q_{J\mu}$$

b) Dynamic Matrix

$$\overline{C}_{I\nu;J\mu} = -\frac{F_{I\nu}(Q_{J\mu}) - F_{I\nu}(-Q_{J\mu})}{2Q_{J\mu}}$$

Average matrix elements
(can be computed numerically!)

ph acoustic/optical

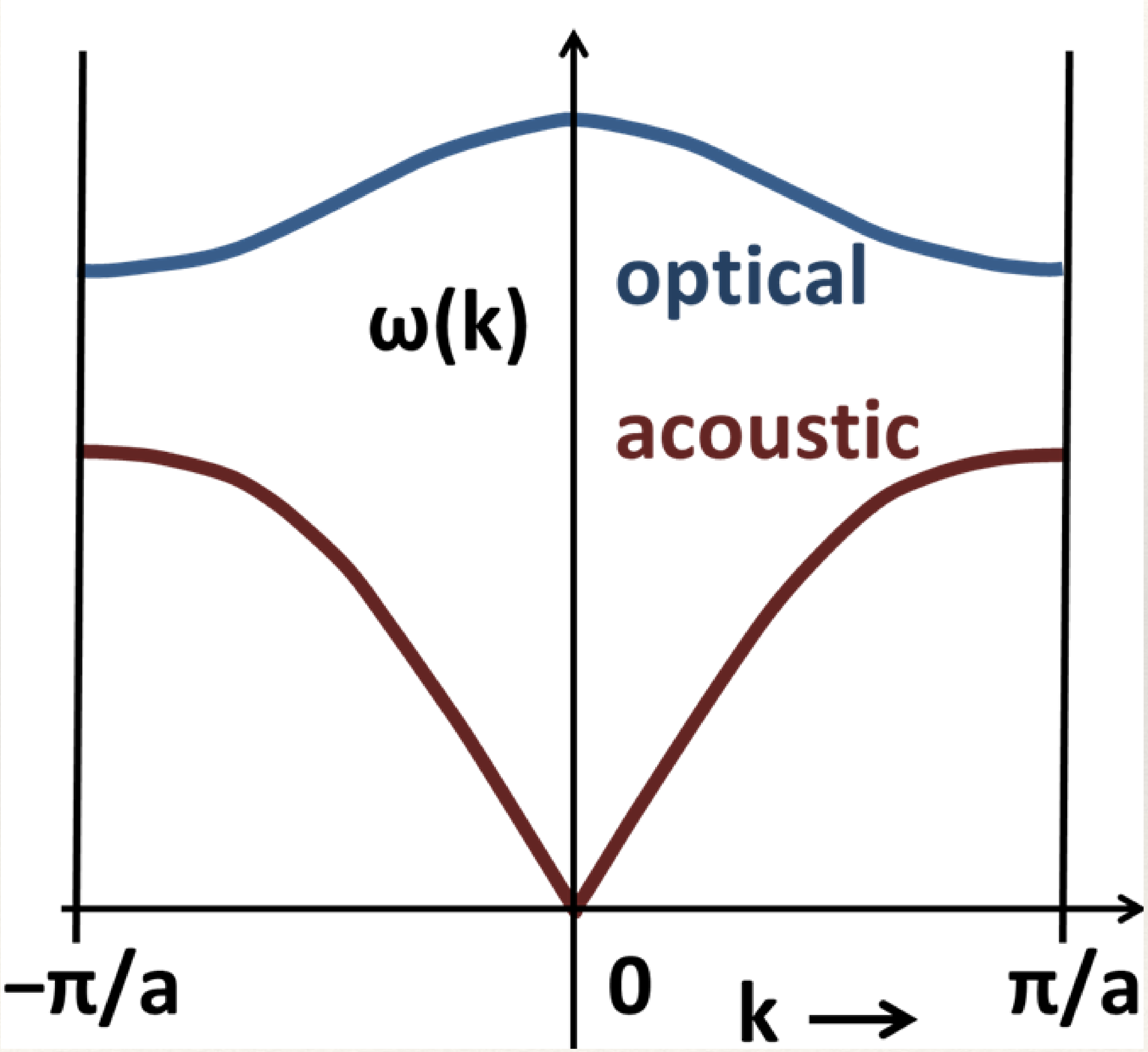

m1, m2 (1D chain, alternating)

See also:
https://physics.uwo.ca/~lgonchar/courses/p9812/Lecture7_Phonons.pdf

Improved numerical calculations

- phonon lifetimes may strongly deviate from HA due to anharmonicity (frequency-dependent lifetimes)
- -> include third-order force constants
- -> include phonon-phonon and 3-phonon interactions.

A. Togo et al., Phys. Rev. B 91, 094306 (2015)

Lattice thermal conductivity

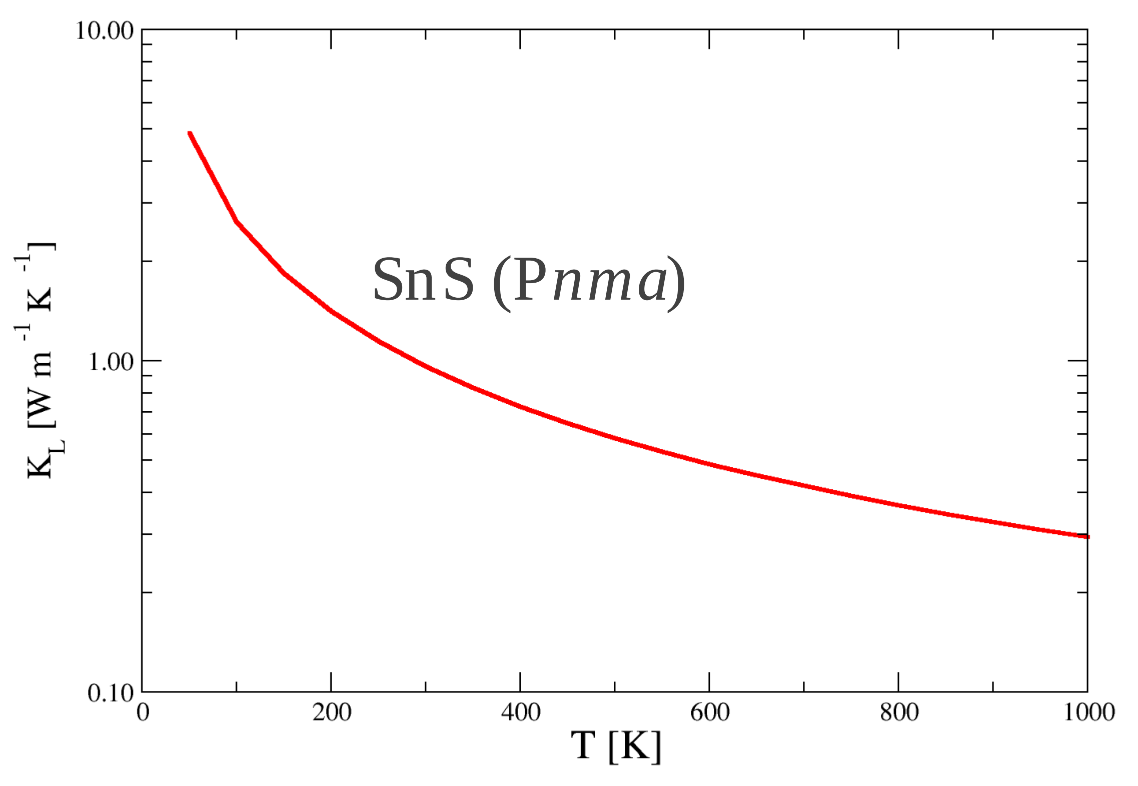

QE, 346 finite displacements
(within Unit Cell). Includes 3rd order terms

KL (300 K) : 0.963888 [W m^{-1} K^{-1}]

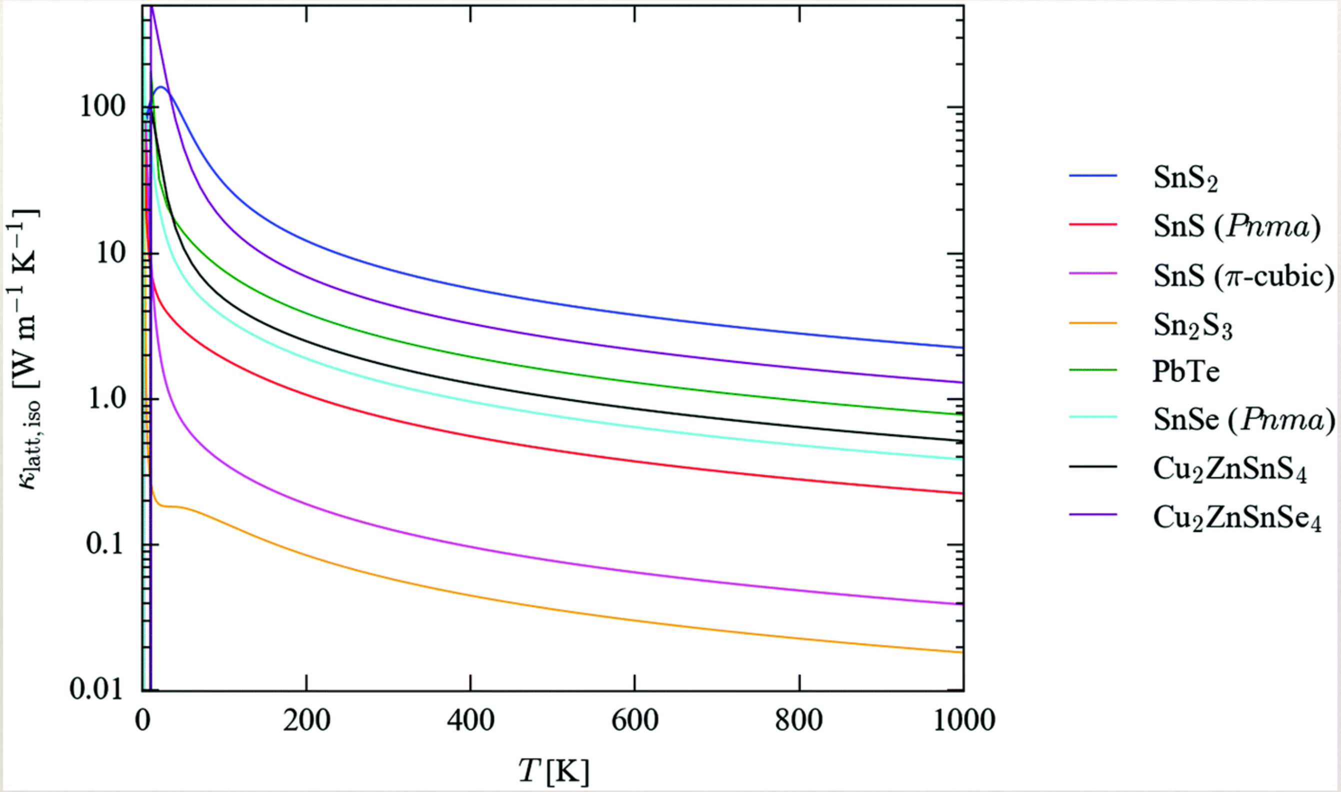

J.M. Skelton et al, PCCP, 2017, 19, 12452-12465

VASP, supercell

KL (300 K) : 0.73 [W m^{-1} K^{-1}]

SnS/SnSe (el.) structure

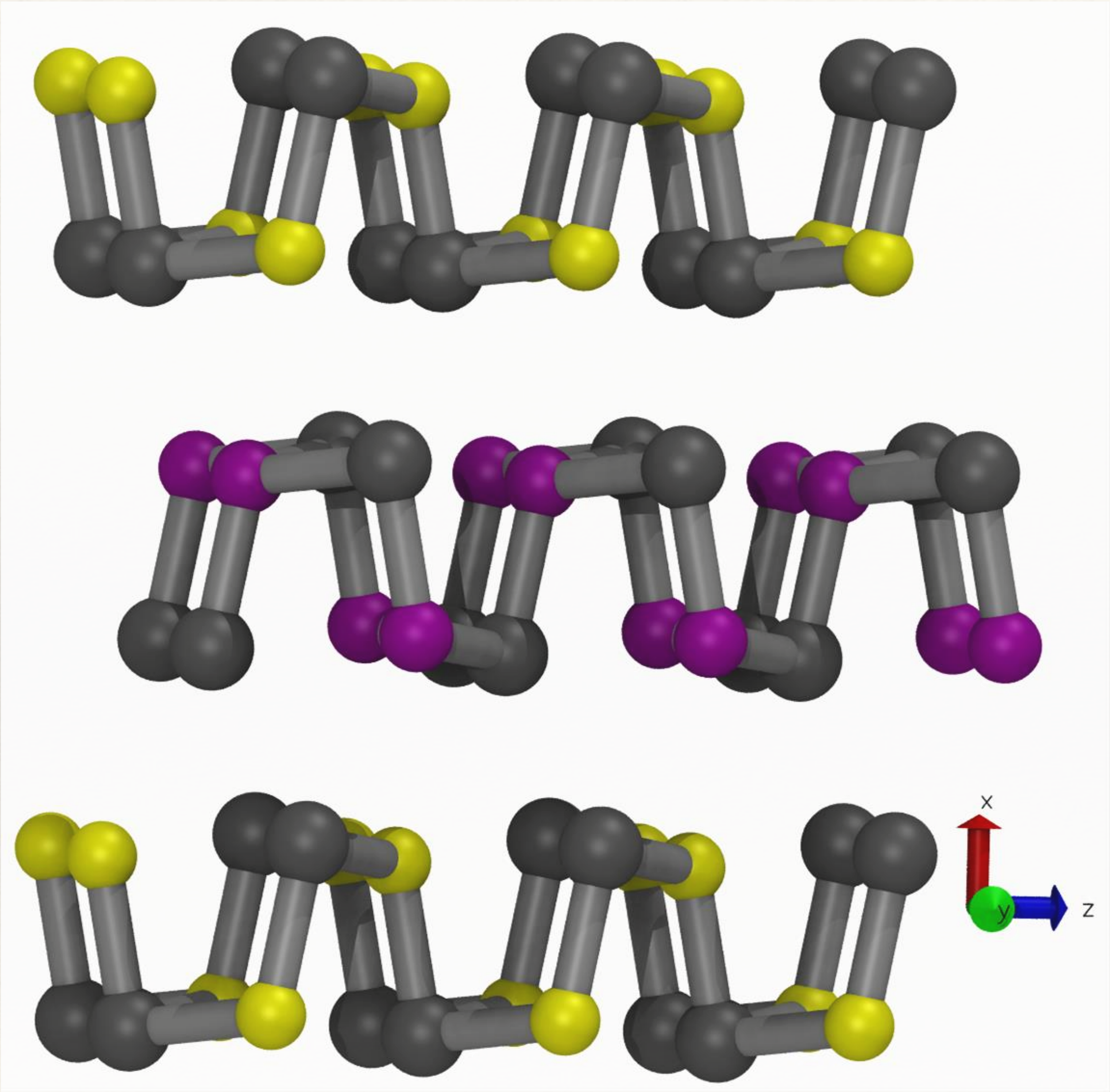

a=11.71, *b*=4.12, *c*=4.58 [Å]

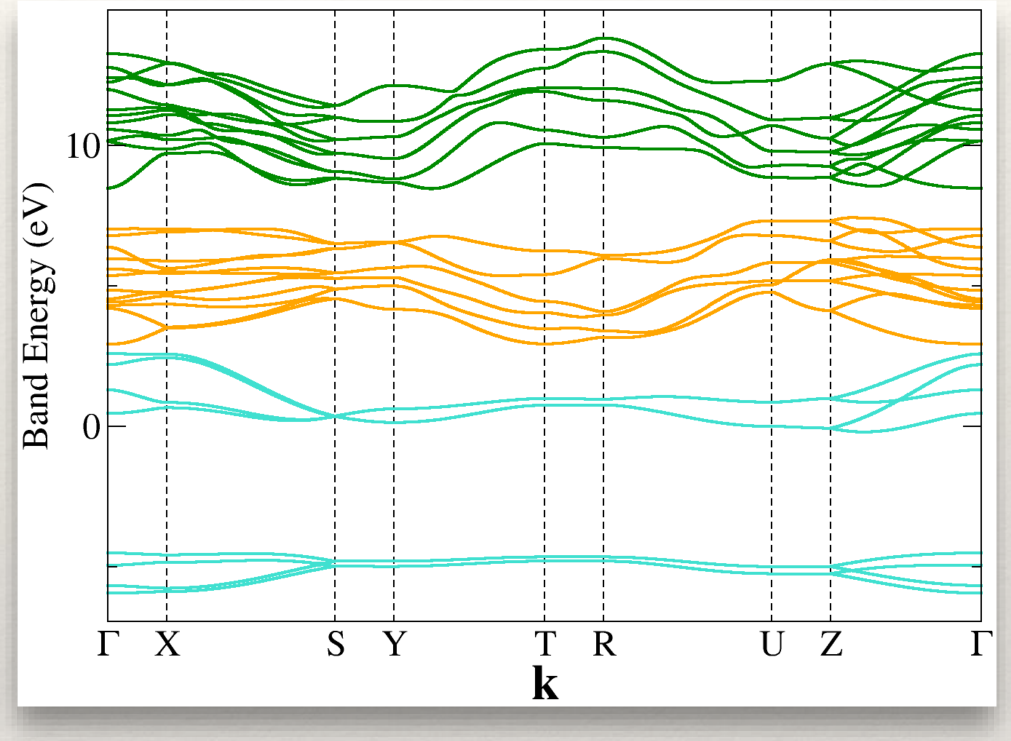

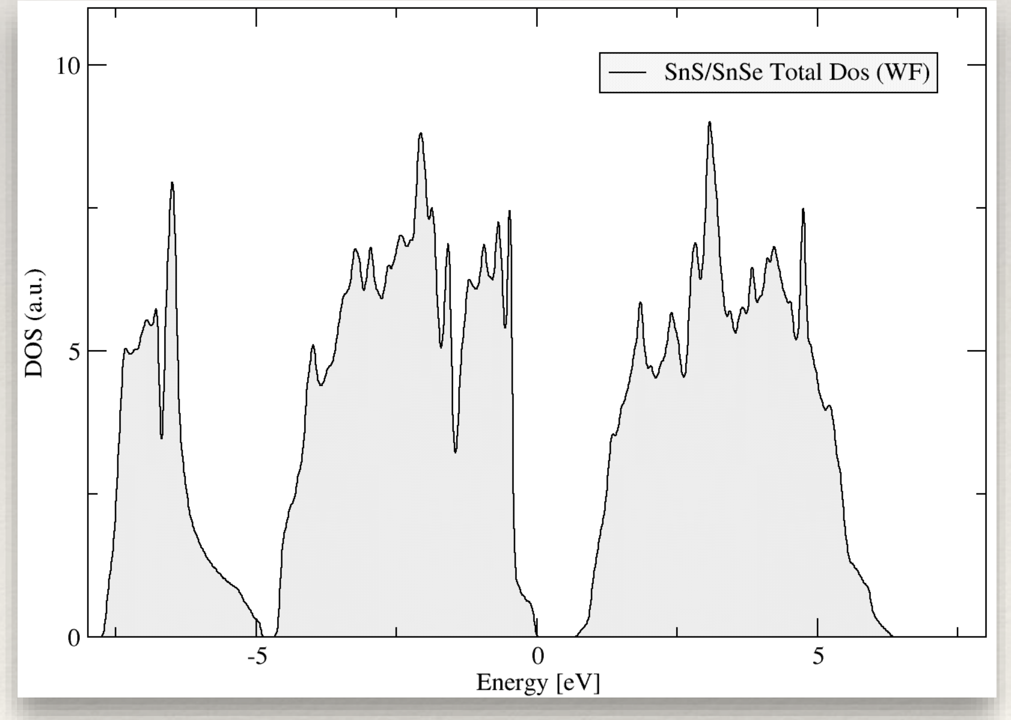

SnS/SnSe Interfaces - k_L

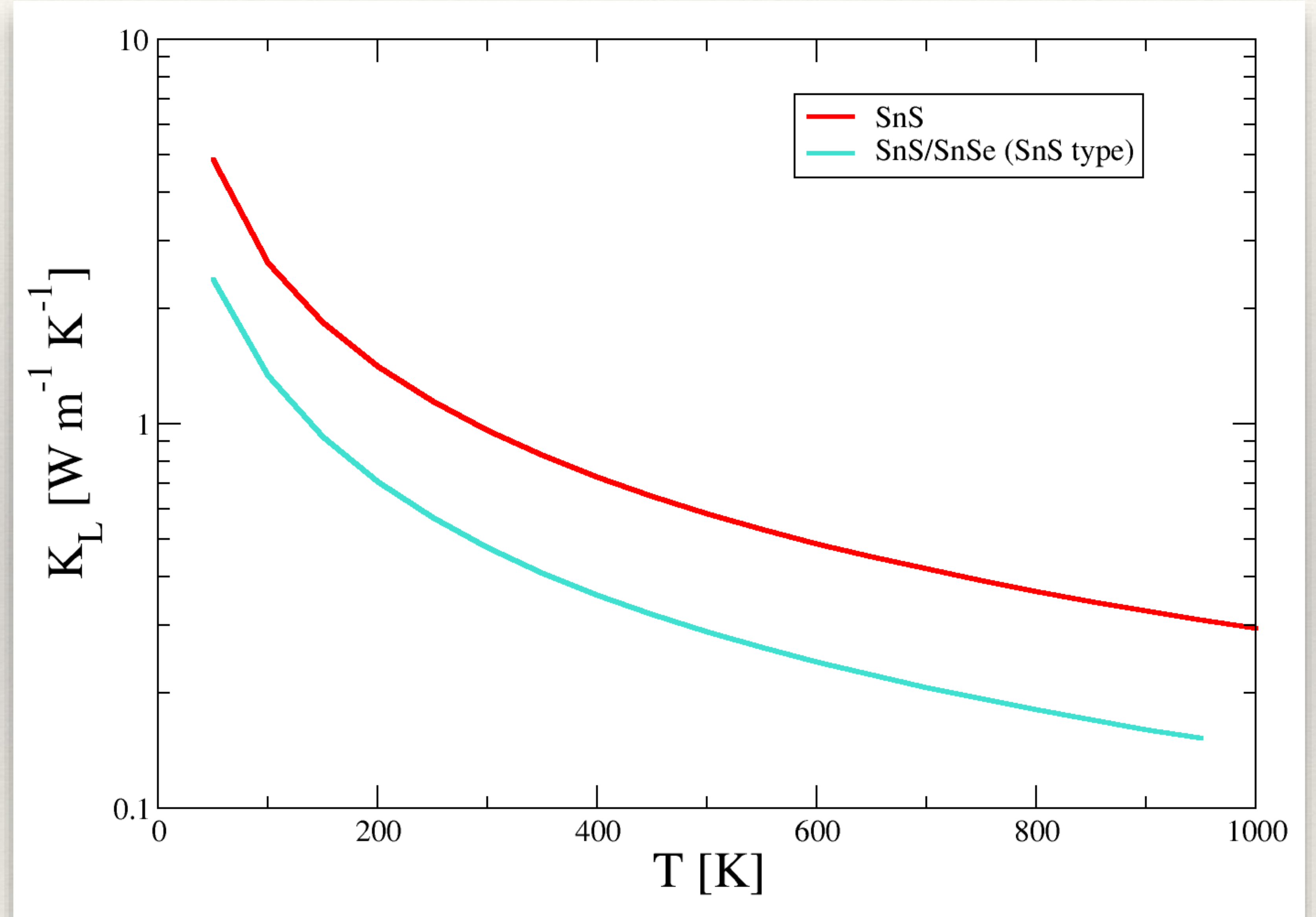

k_L (300 K) : 0.477303 [W m^{-1} K^{-1}]

SnS/SnSe Interfaces - S

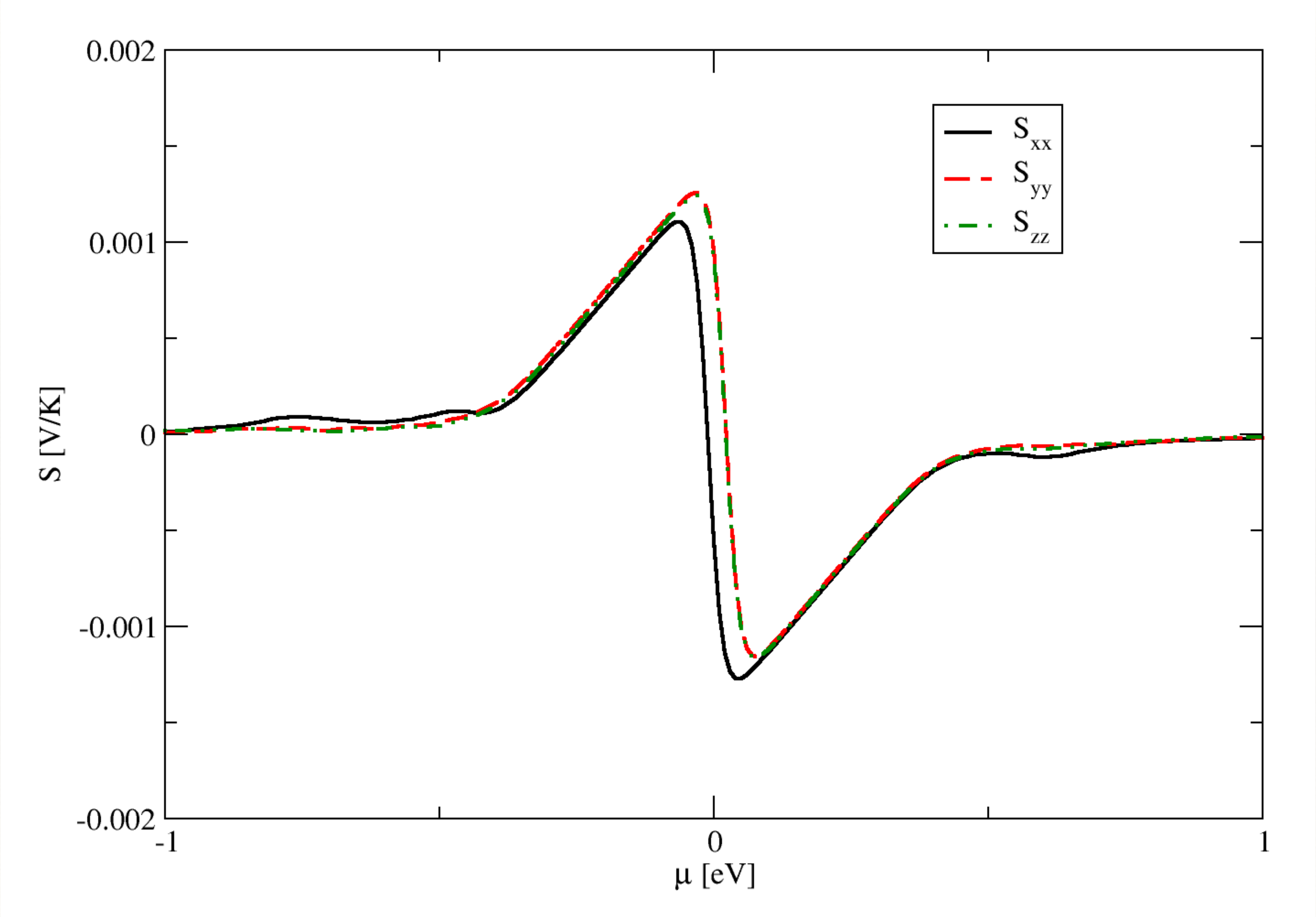

PbSe/PbTe

thermal conductivity

Alloy		**50% of Te**	0.72 ± 0.02		
Layers	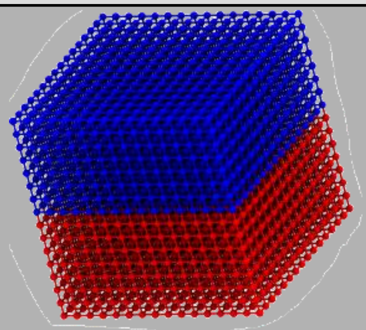	**25 Å**	**Average** 1.48 ± 0.14		
			X 1.80 ± 0.14	**Y** 1.79 ± 0.18	**Z** 0.85 ± 0.11
	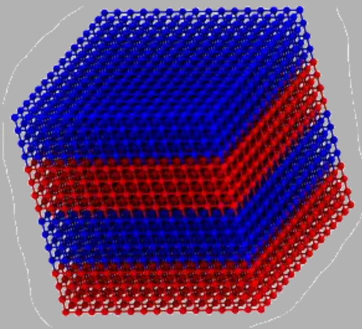	**12.5 Å**	**Average** 1.11 ± 0.18		
			X 1.40 ± 0.27	**Y** 1.44 ± 0.21	**Z** 0.49 ± 0.08
	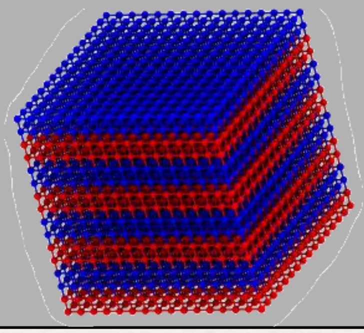	**6.75 Å**	**Average** 1.15 ± 0.08		
			X 1.40 ± 0.12	**Y** 1.32 ± 0.05	**Z** 0.71 ± 0.06

D. Selli, SL, unpublished

Thermal Transport

$$k_L = \frac{1}{3k_B T^2 V} \int_0^\infty \langle J(0) \cdot J(t) \rangle \, dt$$

Green-Kubo

$$J = \frac{1}{V} \left[\sum_i e_i \mathbf{v}_i + \frac{1}{2} \sum_{i<j} (\mathbf{f}_{ij} \cdot (\mathbf{v}_i + \mathbf{v}_j)) \mathbf{x}_{ij} \right]$$

Heat Flux

Equilibrium Molecular Dynamics

PbSe/PbTe

thermal conductivity

Alloy	**50% of Te**	0.72 ± 0.02		
Layers 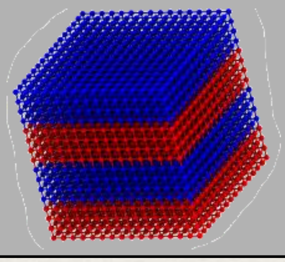	**12.5 Å**	**Average** 1.11 ± 0.18		
		X 1.40 ± 0.27	**Y** 1.44 ± 0.21	**Z** 0.49 ± 0.08

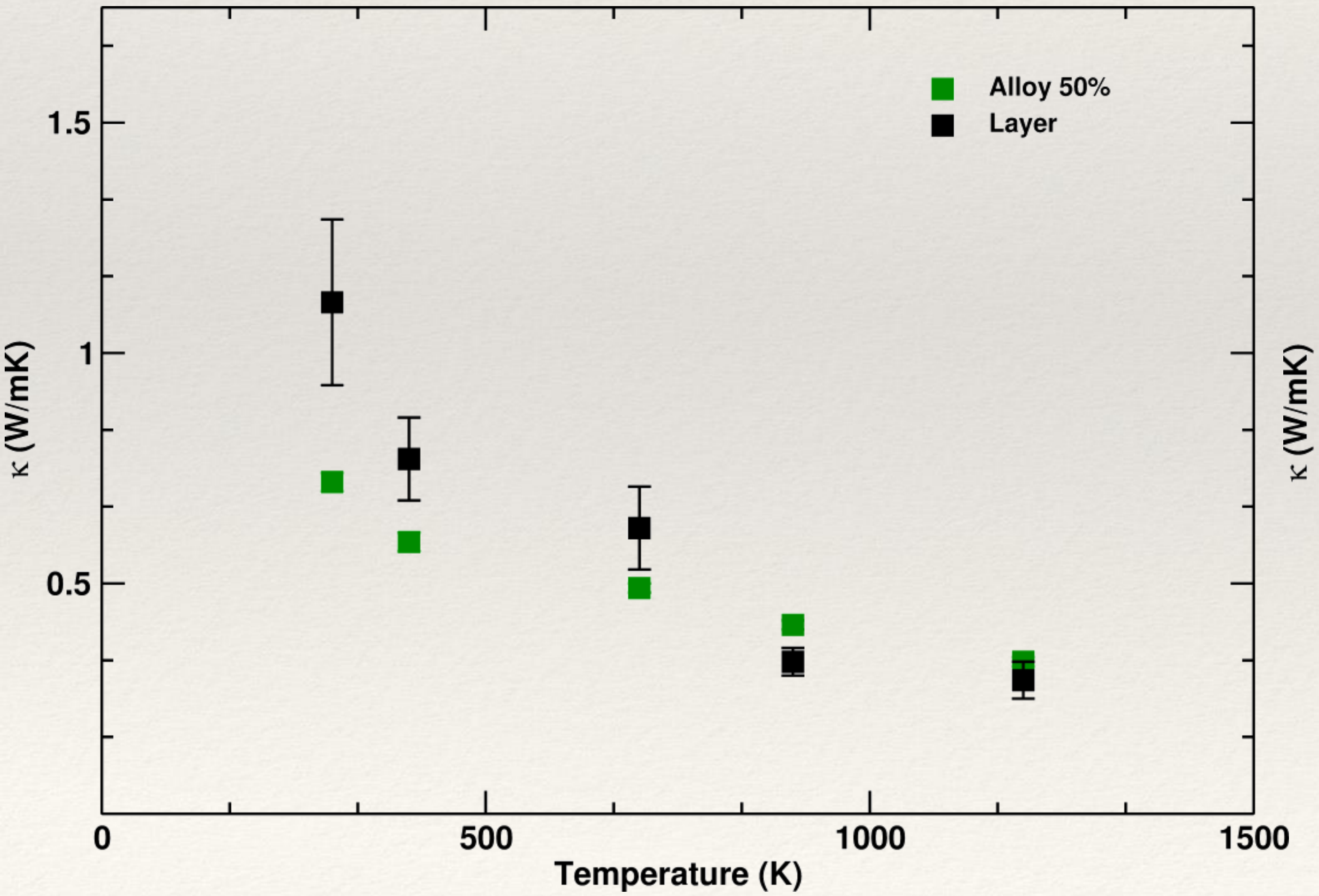

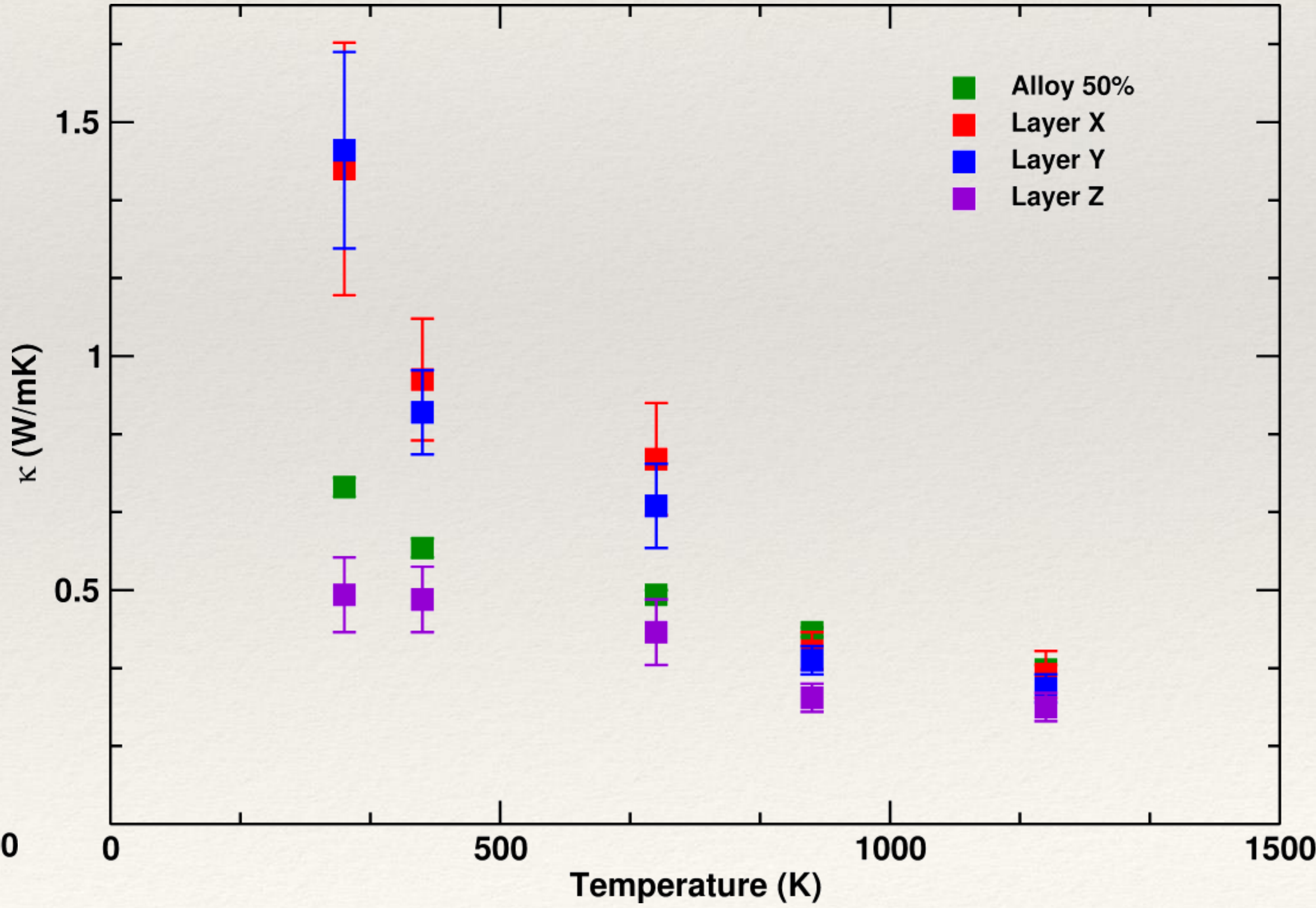

D. Selli, SL, unpublished

Polymorphs (variety)

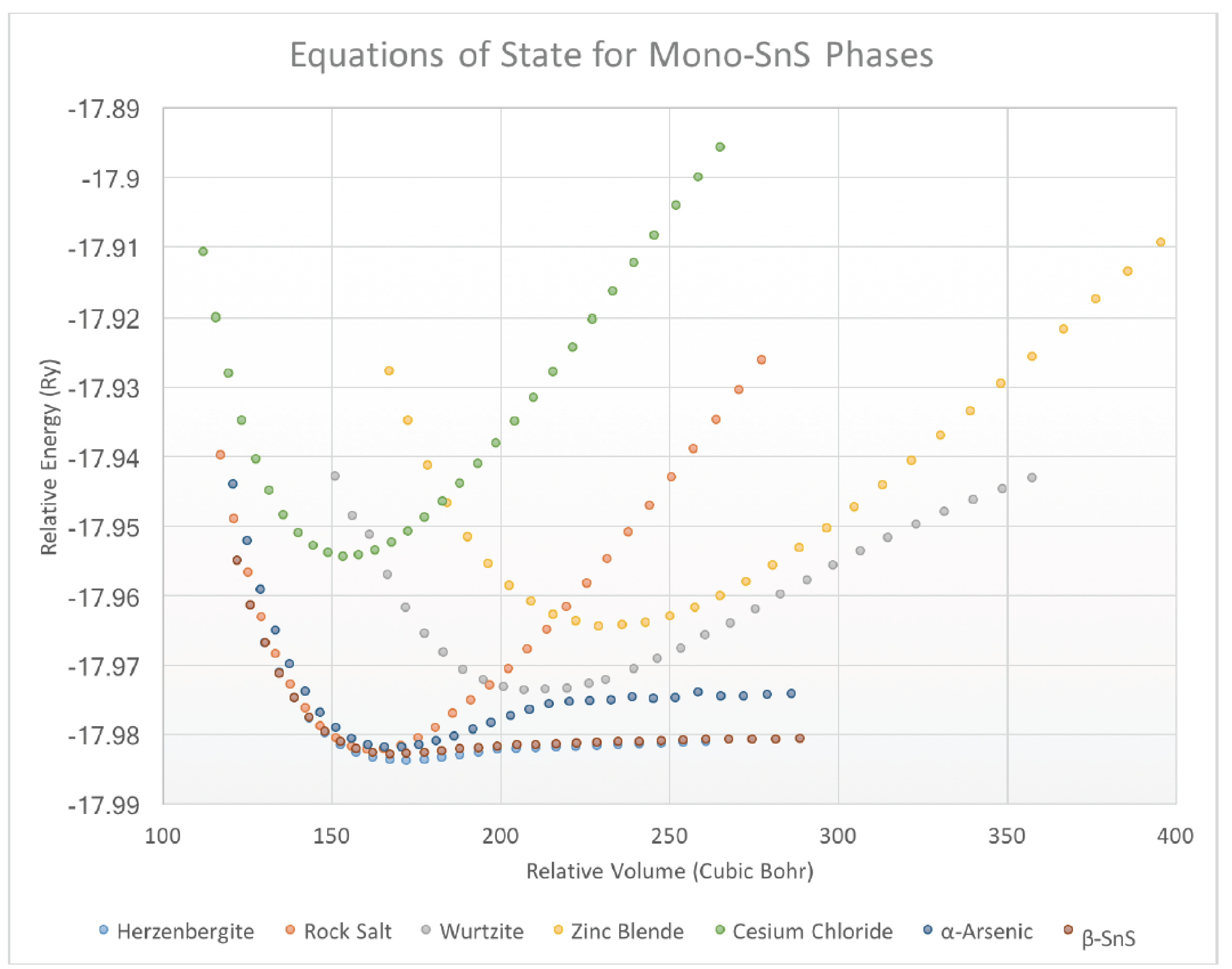

D.H, 2018 Additional degrees of freedom from polymorph “reservoir”

SnS - α-As type

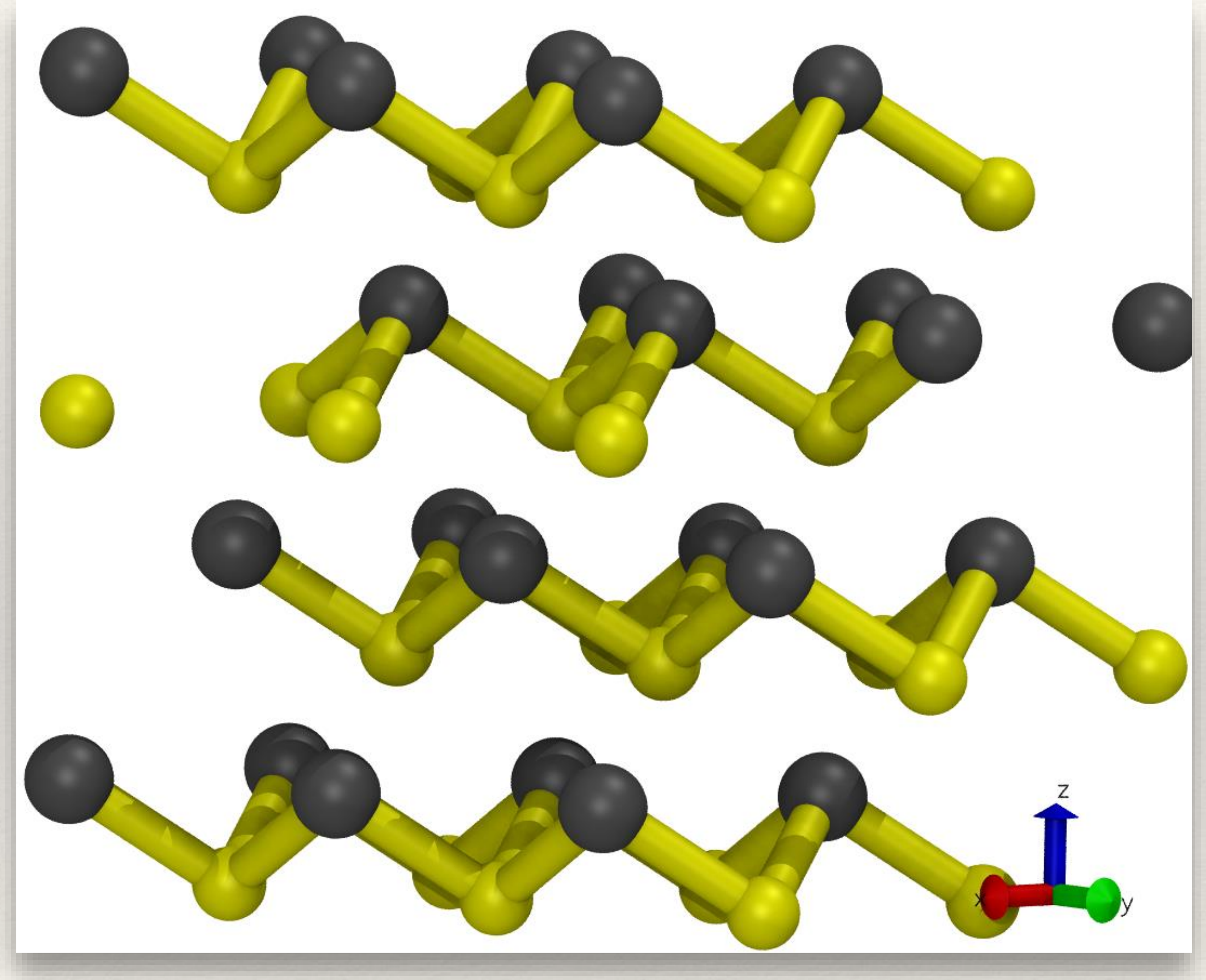

Predicted polymorph based on P system
(accessible under pressure in P)

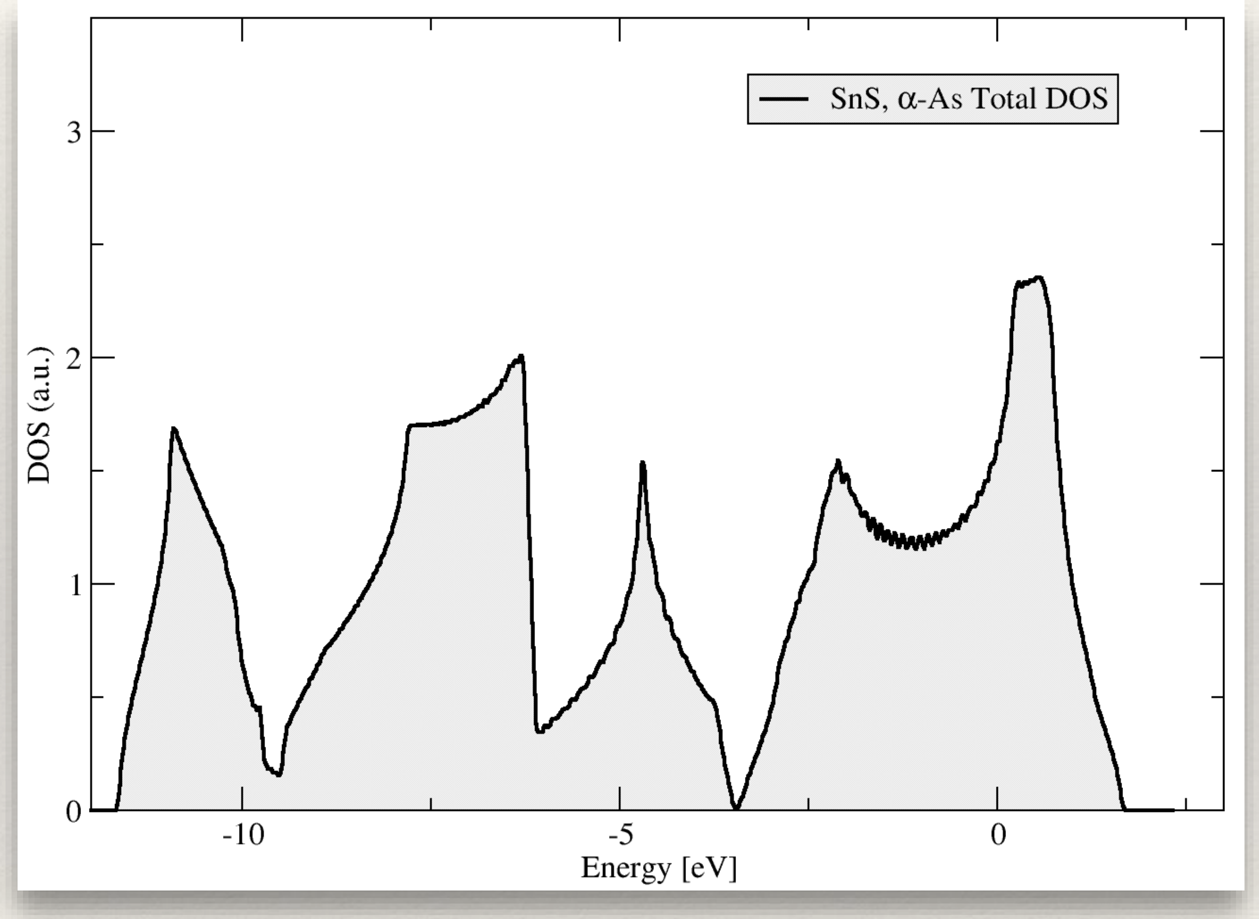

siesta/ wannier90 interface
Boltzmann TE

SnS - α-As type - transport (el)

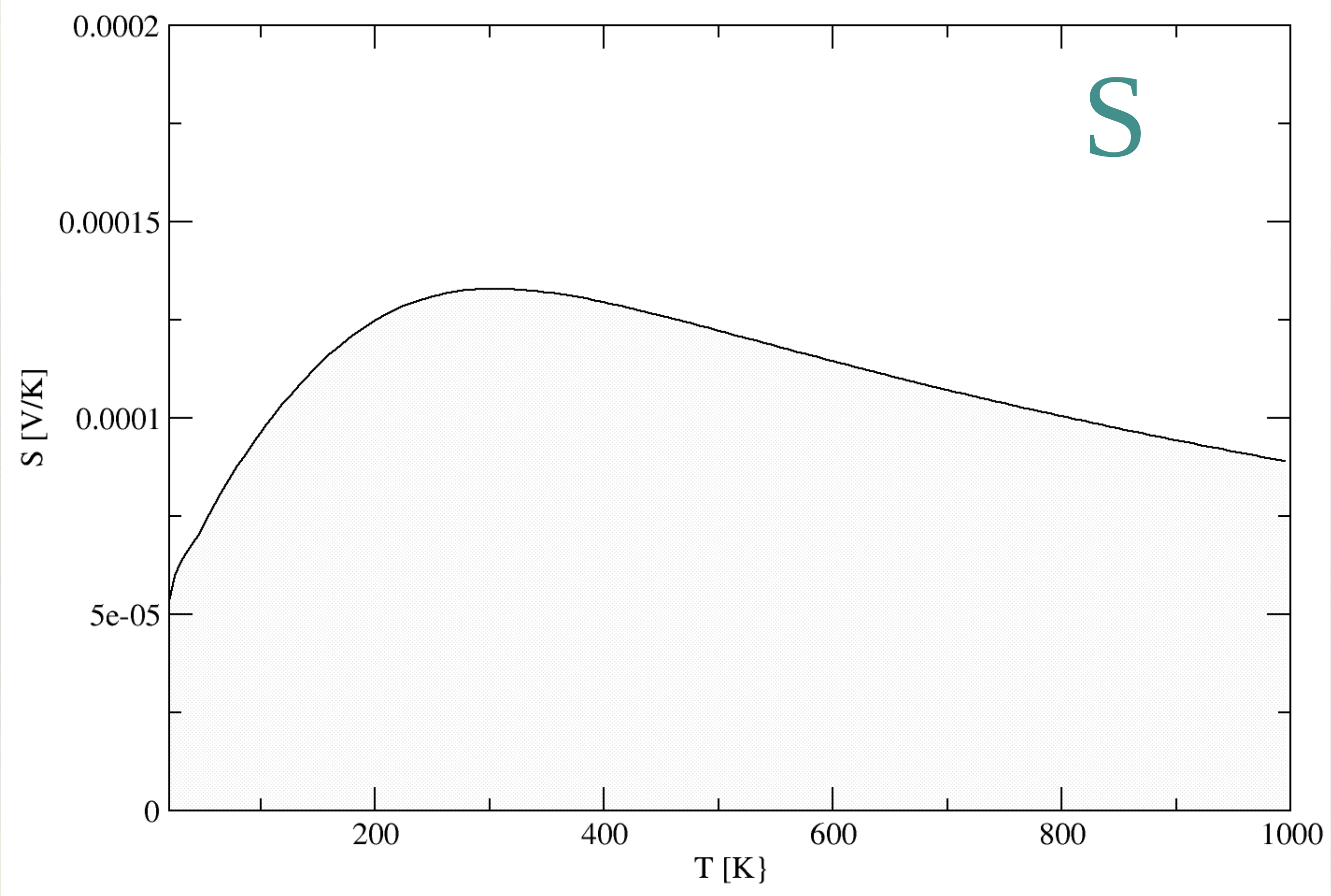

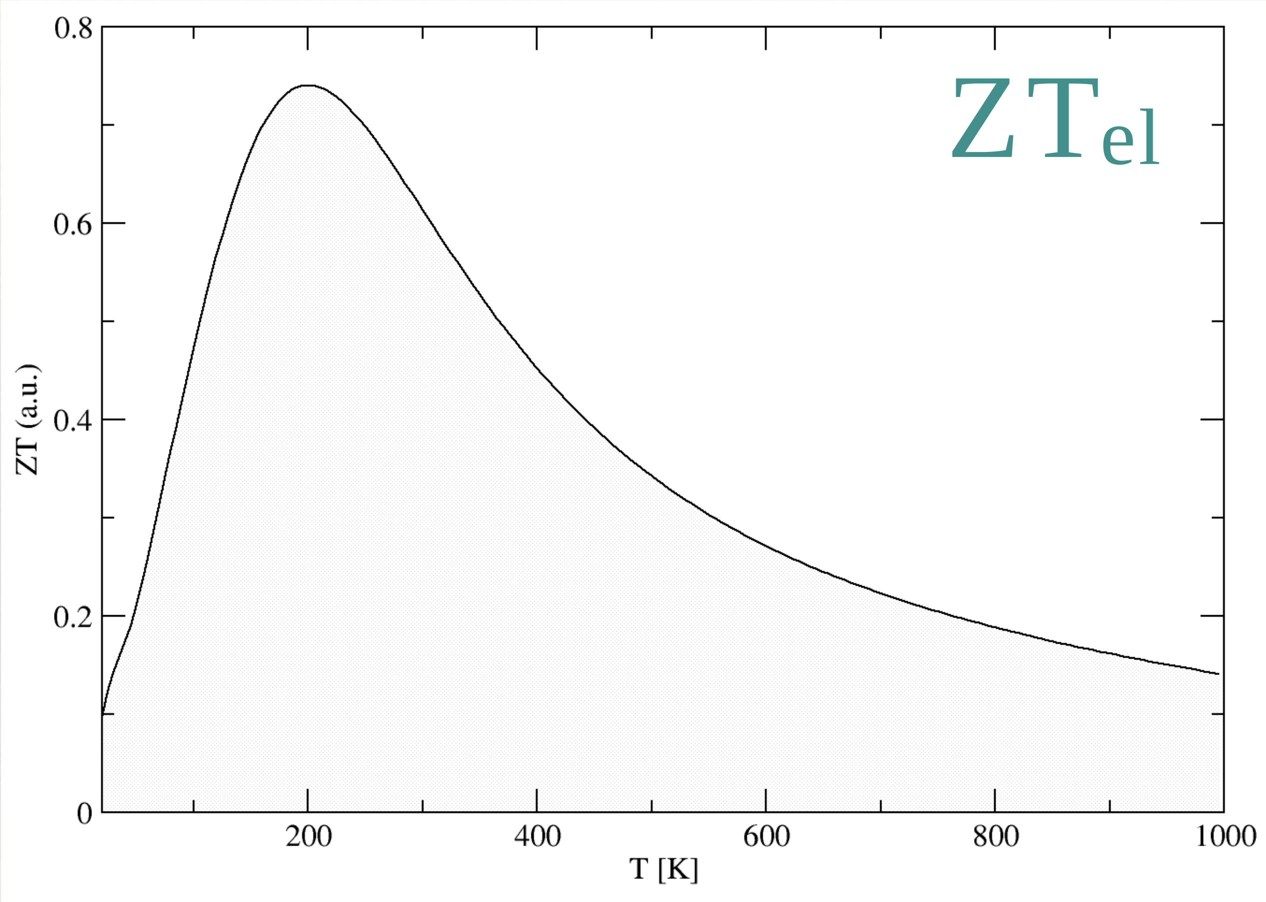

Lower S (compared to SnS BP), counterbalanced by high el conductivity. Promising ZT_{el} -> check k_L

siesta/ wannier90 interface
Boltzmann TE

Approach to large systems

- Large(r) number of atoms needed, to accommodate realistic features (grains, stacking faults…)
- DFT rapidly inefficient (el) - finite displacements methods need an efficient force driver for large number of atoms (ph)
- DFTB (TB DFT) is an efficient alternative
- Transmission can be calculated (el, ph)
- to do: driver for Finite displacements calculations

Structural variety & anisotropy

Derived from P under pressure

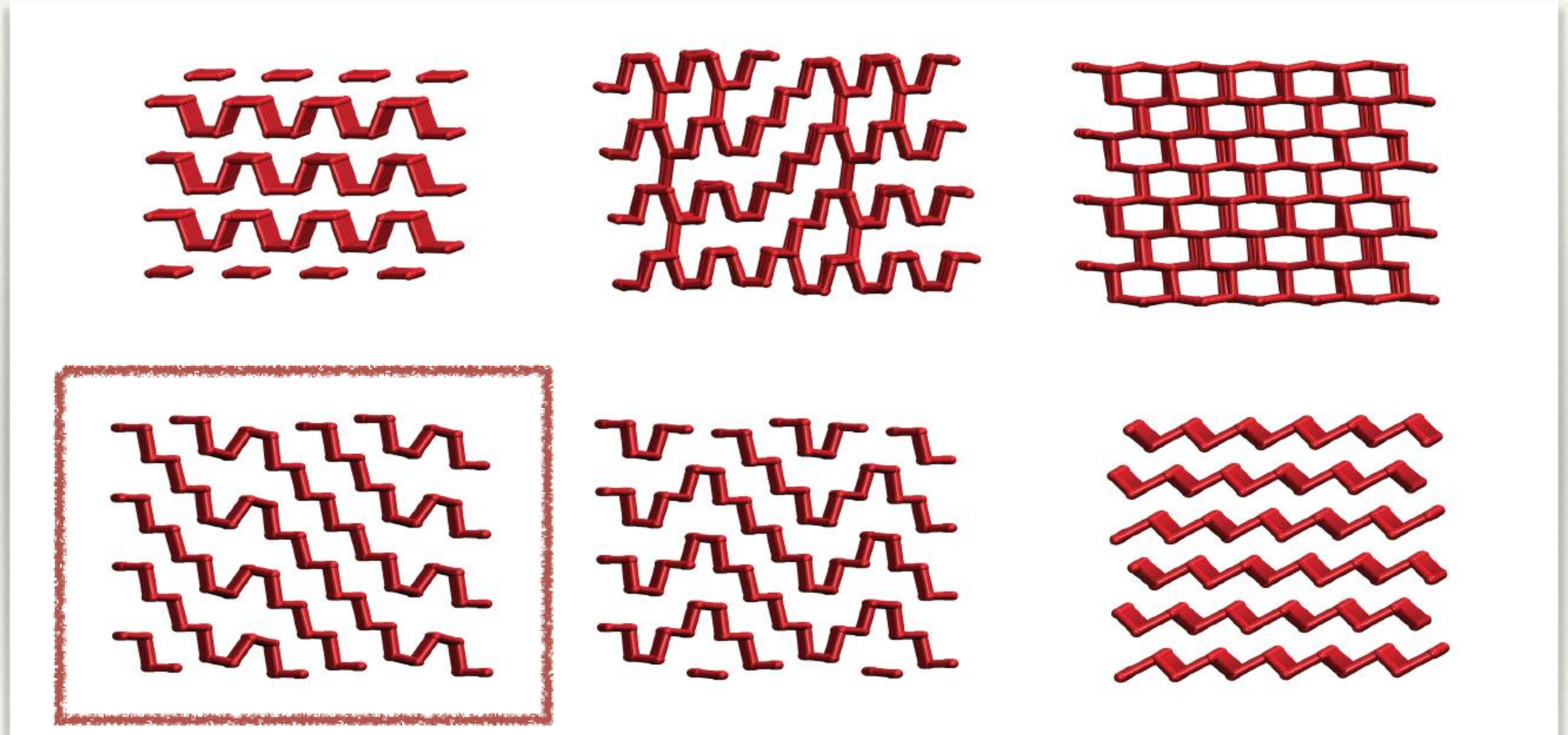

Co-existing structural features under pressure

Impact on Seebeck/ZT

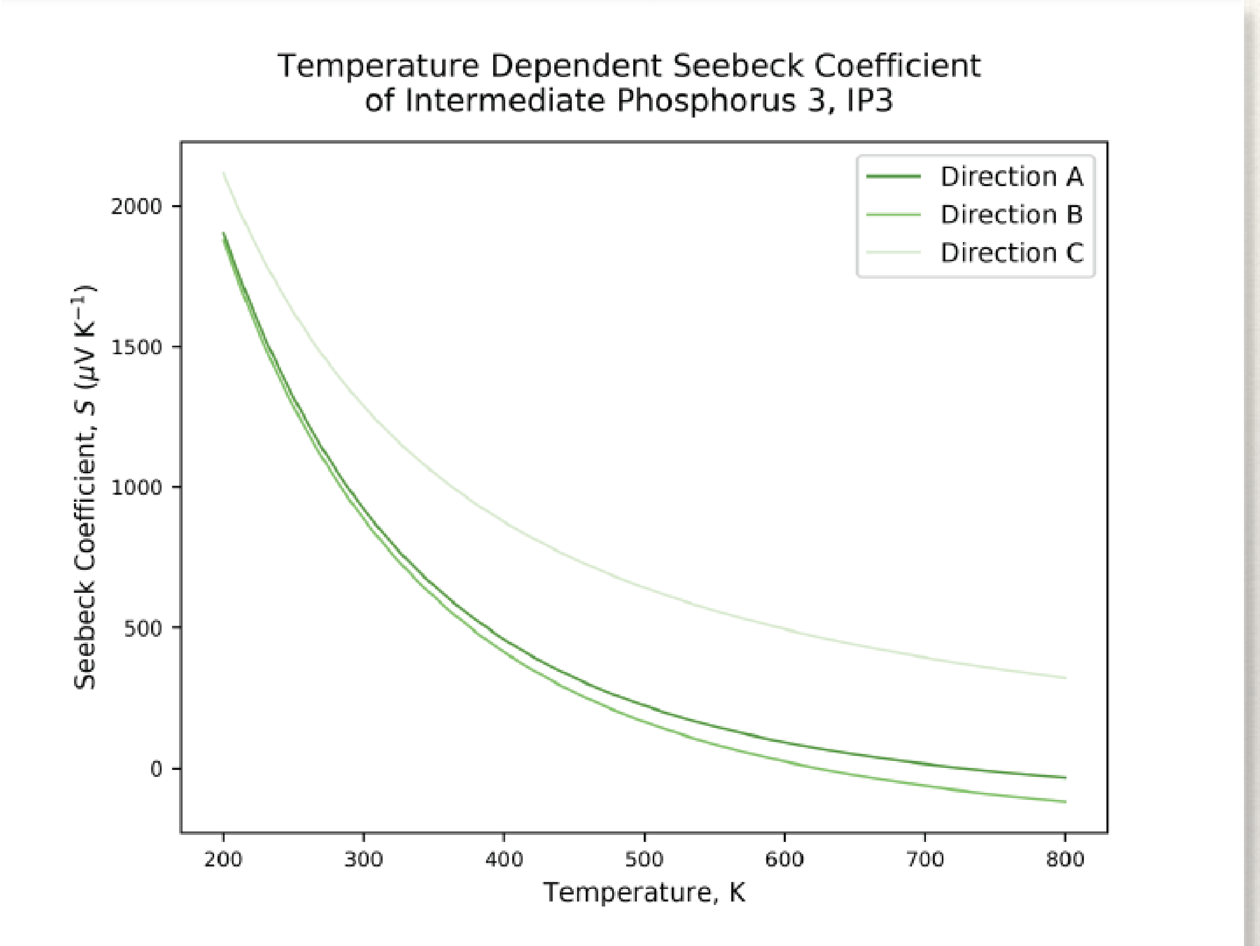

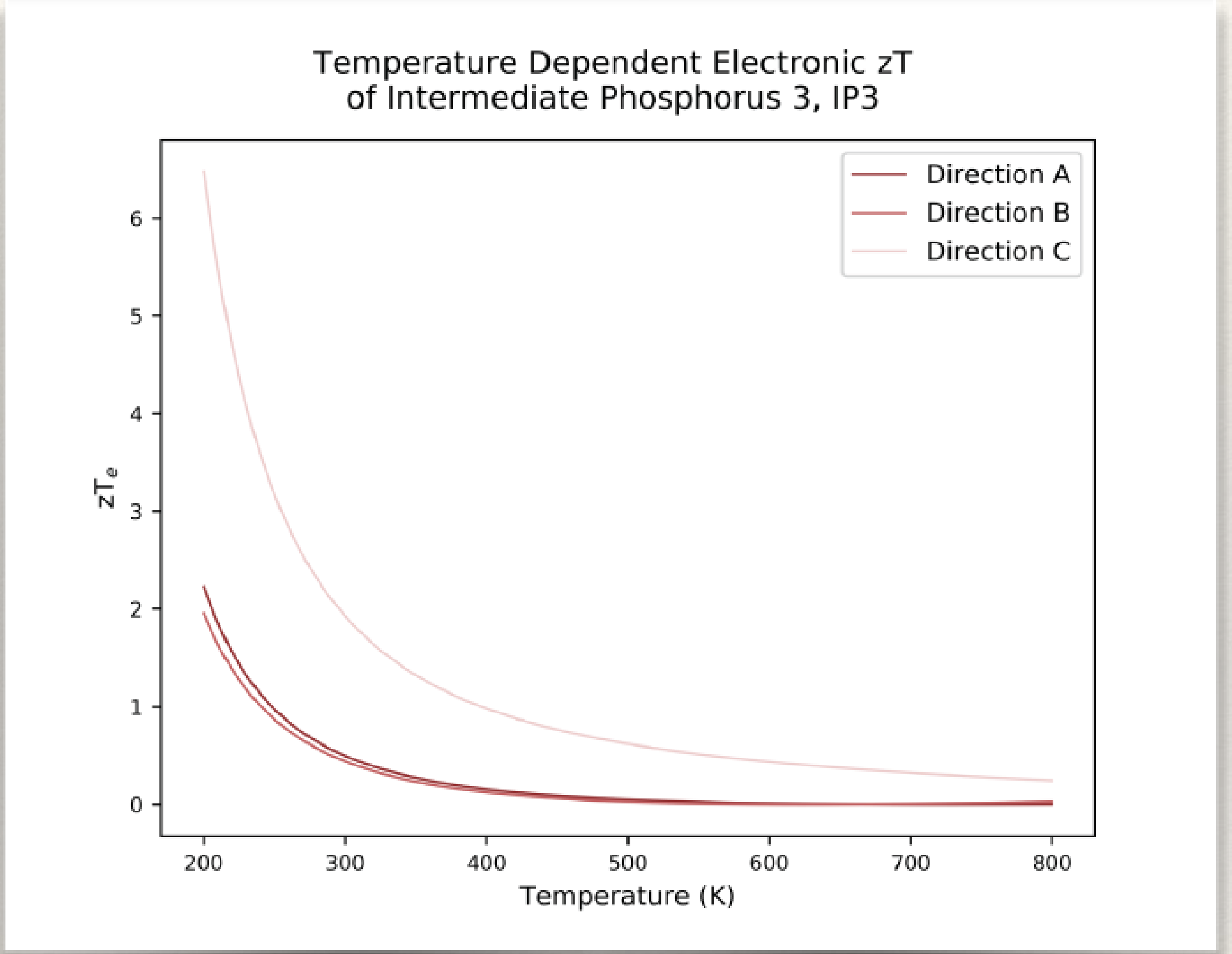

Increase in Seebeck & ZT (electronic)
Less anisotropic under pressure

Landauer-Büttiker

- Evaluate transmission as key quantity.

Non-Equilibrium

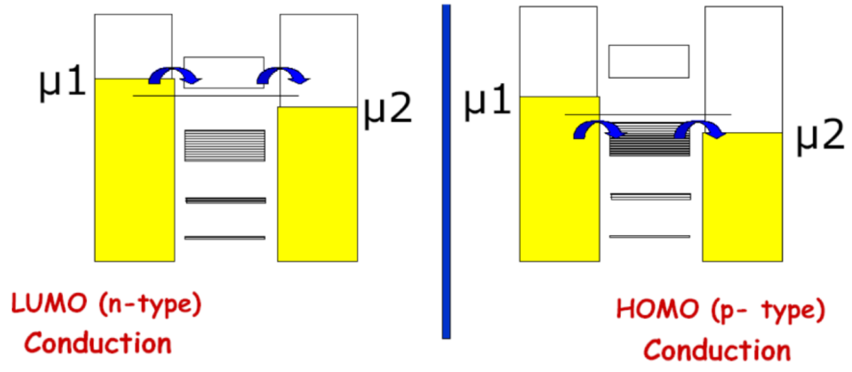

Flow of electrons

$$I = -\frac{2q}{h}\int_0^{\infty} d\varepsilon_k [f_0(\varepsilon_k - \mu_1) - f_0(\varepsilon_k - \mu_2)] = -\frac{2q}{h} T(E)[\mu_1 - \mu_2]$$

$$K_n = \frac{2}{h}\int dE\, T(E)\left(-\frac{\delta f}{\delta E}\right)(E-\mu)^n$$

$$\sigma = q^2 K_0 \qquad S = \frac{K_1}{qTK_0} \qquad k_e = \frac{K_2 - \frac{K_1^2}{K_0}}{T}$$

SnS - DFTB

Geometry, forces and el structure

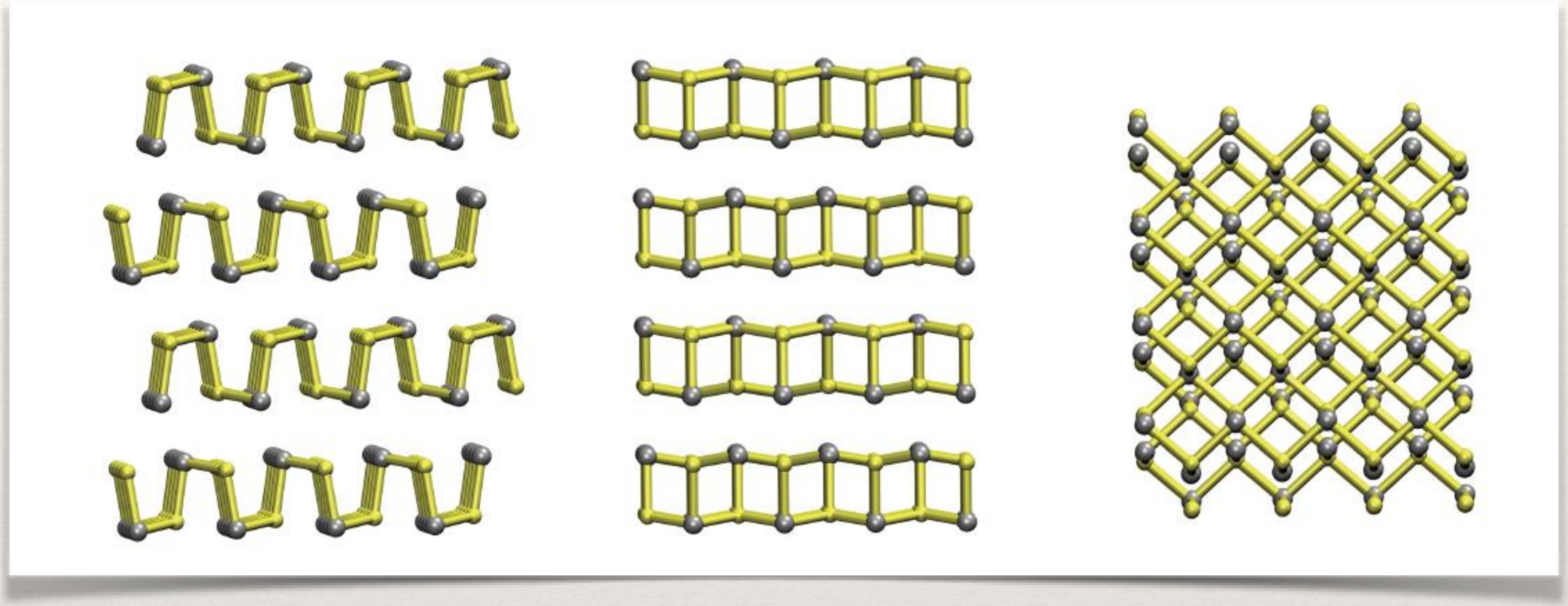

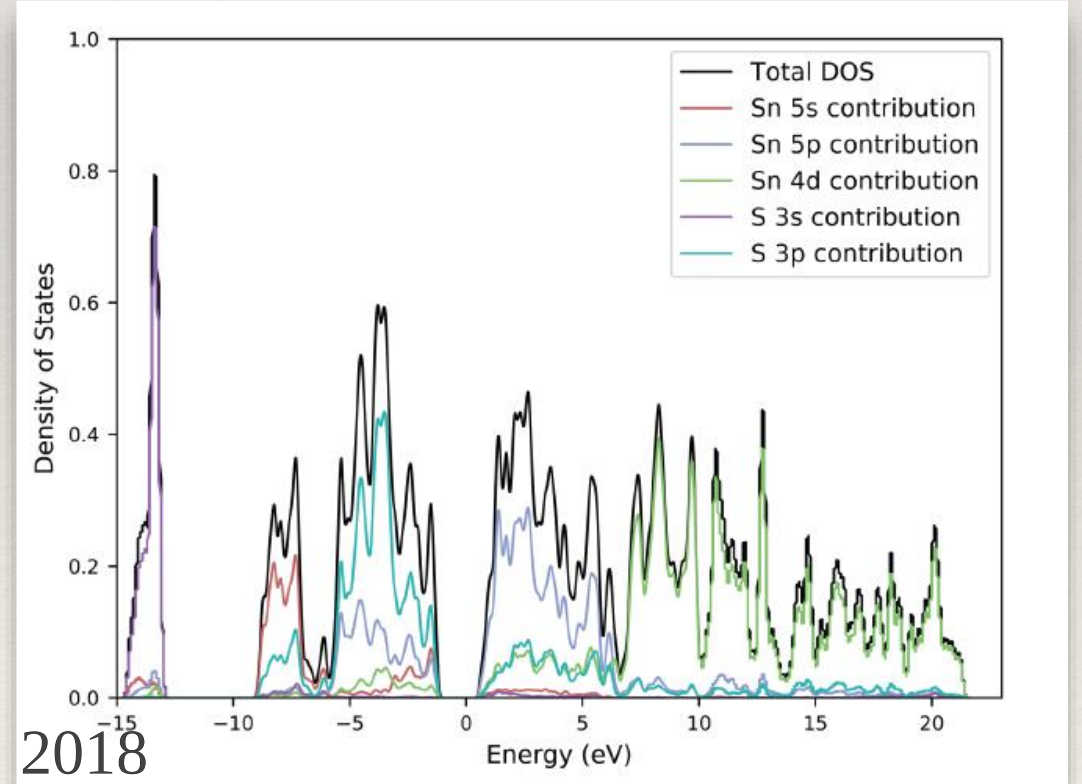

D.H, 2018

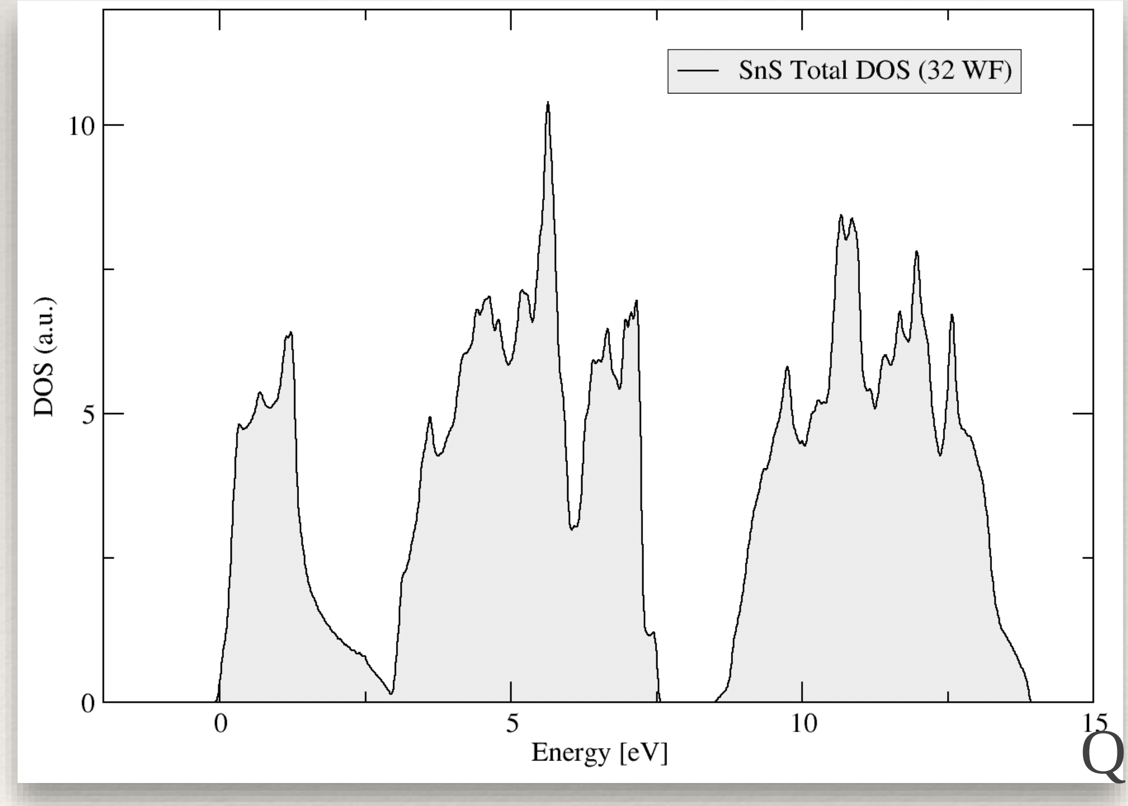

QE

Advantages of DFTB

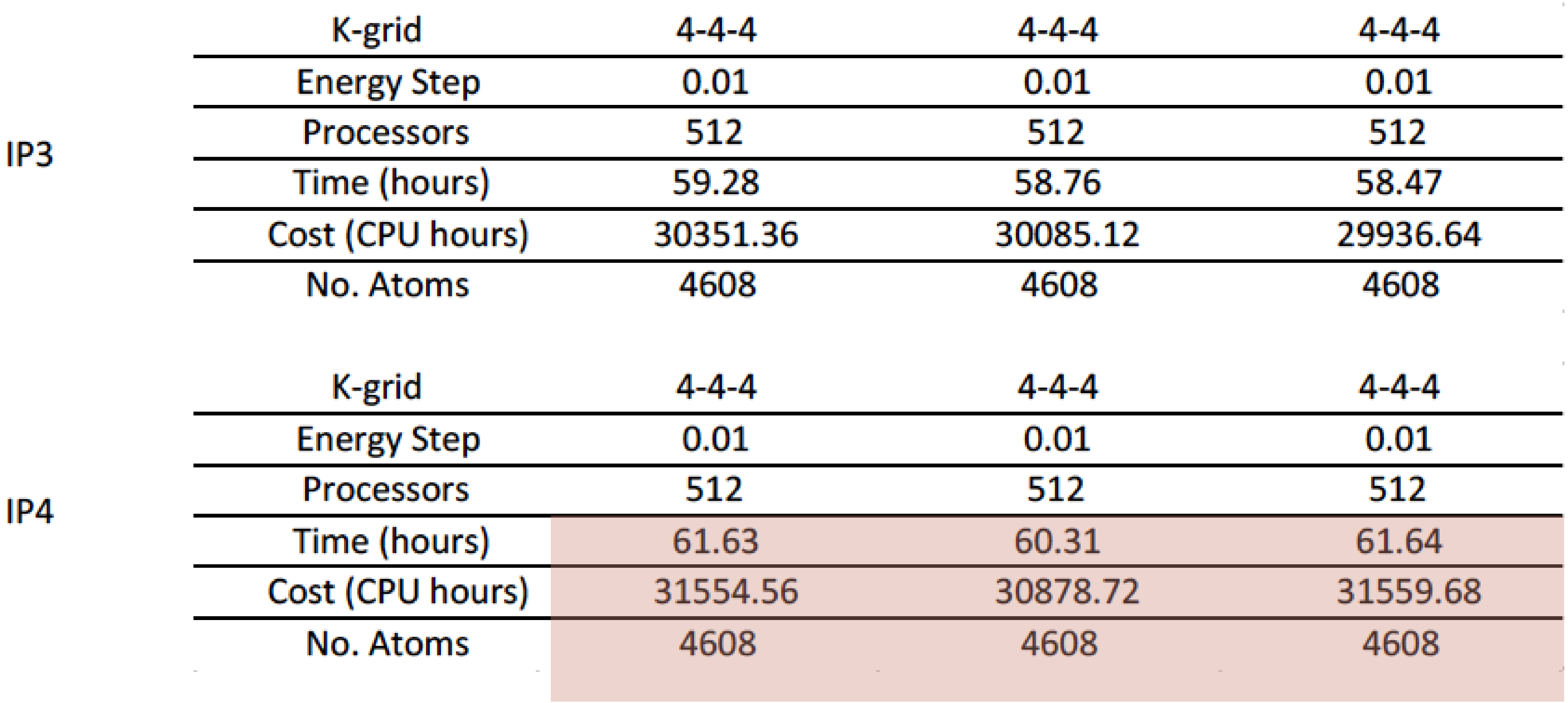

IP3

K-grid	4-4-4	4-4-4	4-4-4
Energy Step	0.01	0.01	0.01
Processors	512	512	512
Time (hours)	59.28	58.76	58.47
Cost (CPU hours)	30351.36	30085.12	29936.64
No. Atoms	4608	4608	4608

IP4

K-grid	4-4-4	4-4-4	4-4-4
Energy Step	0.01	0.01	0.01
Processors	512	512	512
Time (hours)	61.63	60.31	61.64
Cost (CPU hours)	31554.56	30878.72	31559.68
No. Atoms	4608	4608	4608

SnS - DFTB - Transport

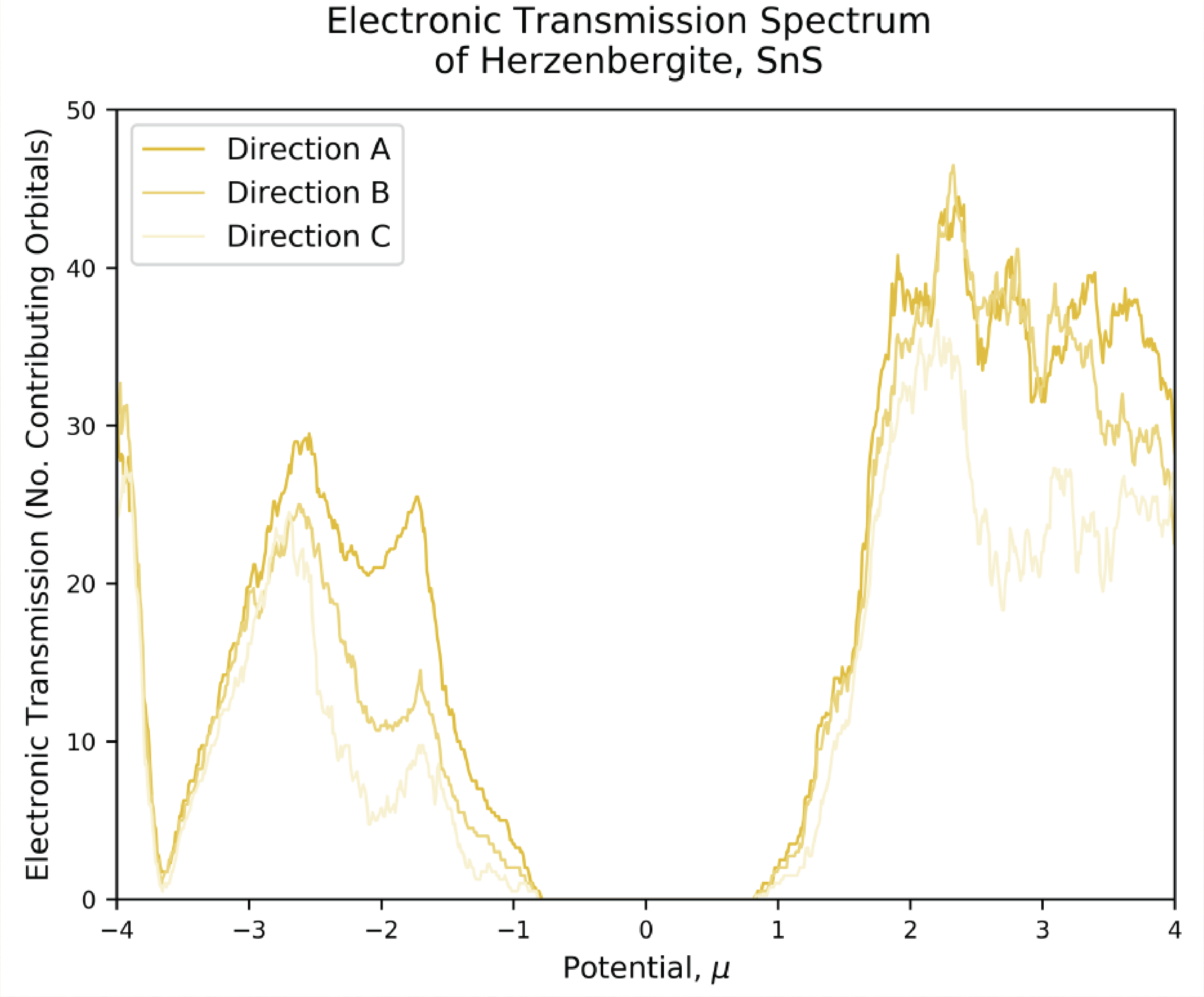

C direction corresponds to long axis (a in P*nma*)

D.H, 2018

SnS - ZT$_{el}$

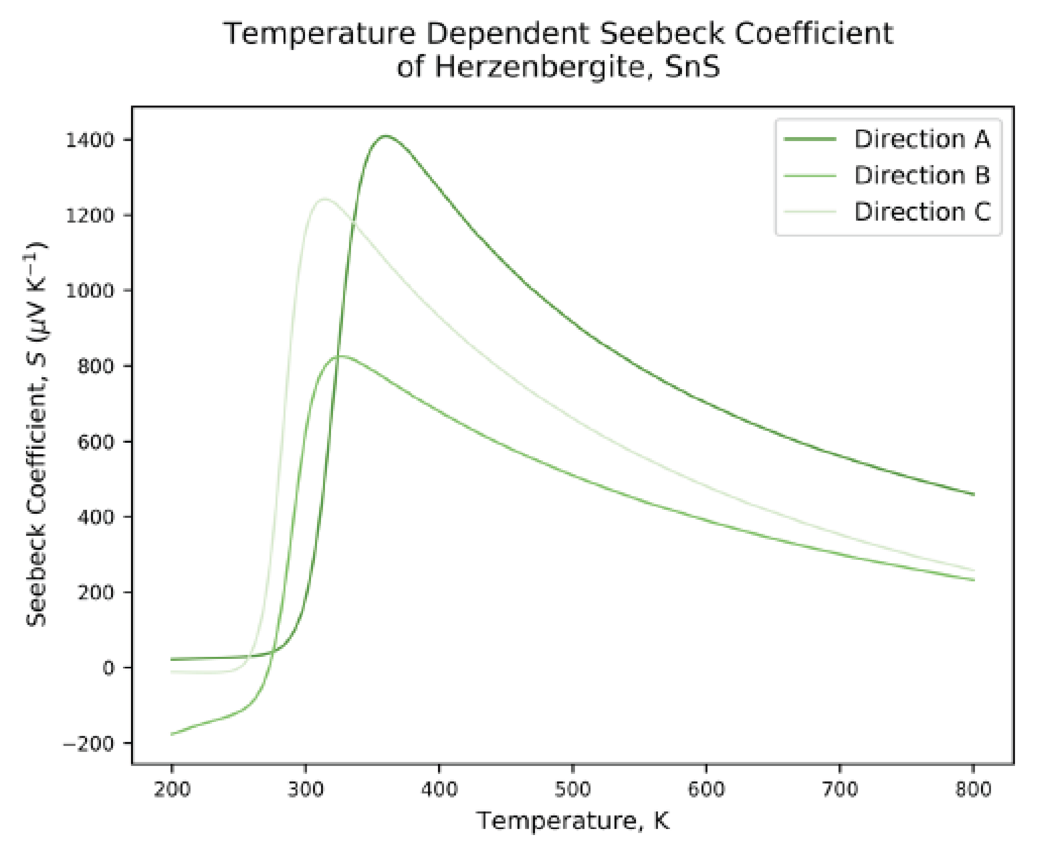

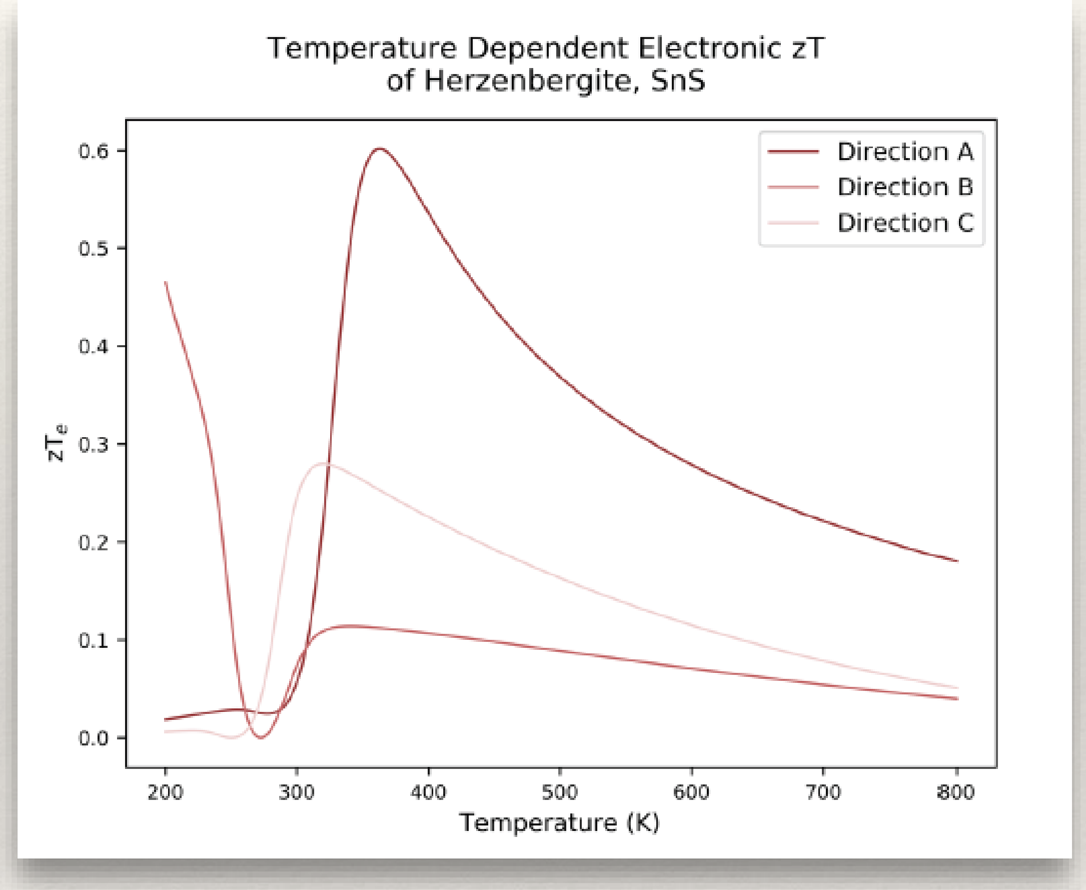

S value in the range of QE calculations (notice 2 order of magnitude difference!)
ZT$_e$ consistent, comparable to other studies & experiments.

D.H, 2018

SnS - Seebeck

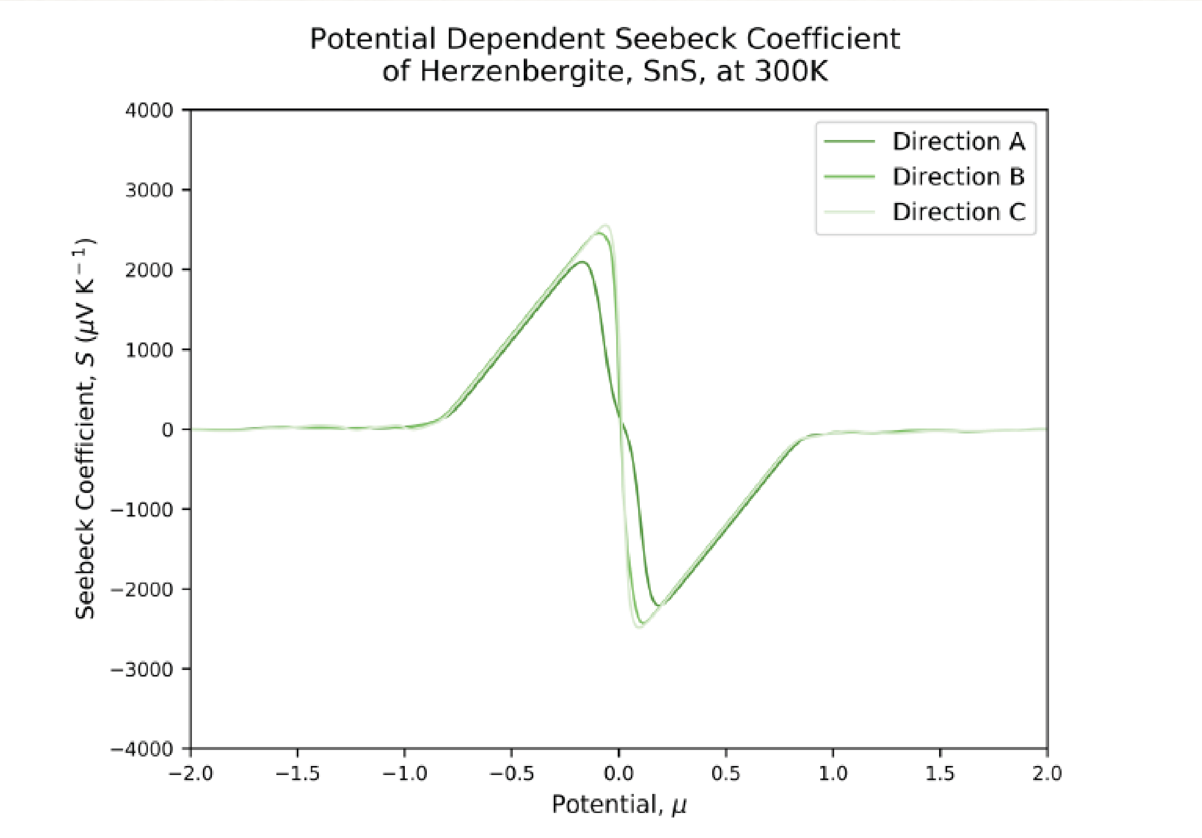
Potential Dependent Seebeck Coefficient
of Herzenbergite, SnS, at 300K
Seebeck Coefficient, S (μV K^{-1})
4000
3000
2000
1000
0
−1000
−2000
−3000
−4000
−2.0
−1.5
−1.0
−0.5
0.0
0.5
1.0
1.5
2.0
Potential, μ
Direction A
Direction B
Direction C

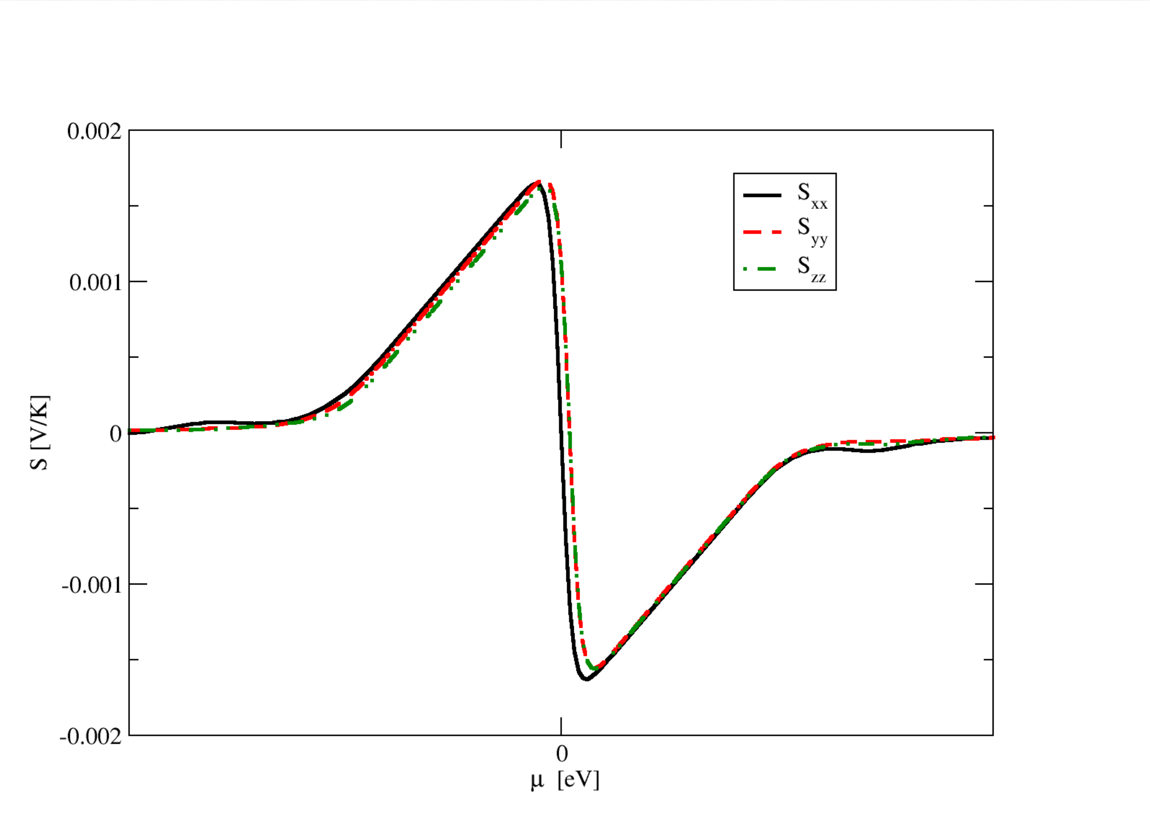
0.002
0.001
0
-0.001
-0.002
S [V/K]
0
μ [eV]
S_{xx}
S_{yy}
S_{zz}

Grain(-boundaries) - SnS

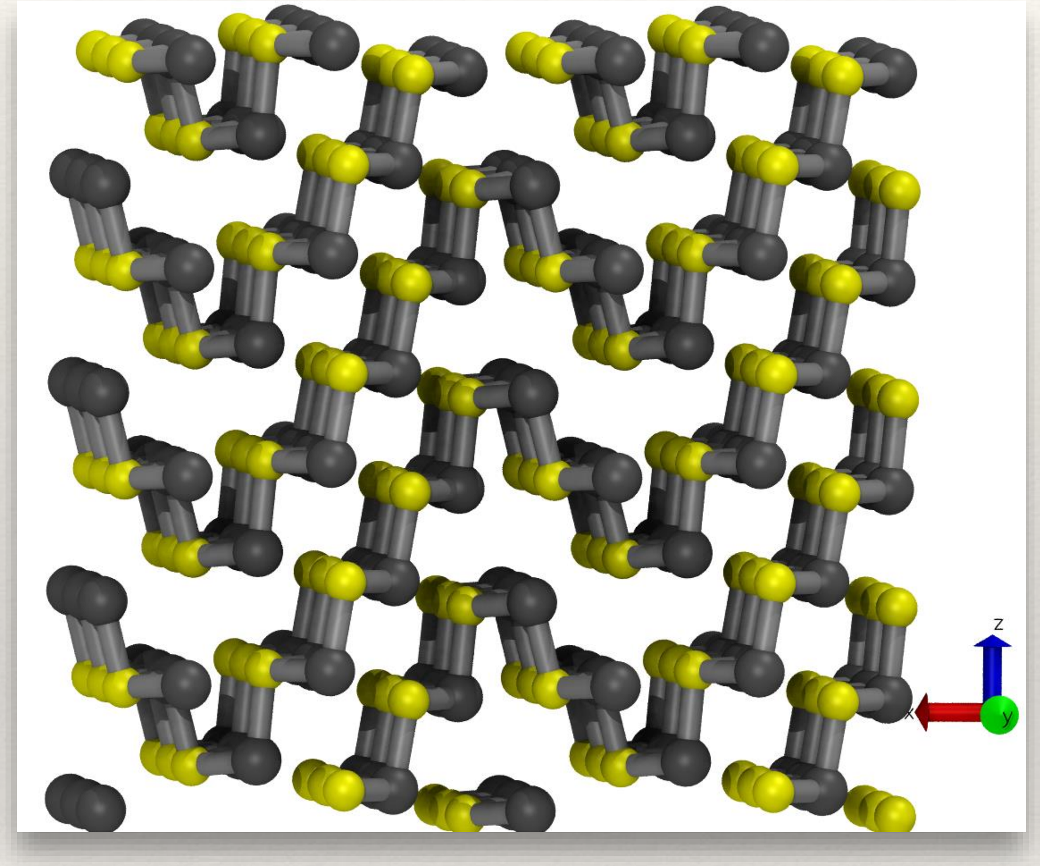

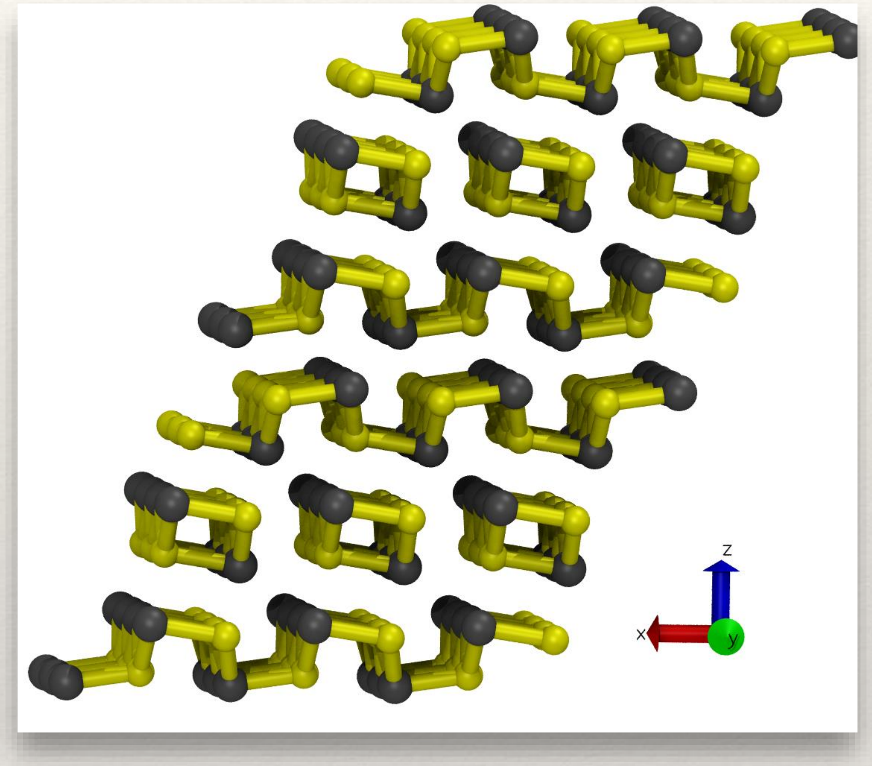

SnS tends to avoid too large spaces between layers.
Mixed structures tend to have smaller bandgap.
Some consequences on k_{el},
which nonetheless is still < 1.0 (300 K).

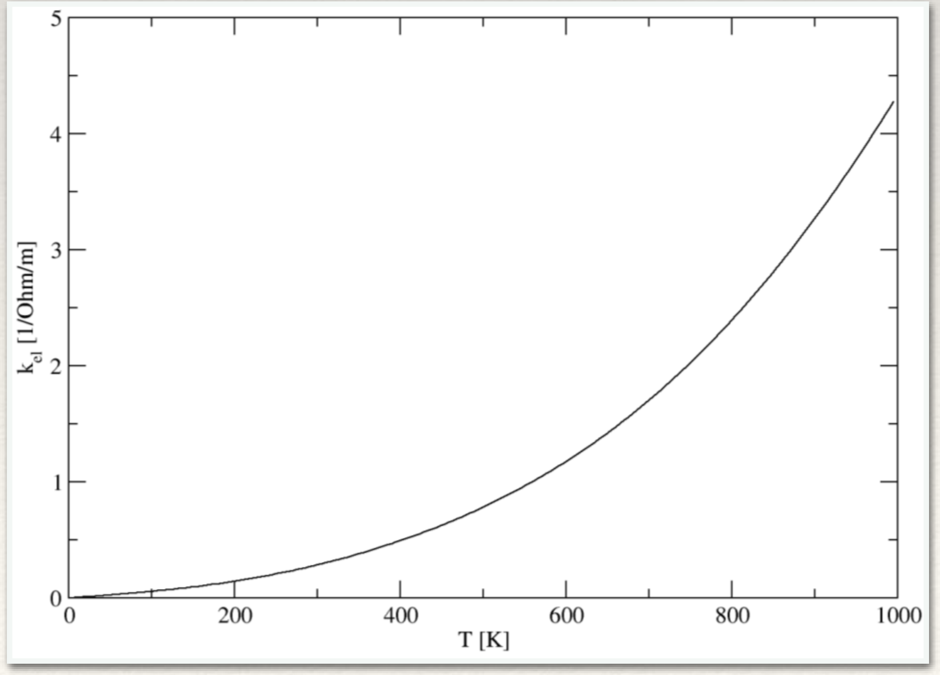

SnS - Force Field (ongoing)

- Parametrisation of a force field in progress
- Advantages: large systems, efficient, can use MD for thermal flux calculations (10^5-10^6 atoms easily reachable)
- Some success with a core-shell polarisable model (w/ point charges)
- However, better fit with a BO (Tersoff type) potential
  - works well for semiconductors
  - can (surprisingly) accommodate layered features, and deviation from symmetric structures (like NaCl for SnS)
  - fitting ongoing

ZT Computation Environment

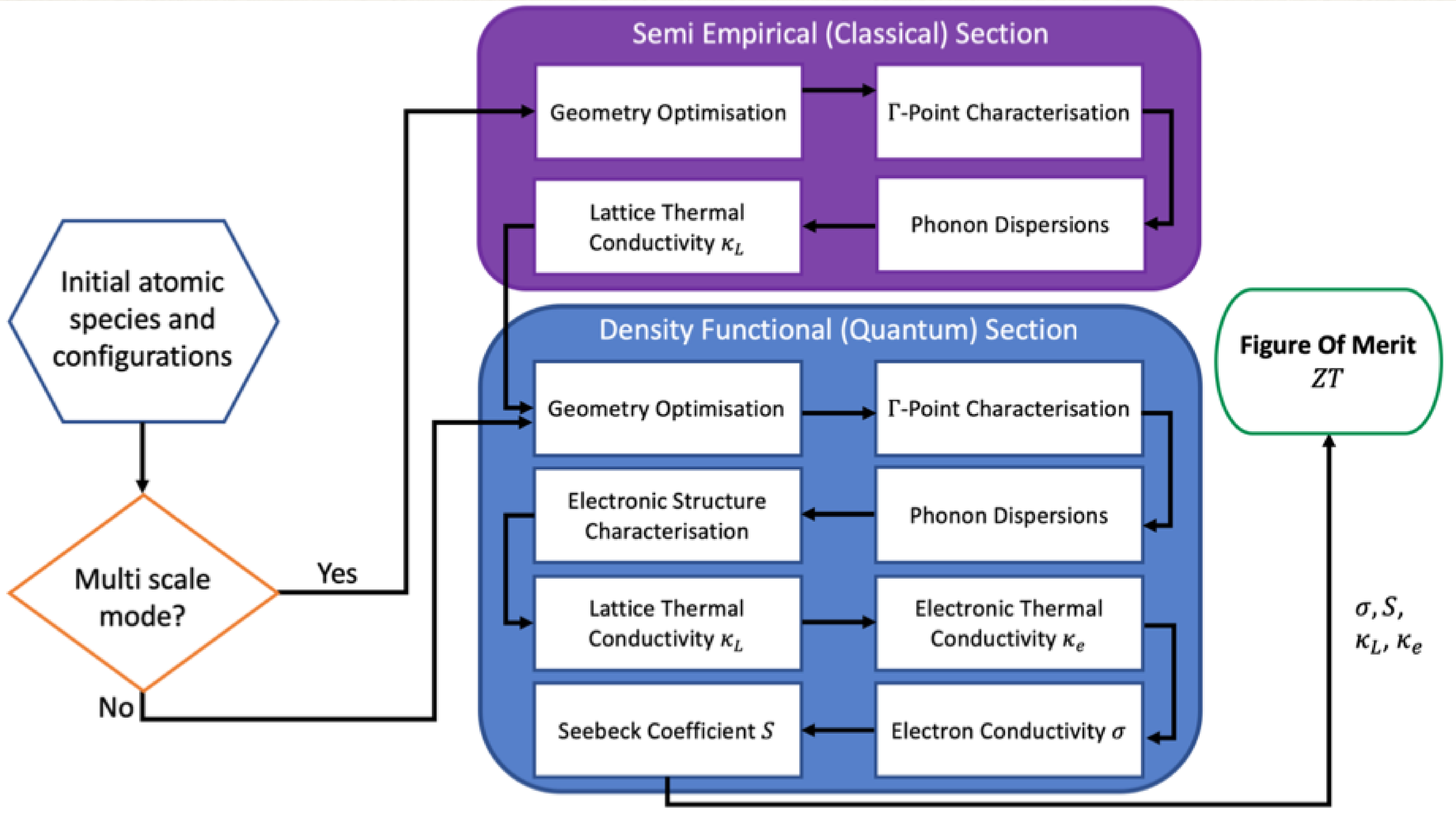

Initial atomic species and configurations

Multi scale mode?

Yes

No

Semi Empirical (Classical) Section

Geometry Optimisation

Γ-Point Characterisation

Phonon Dispersions

Lattice Thermal Conductivity κ_L

Density Functional (Quantum) Section

Geometry Optimisation

Γ-Point Characterisation

Phonon Dispersions

Electronic Structure Characterisation

Lattice Thermal Conductivity κ_L

Electronic Thermal Conductivity κ_e

Electron Conductivity σ

Seebeck Coefficient S

$\sigma, S,$
κ_L, κ_e

Figure Of Merit
ZT

Conclusions

- el transport calculations at ab initio level (QE, siesta),
    - some approximations
- thermal transport including anharmonicity and 3 order force terms,
- DFTB for large system, efficient and parallel,
    - el transport
    - ph transport in progress (calculation of ph transmission)
    - full ZT for large systems (upper 10^3 atoms)
    - including structural features (grains, stacking disorder)